Ренессанс в резонансном рассеянии (новые задачи-новая техника)

В.З. Гольдберг
Texas A&M University, РНЦ «Курчатовский институт»

МГУ 30 июля 2009 г.

coauthors

- Texas A&M University, USA
- Changbo Fu, V. Z. Goldberg, G. Chubarian, A. Mukhamedganov, G. Tabacaru, X. D. Tang, R. E. Tribble.

- Institute of Structure and Nuclear Astrophysics, USA
- B. Skorodumov, A. Aprahamian, P. Boutachkov, J. Kolata, L.O. Lamm, M. Quinn and A. Woehr

- Lawrence Berkeley National Laboratory, USA
- K. Peräjärvi, F. Q. Guo, D. Lee, D. M. Moltz, J. Powell and Joseph Cerny

- Florida State University, USA
- G. V. Rogachev, A. Volya

- Michigan State University, USA
- B. A. Brown

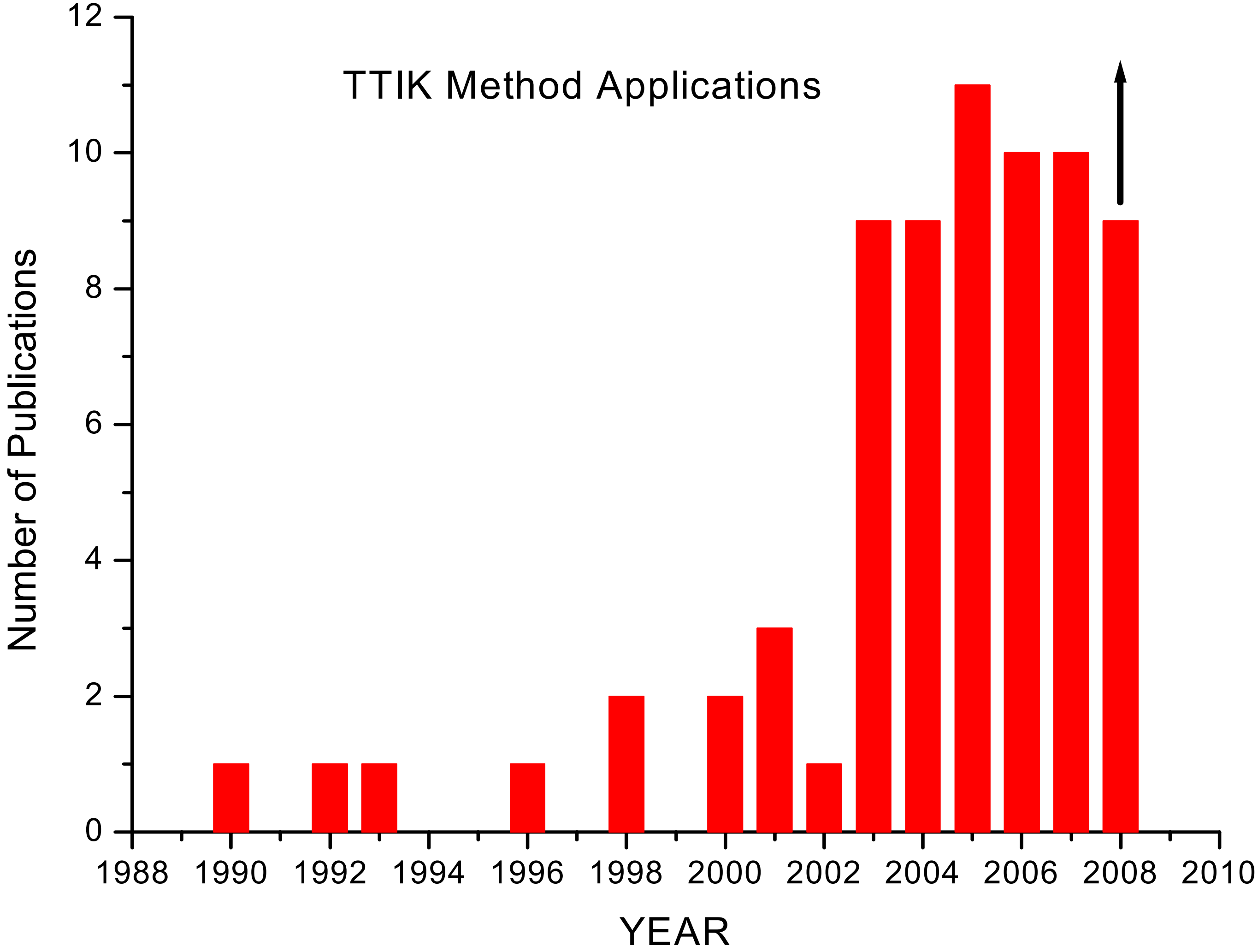
TTIK Method Applications
Number of Publications
YEAR
0
2
4
6
8
10
12
1988
1990
1992
1994
1996
1998
2000
2002
2004
2006
2008
2010

Resonance reaction

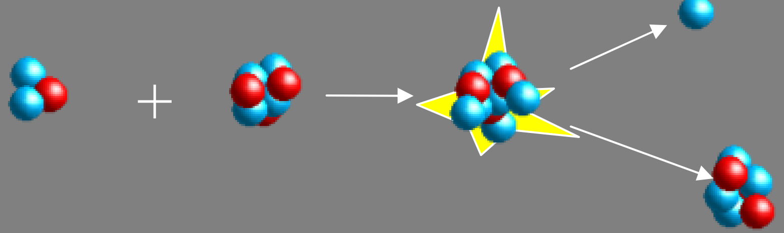

The goal is to study properties (level structure) of compound nuclei rather then the properties of the residual species.

$$\sigma \propto \frac{\Gamma_{in}\Gamma_{out}}{(E-E_0)^2 + (\frac{\Gamma_{tot}}{2})^2}$$

Cross section strongly depends on energy

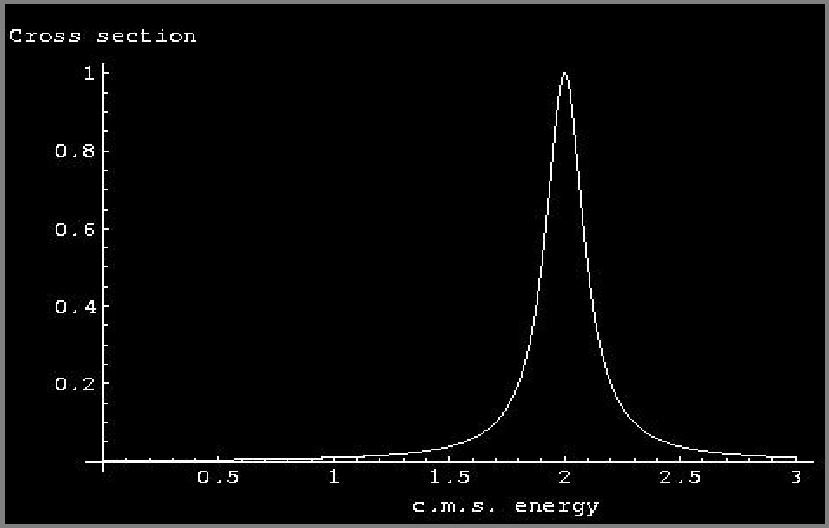

Resonance elastic scattering

Cross section in case of single isolated resonance
(spin zero particles)

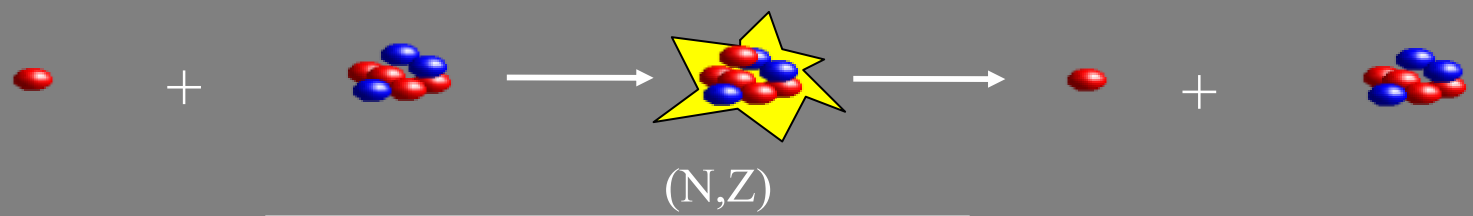

$$\frac{d\sigma(\theta)}{d\Omega}=\frac{(2L+1)^2}{4k^2}\frac{\Gamma^2 el}{(E-E_0)^2+\frac{1}{4}\Gamma^2{}_{tot}}P^2{}_L(\cos\theta)$$

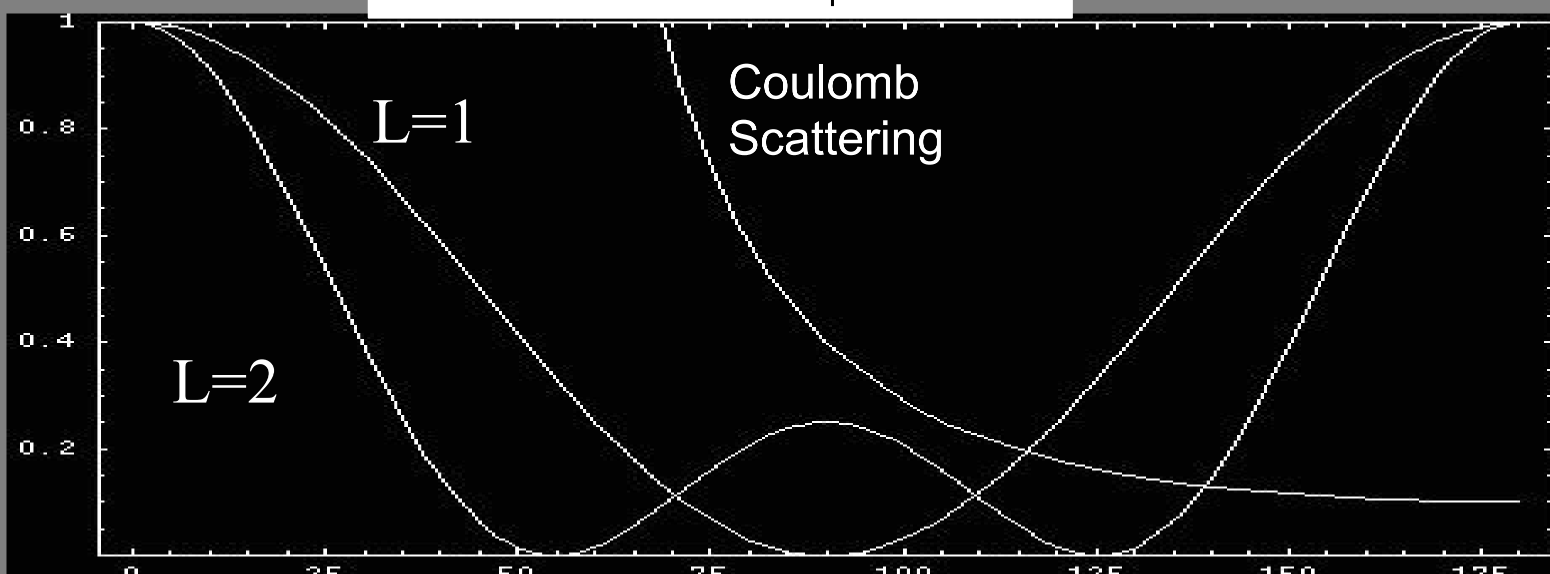

W.M. Wilson,
E.G. Bilpuch,
G.E. Mitchel

N.P. A 271
(1976)

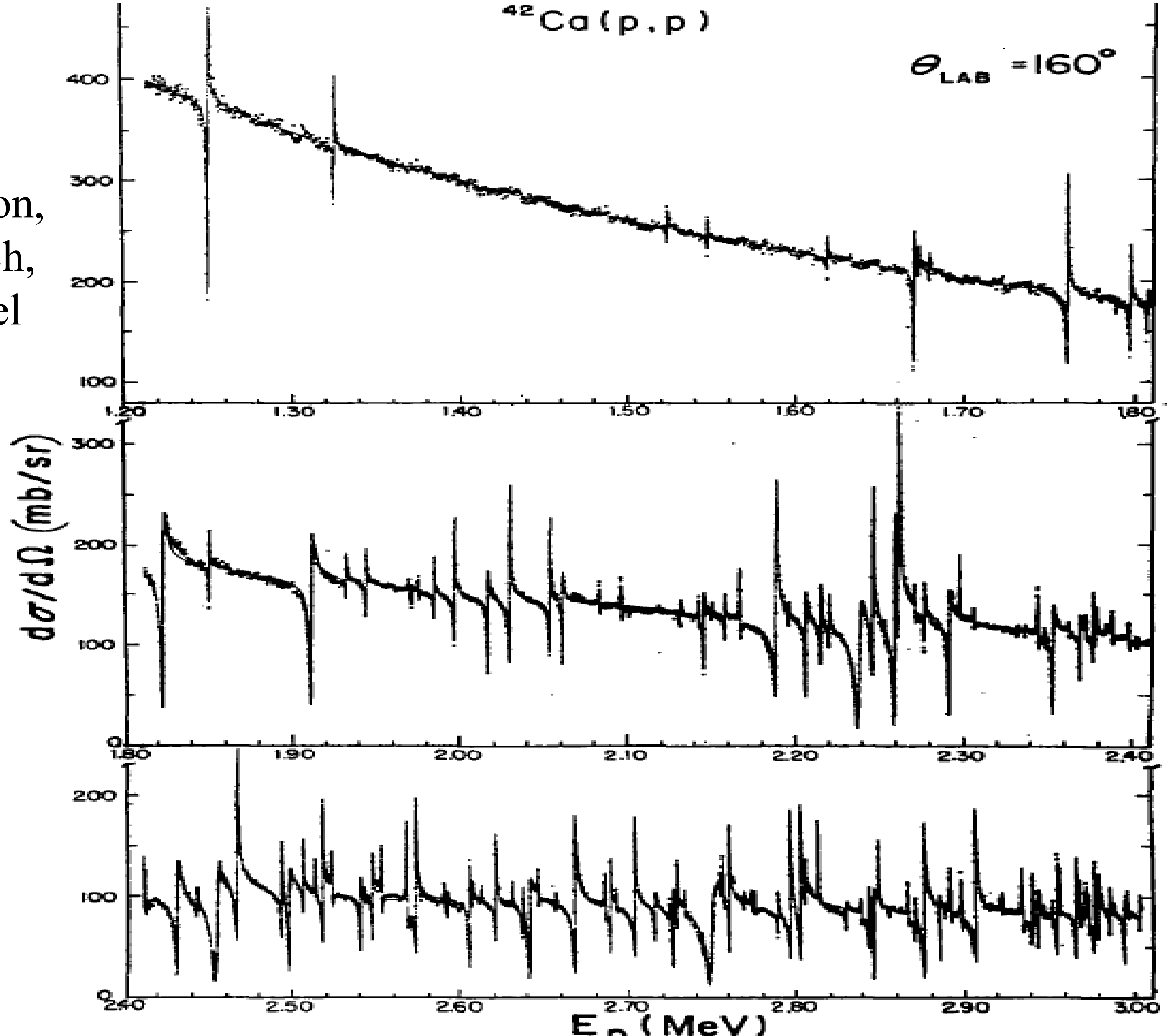

Fig. 1. The ^{42}Ca(p, p) differential cross section at 160° over the entire energy range. The solid line represents a multi-level fit to the data.

$$^{42}Ca_{20} + p \rightarrow {}^{43}Sc$$

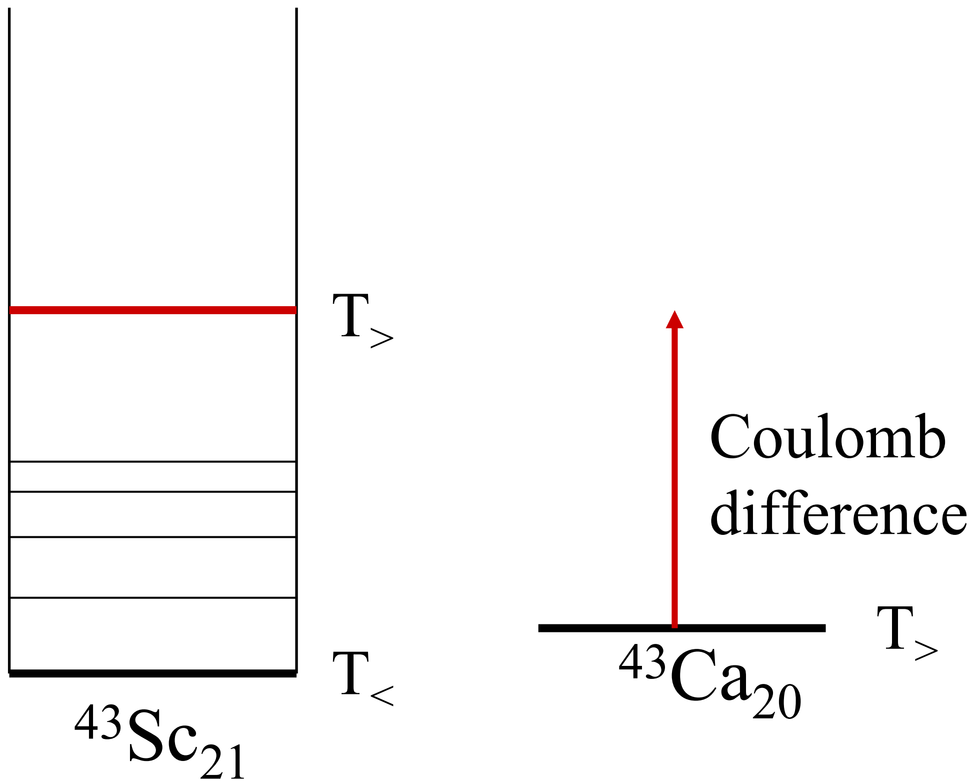

NEW

Radioactive beams (beams of exotic nuclei)

Main goals:

1. To obtain information on exotic nuclei
2. Nuclear astrophysics
3. α clusters in exotic nuclei

motivation (1) nuclear astrophysics

Insik Hahn

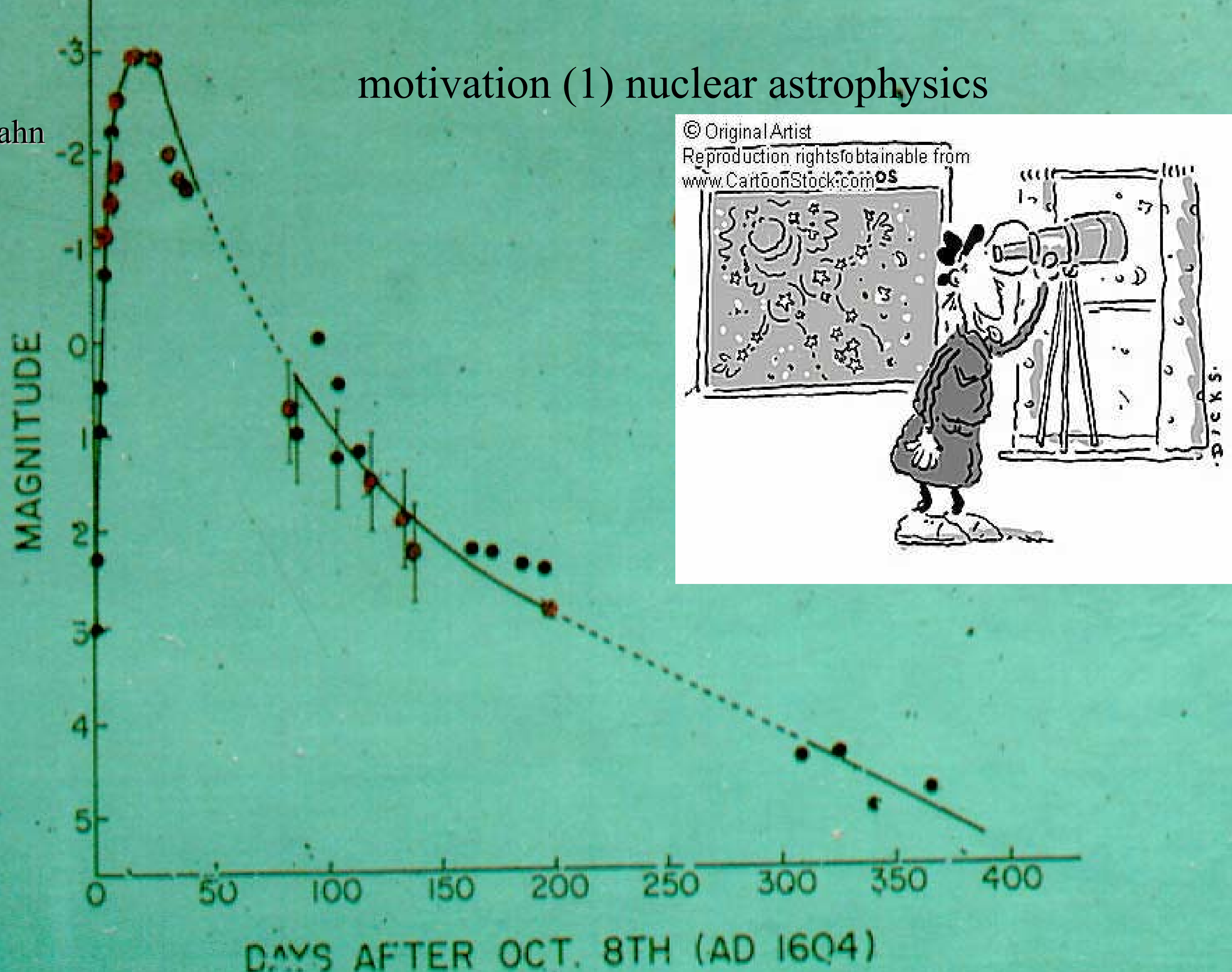

X-ray burst and novae

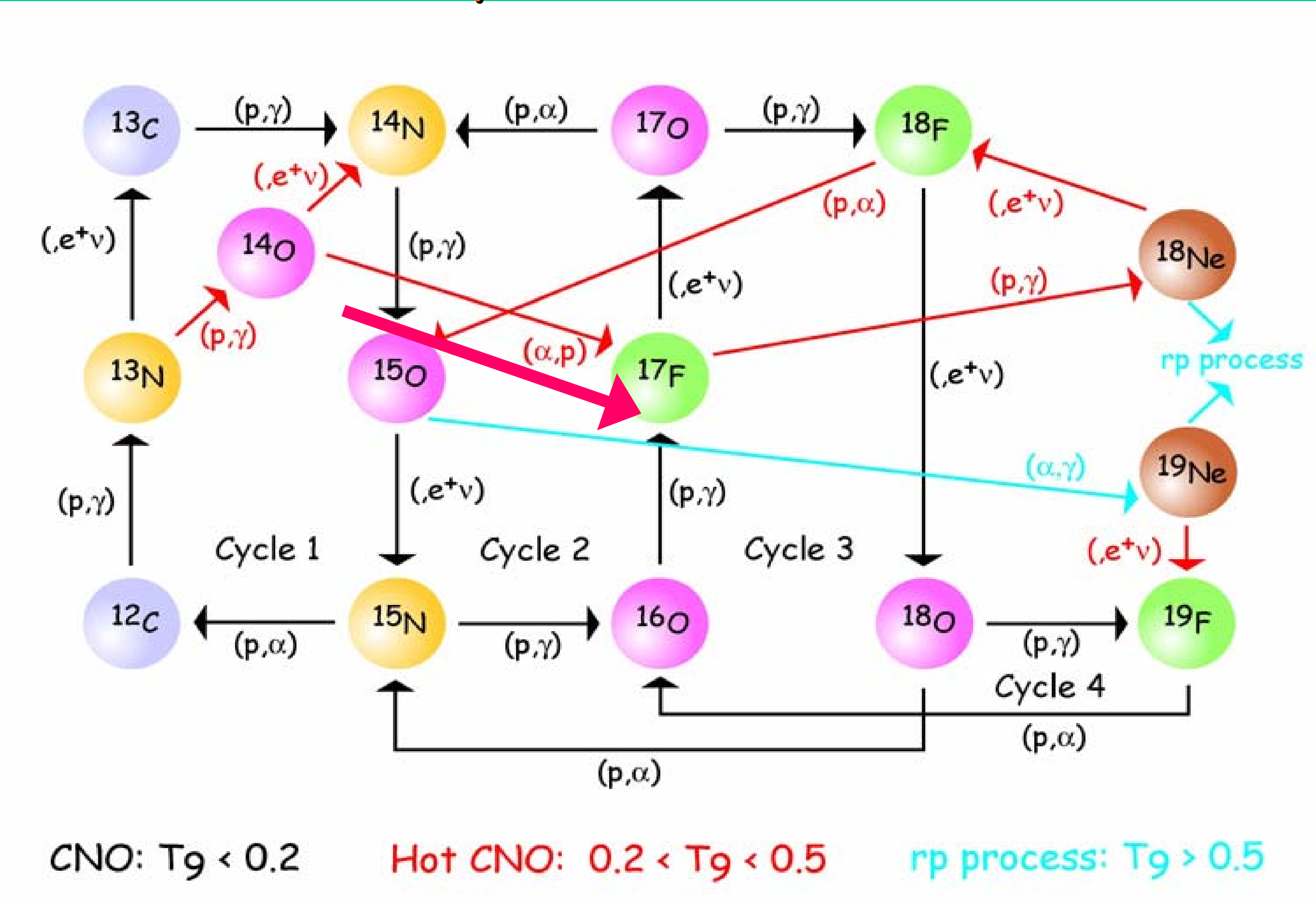

Resonances in exotic nuclei

Conventional nucleus

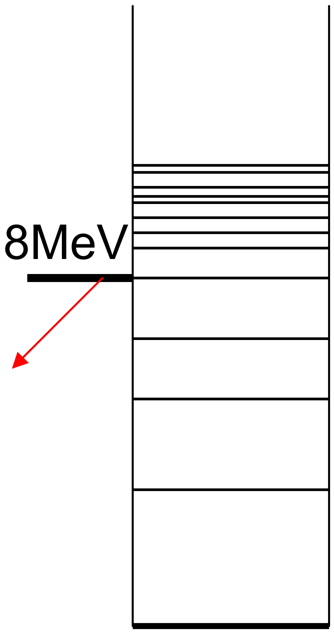

Density of levels is high. Practically it is not possible to use theoretical predictions

Proton rich exotic

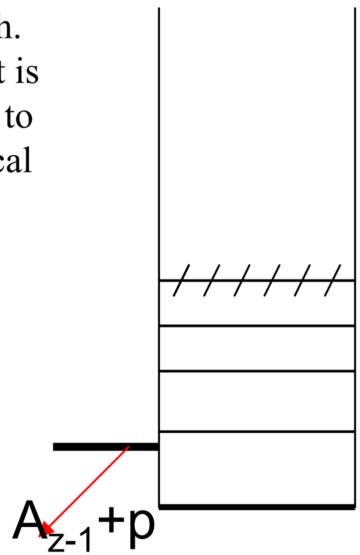

Density of levels is low. Even simple considerations can work

Neutron rich exotic

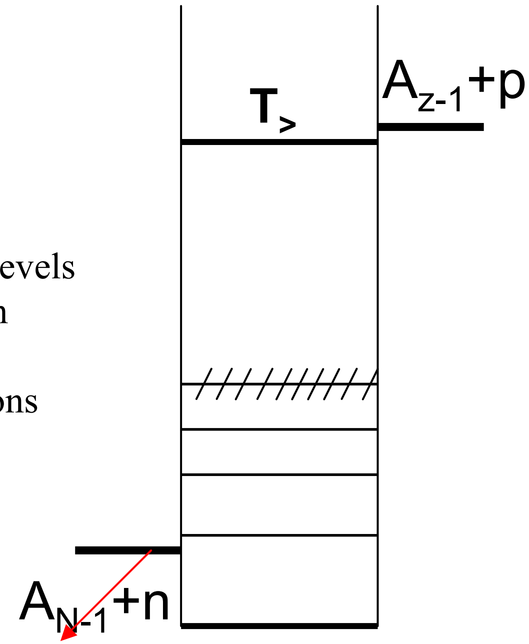

^{9}He? ^{8}He+p→^{9}Li (T=5/2)

Inverse geometry and thick target technique

- High efficiency
- Good energy resolution
- 180 degree (c.m.) measurements are possible
- Excitation function is continuous
- Low excitation energies could be measured due to energy amplification in inverse kinematics

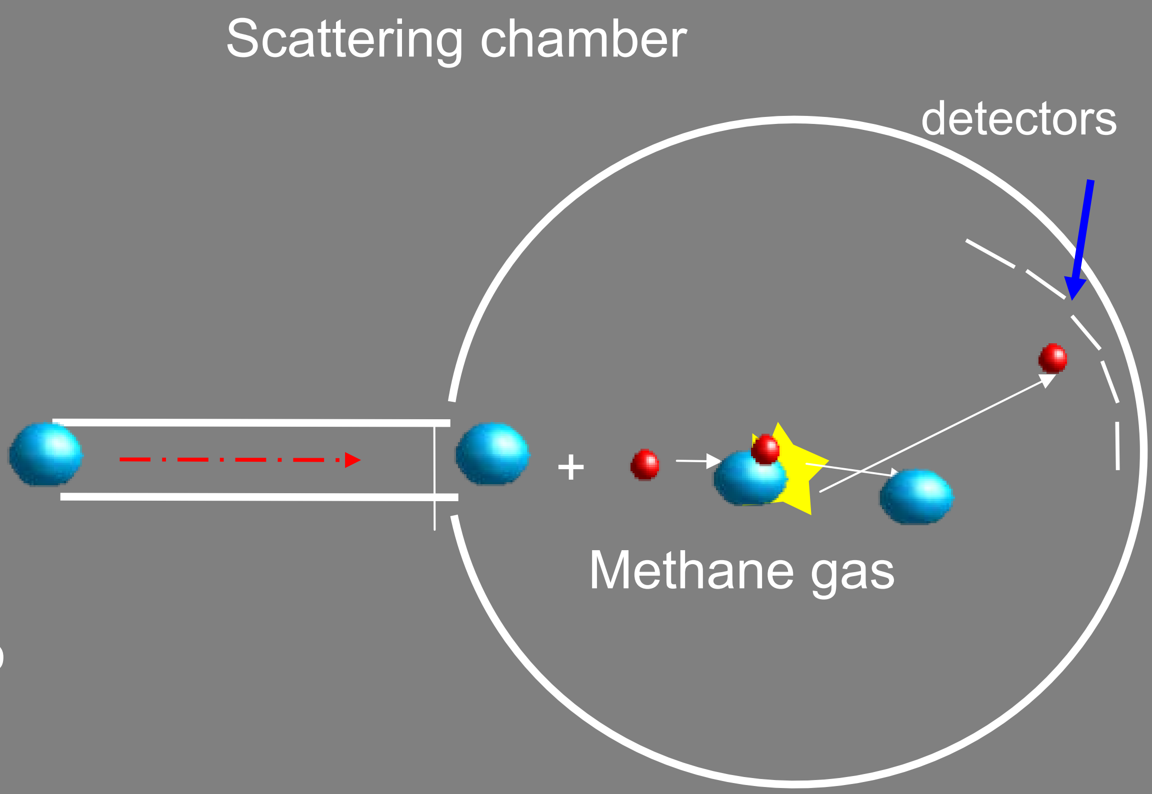

just kinematics

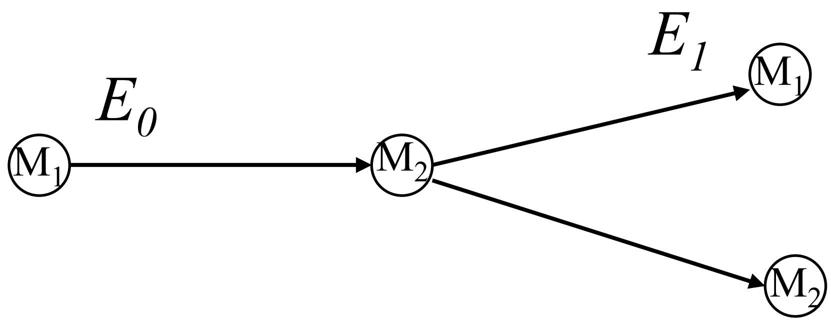

elastic (conventional)

$$E_1 = E_0\ (M_2 - M_1)^2/(M_2 + M_1)^2 \sim E_0 \sim E_{cm} \qquad M_2 >> M_1$$

elastic (inversed)

$$\Theta_{cm} = 180^0 \qquad E_2 = 4E_0\ M_1M_2/\ (M_2 + M_1)^2 \sim 4E_0\ M_1/M_2 \sim 4E_{cm} \qquad M_1 >> M_2$$

inelastic (inversed)

$$E_2 = 4\{E_0 - Q\ (M_2 + M_1)/2M_2\}\ M_1M_2/\ (M_2 + M_1)^2 \qquad Q/E_0 << 1$$

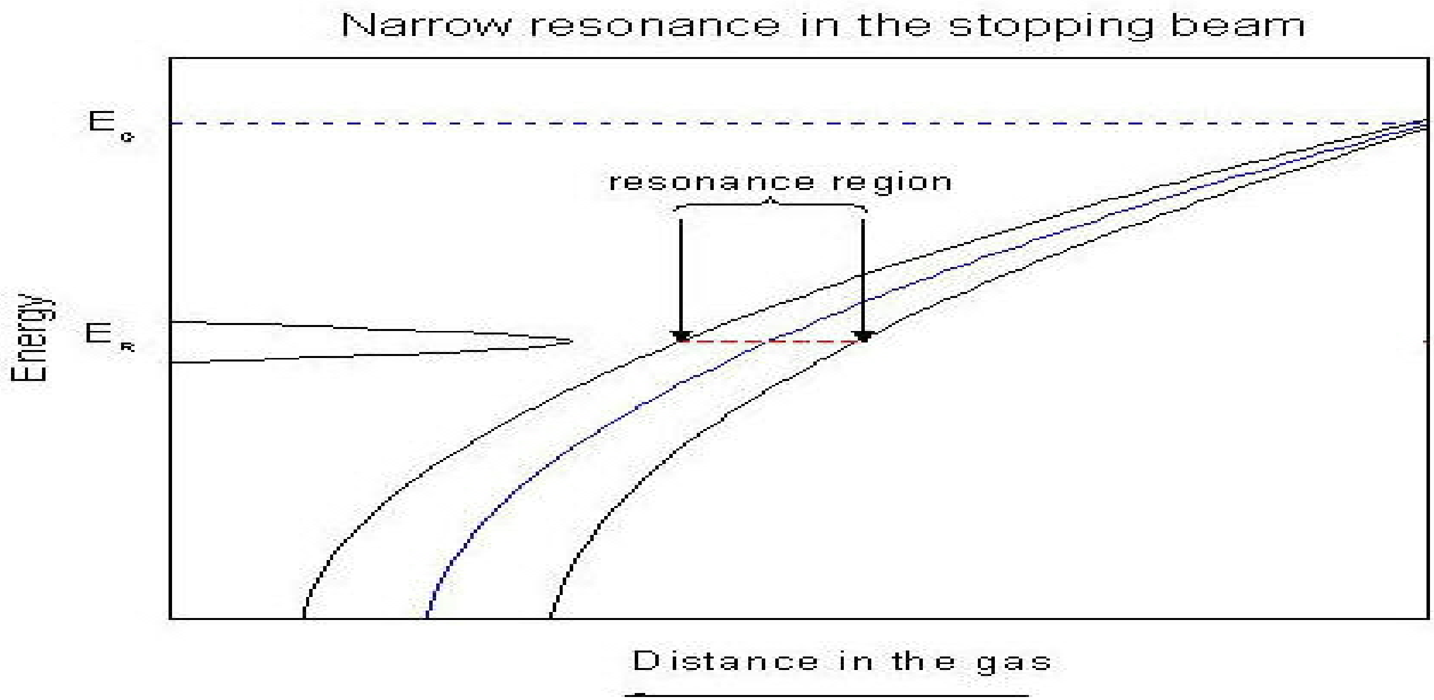

$$E_{rec}(0^{o}) = 4E_{0}\frac{m_{rec}M}{(m_{rec}+M)^{2}}$$

$E_{rec} \approx$ 3 MeV for a resonance, corresponding 1 MeV cm energy of the $^{16}O+\alpha$ interaction (while in the conventional kinematics of $^{16}O+\alpha$ interaction, the corresponding energy of α particles at 180^{o} will be only 300 keV.)

Assumptions:

1.The recoil energy loss in the target is much smaller than that of the heavy ions

2. The resonant scattering is the dominant process

Resonance states in ^{20}Ne
^{16}O+He

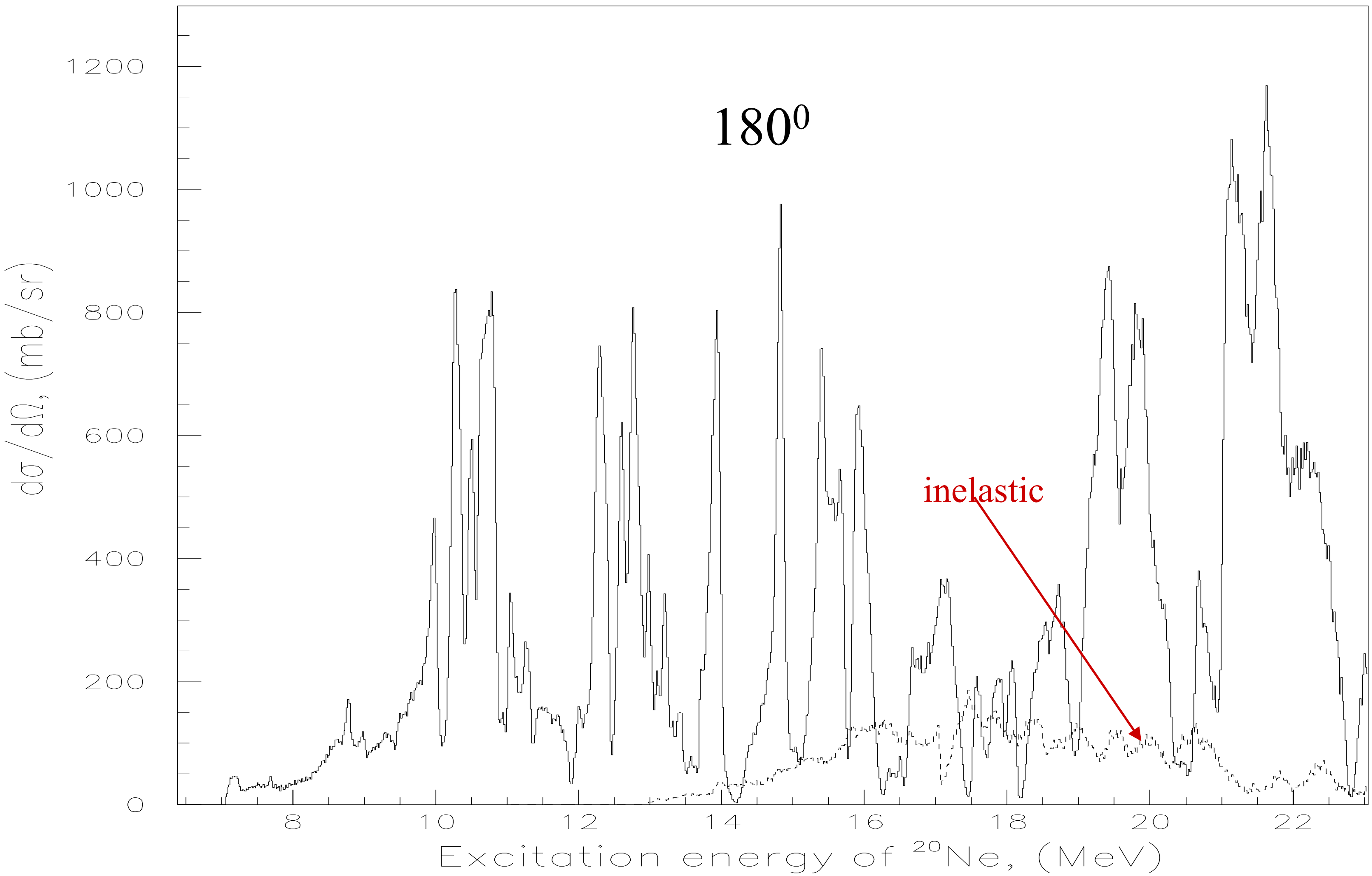

MARS

Momentum Achromat Recoil Separator

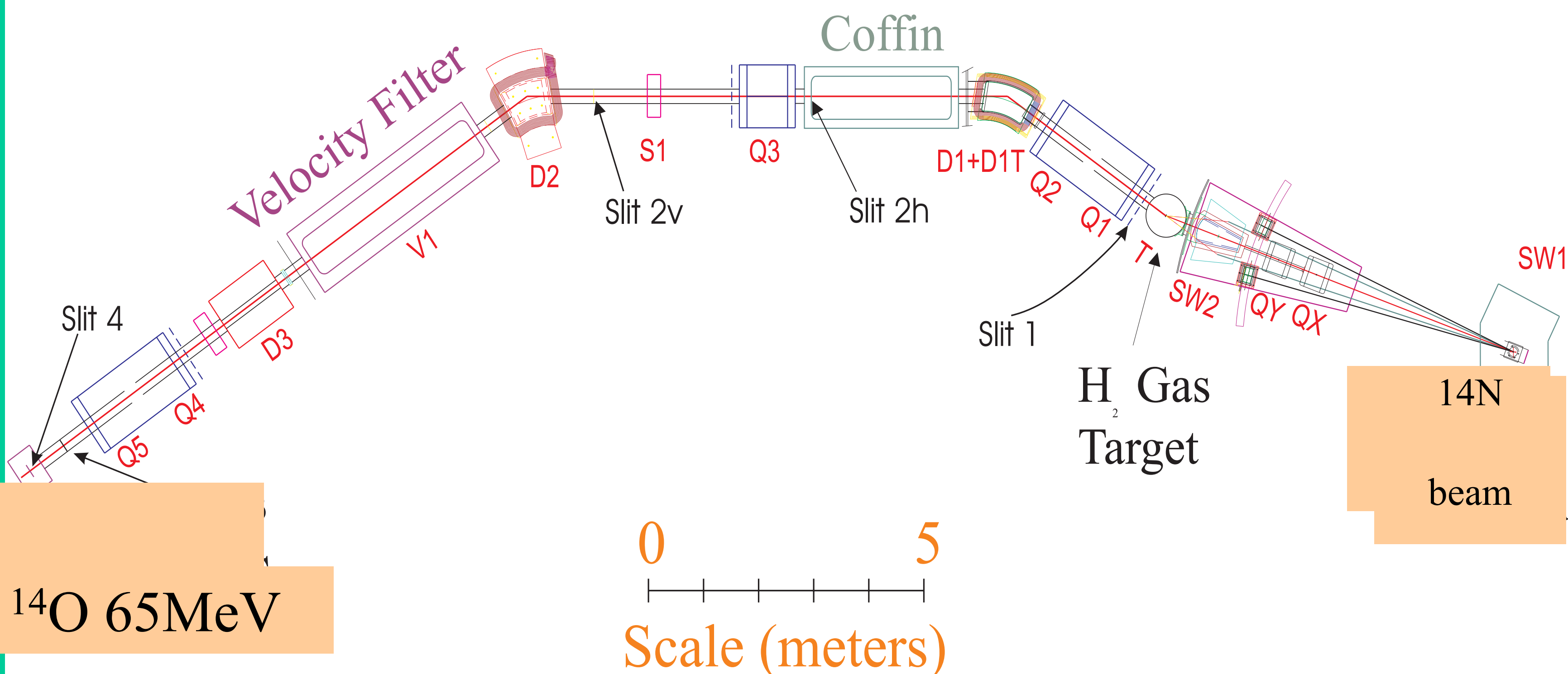

- **Primary beam ^{14}N@ 12 MeV/A – K500 Cyclotron**
- **Primary target LN_2 cooled gas target H_2 p=3.0 atm**
- **Secondary beam ^{14}O @ 4.5 MeV/A**

Purity: >99%
Intensity: ~10^6pps

Facility Layout

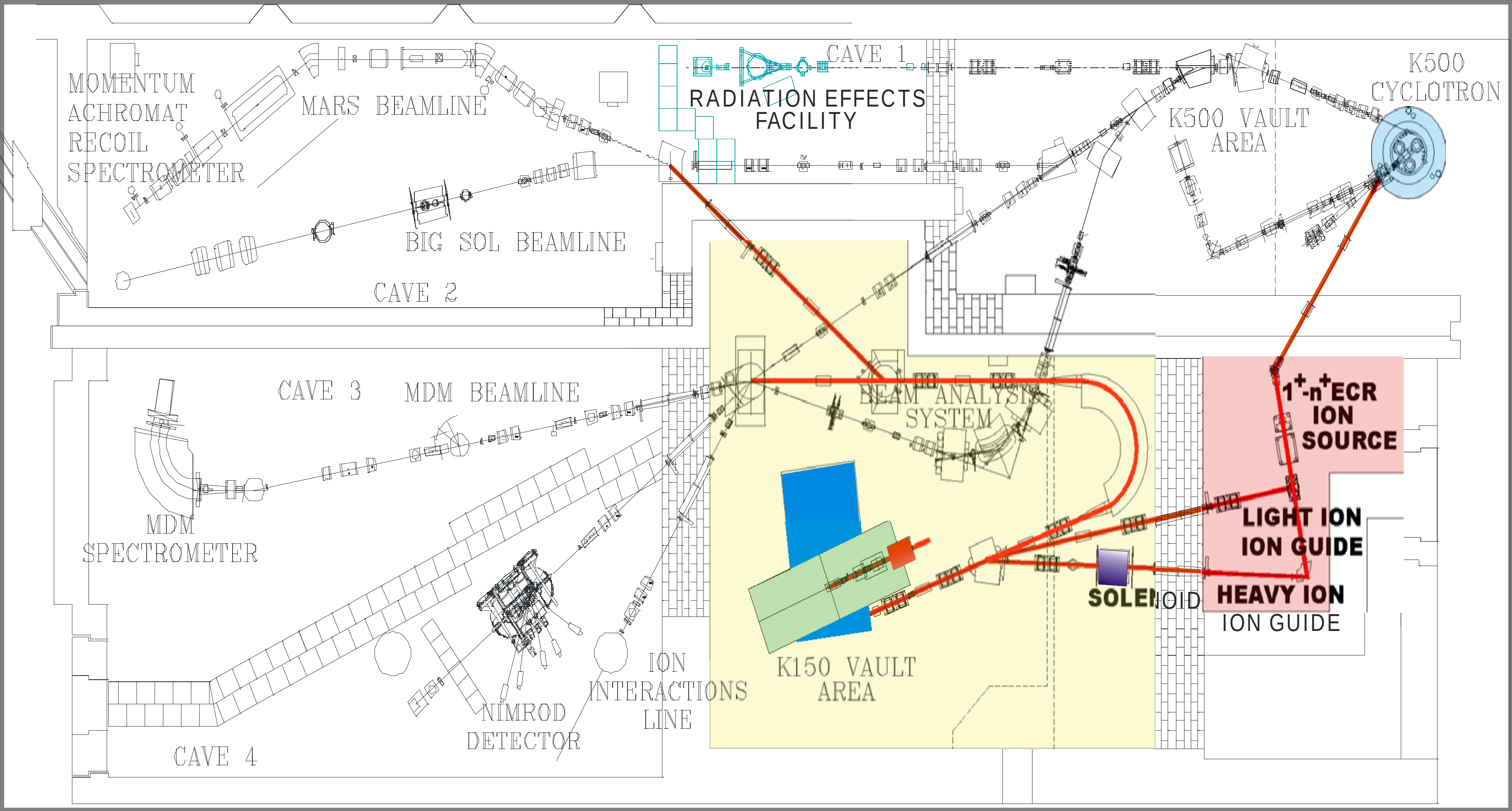

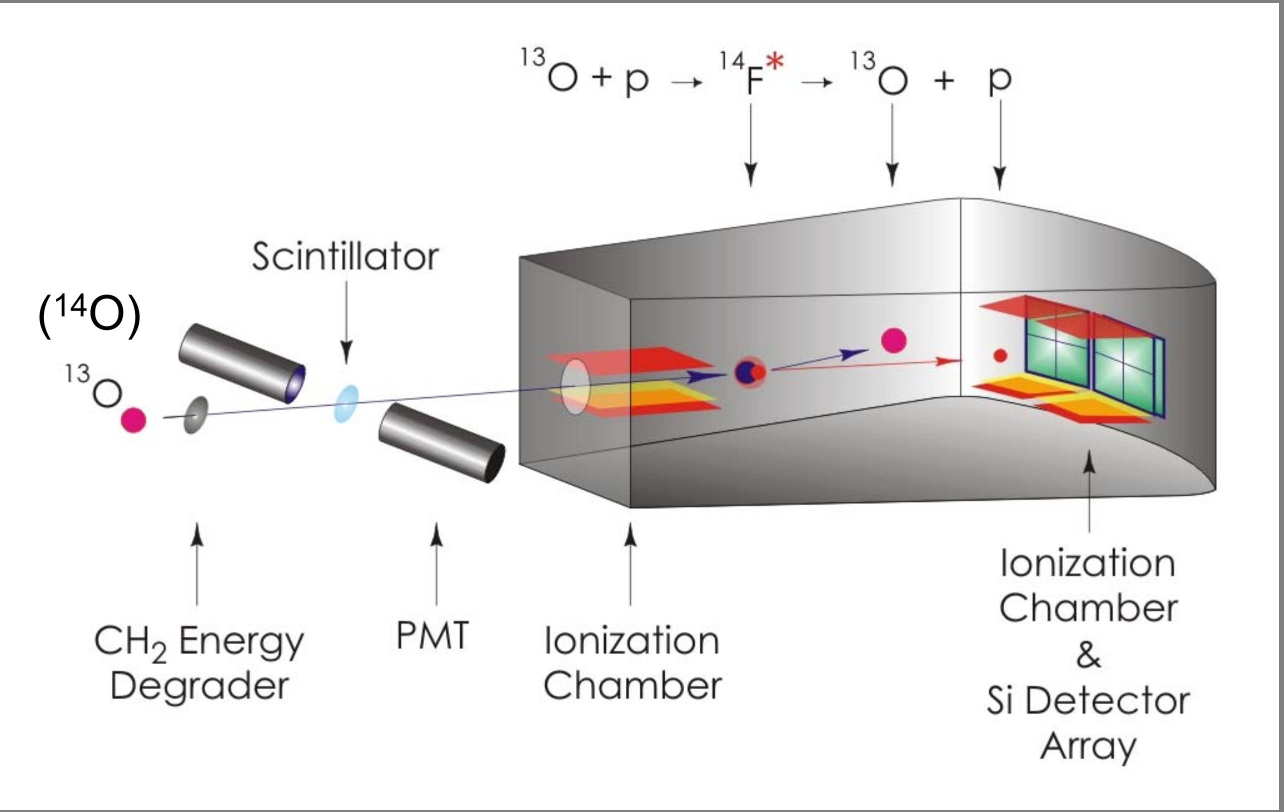

$^{13}O + p \rightarrow {}^{14}F^{*} \rightarrow {}^{13}O + p$
Scintillator
(^{14}O)
^{13}O
CH_2 Energy Degrader
PMT
Ionization Chamber
Ionization Chamber & Si Detector Array

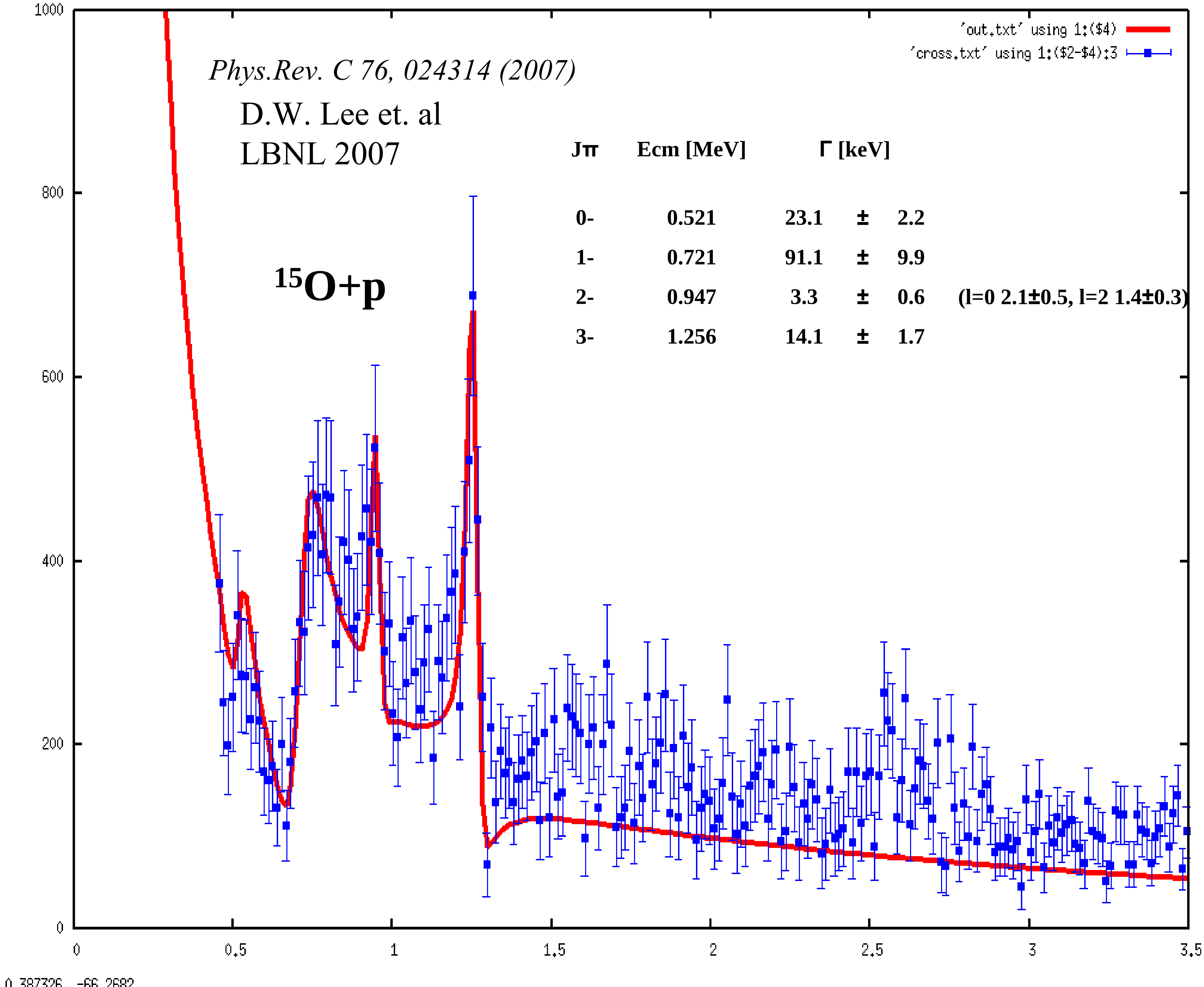

'out.txt' using 1:($4)
'cross.txt' using 1:($2-$4):3
Phys.Rev. C 76, 024314 (2007)
D.W. Lee et. al
LBNL 2007
Jπ Ecm [MeV] Γ [keV]
0- 0.521 23.1 ± 2.2
1- 0.721 91.1 ± 9.9
2- 0.947 3.3 ± 0.6 (l=0 2.1±0.5, l=2 1.4±0.3)
3- 1.256 14.1 ± 1.7
15O+p
1000
800
600
400
200
0
0
0.5
1
1.5
2
2.5
3
3.5
0.387326, -66.2682

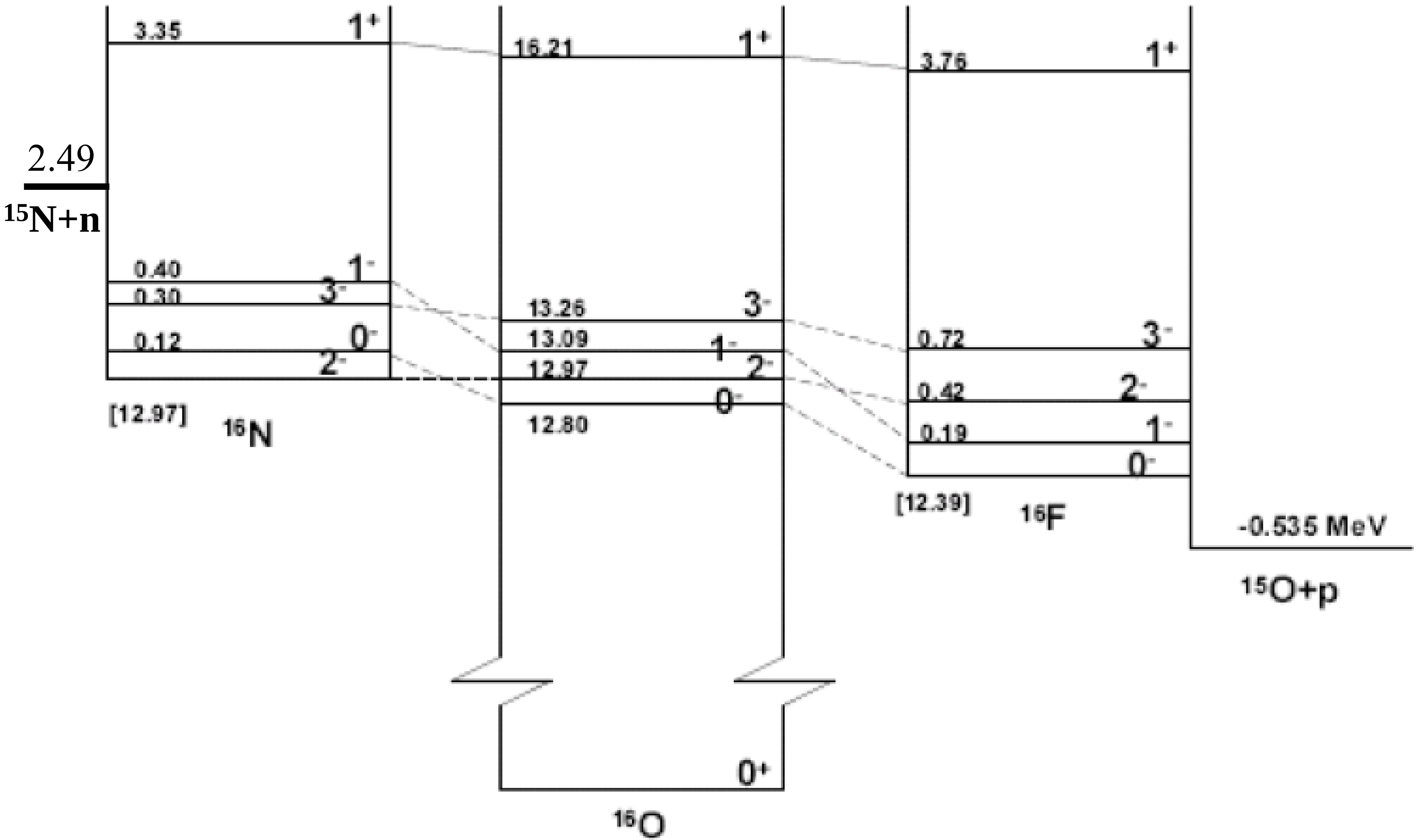

FIG. 1. An isobaric energy level diagram for the A=16, T=1 nuclear states

Table II. Comparison of ^{16}F experimental results with the isobaric analog states in ^{16}N and with theoretical calculations in the framework of the potential model.

^{16}N			^{16}F			^{16}F Theory			
						Parameter set #1 (a=0.65 fm)	Parameter set #2 (a=0.75 fm)		
Ex [MeV]	J^π	C^2S [a]	E_x [MeV±keV]	J^π	Γ_p[keV][b]	Γ_{sp}[keV]	Γ_{sp} [keV]	C^2S (Exp.)	C^2S (Shift)
0.120	0^-	0.95	0	0^-	23.1±2.2	21.8	22	1.05	0.91
0.397	1^-	0.96	0.190±20	1^-	91.1±9.9	89.5	96	0.95	0.88
0	2^-	0.93	0.422±19	2^-	3.3±0.6	3.6	4.3	0.77	
0.296	3^-	0.87	0.721±17	3^-	14.1±1.7	12.7	15.0	0.94	

[a] OXBASH calculation reported in Ref. [36].

[b] This work.

Problem of 7th nucleon

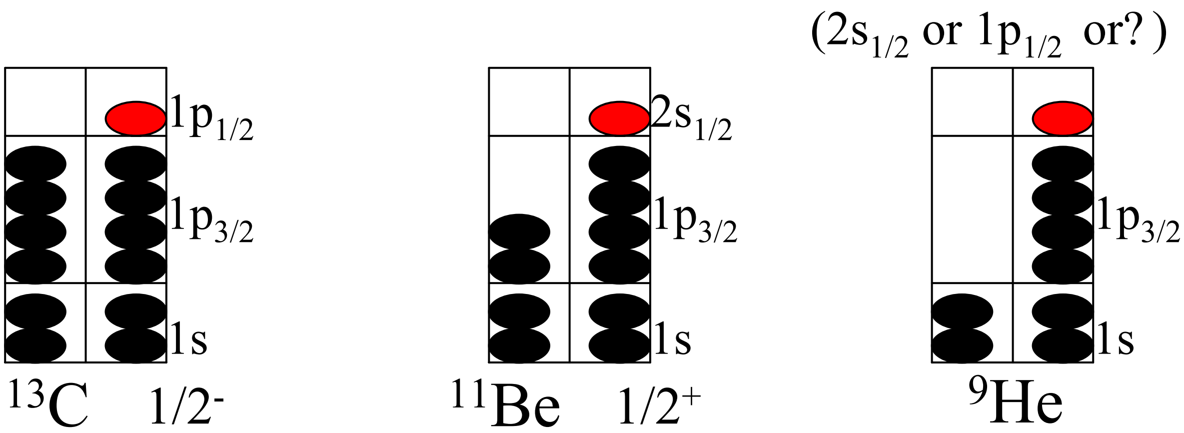

If our identifications are correct it is indeed remarkable that shell-model calculations whose parameters are optimized in the valley of stability should work so well so far from the valley

..since this nucleus is only produced in an exotic reaction.., it is rather unlikely that even the *L* transfers can be determined..

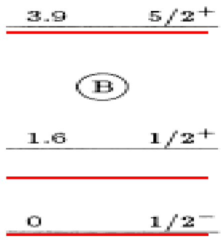

N.A.F.M. Poppelier et al., PL **157B**, 120 (1985)

Calculations

Experiment

Phys. Rev. C54 R1512 (1996)

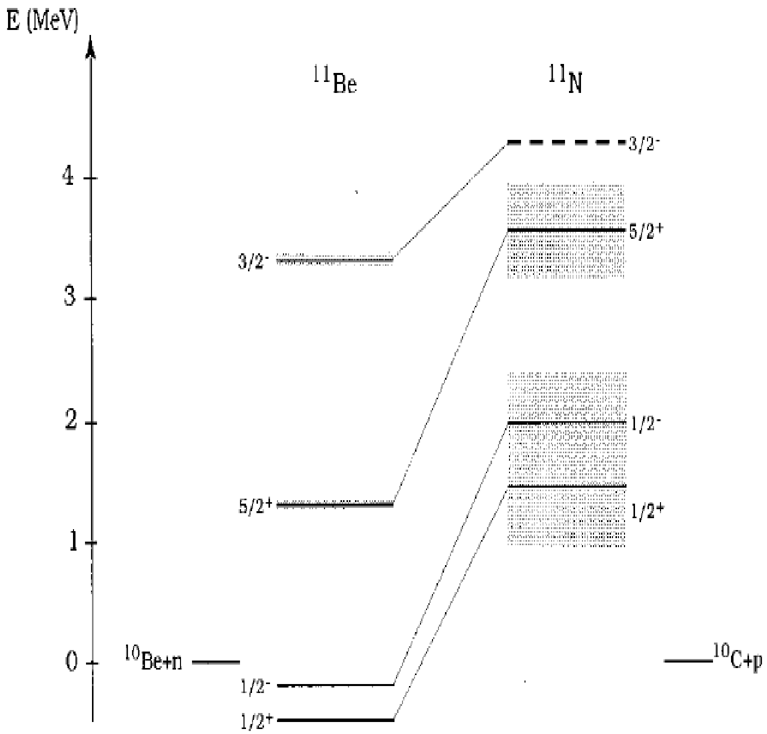

FIG. 4. The lowest energy levels for ^{11}Be and ^{11}N.

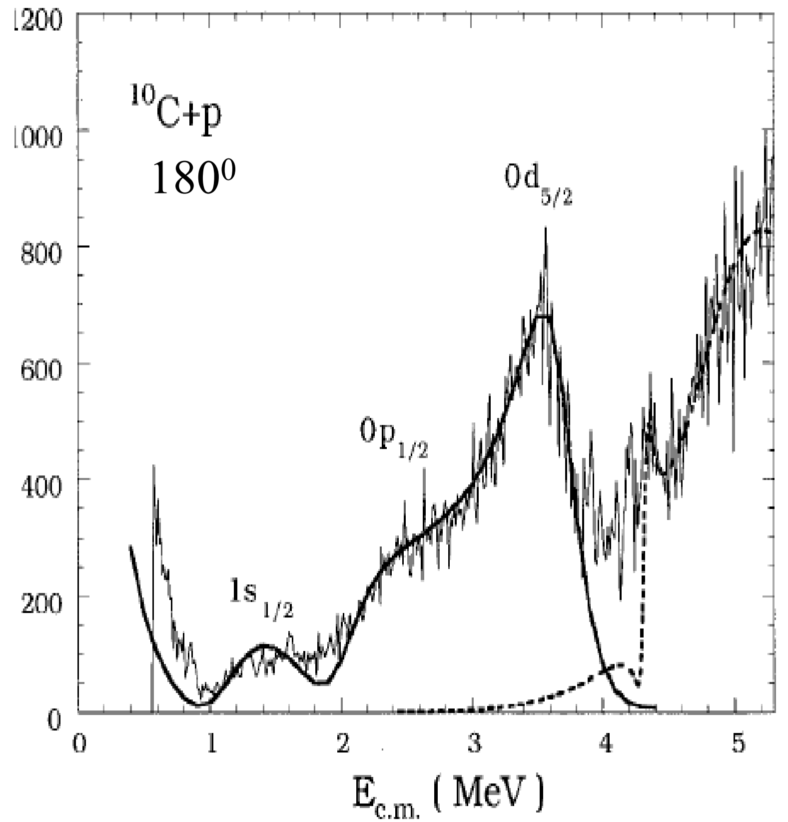

Excitation function for the ^{10}C+p elastic scattering

Shell model neutron binding energies versus the ratio of the diffuseness parameter to the radius of the potential.

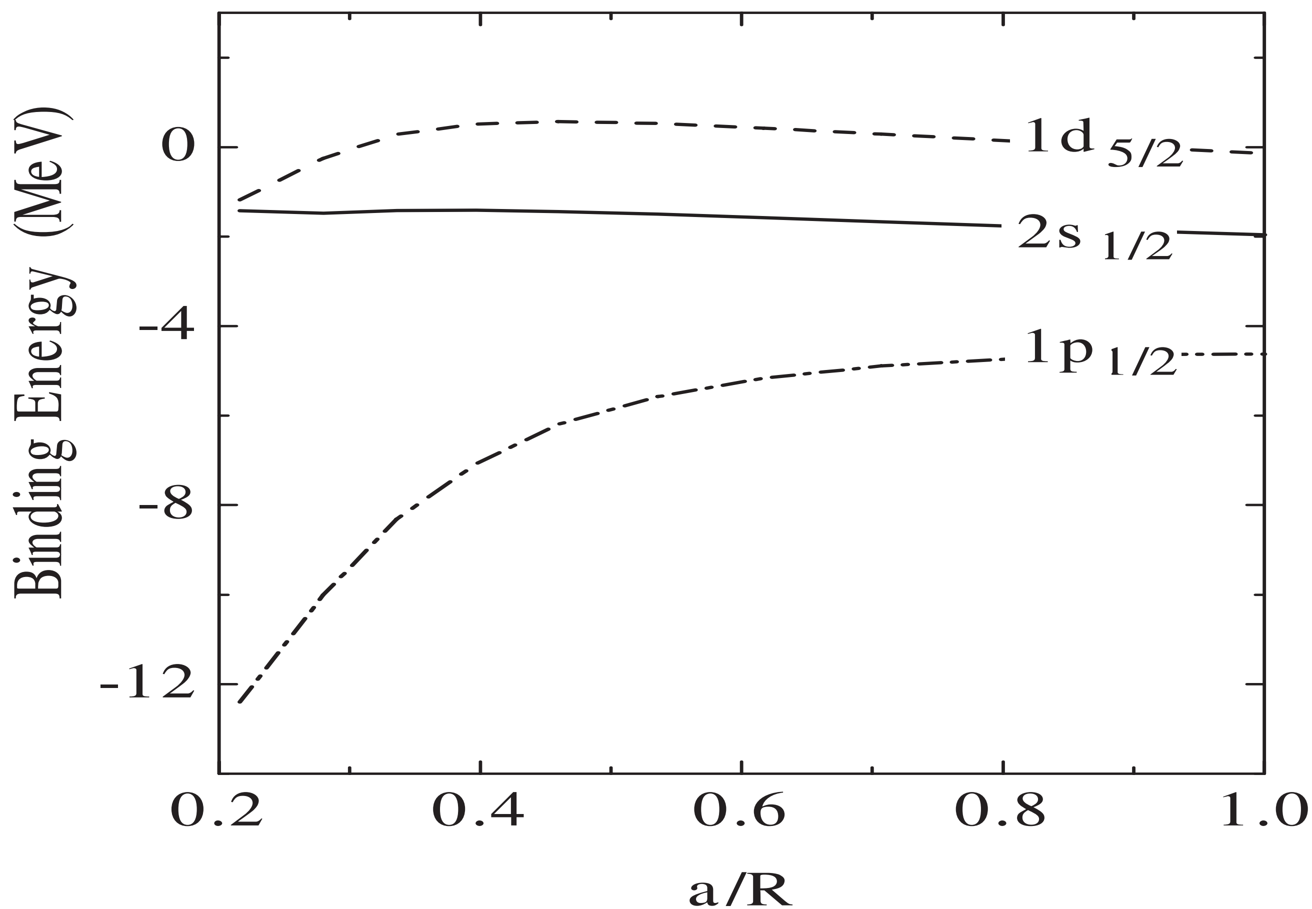

The calculations are made for a light nucleus (A=11), starting with typical parameters: V_0=-55 MeV; $V\ (ls)$=6 MeV; R=r_0A$^{1/3}$; $r_0 = r_0\ (ls)$=1.2 fm; $a = a\ (ls)$=0.6 fm, and keeping a + R=constant.

Single particle levels in A=15 and 17

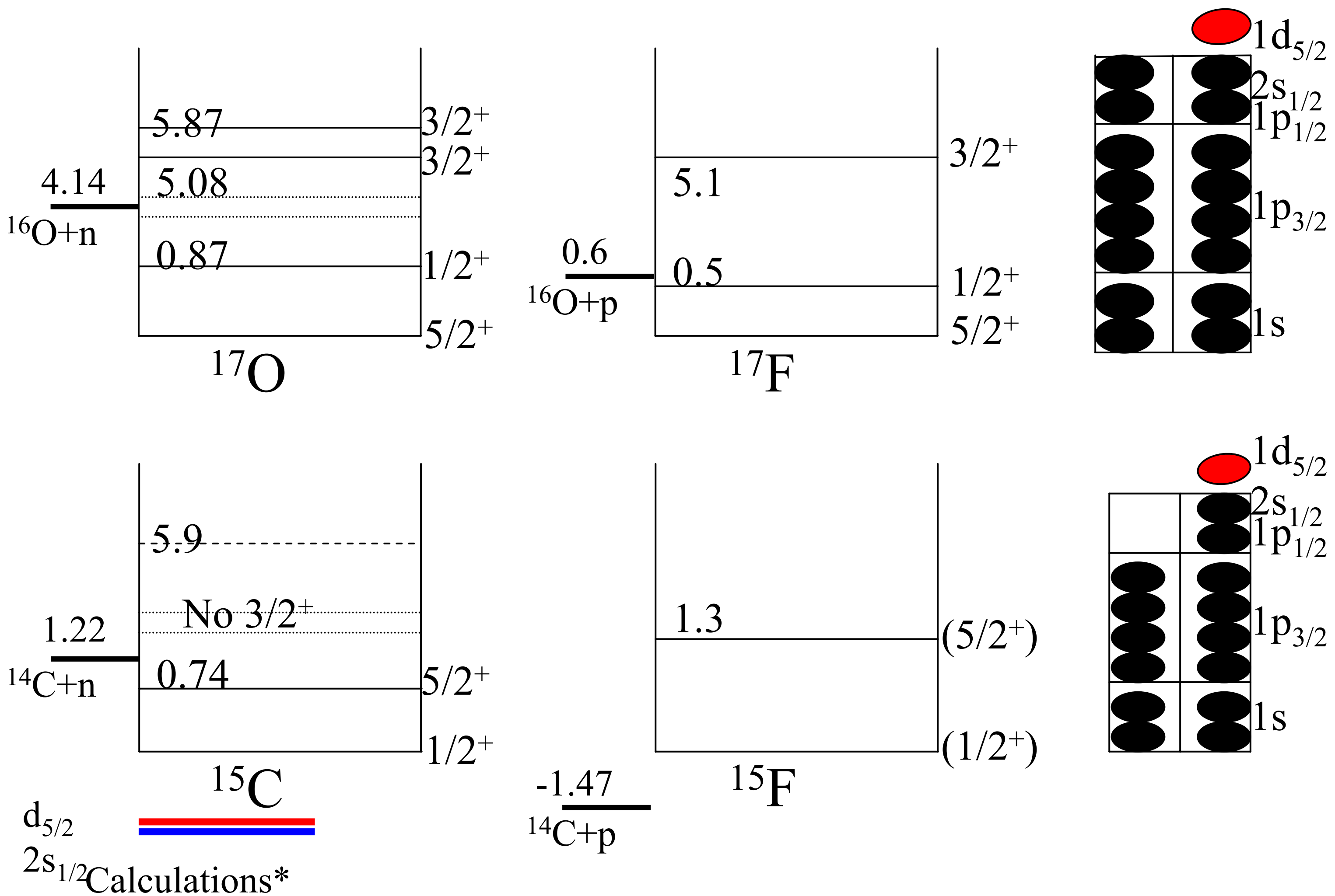

Excitation functions for ^{14}O+p elastic scattering

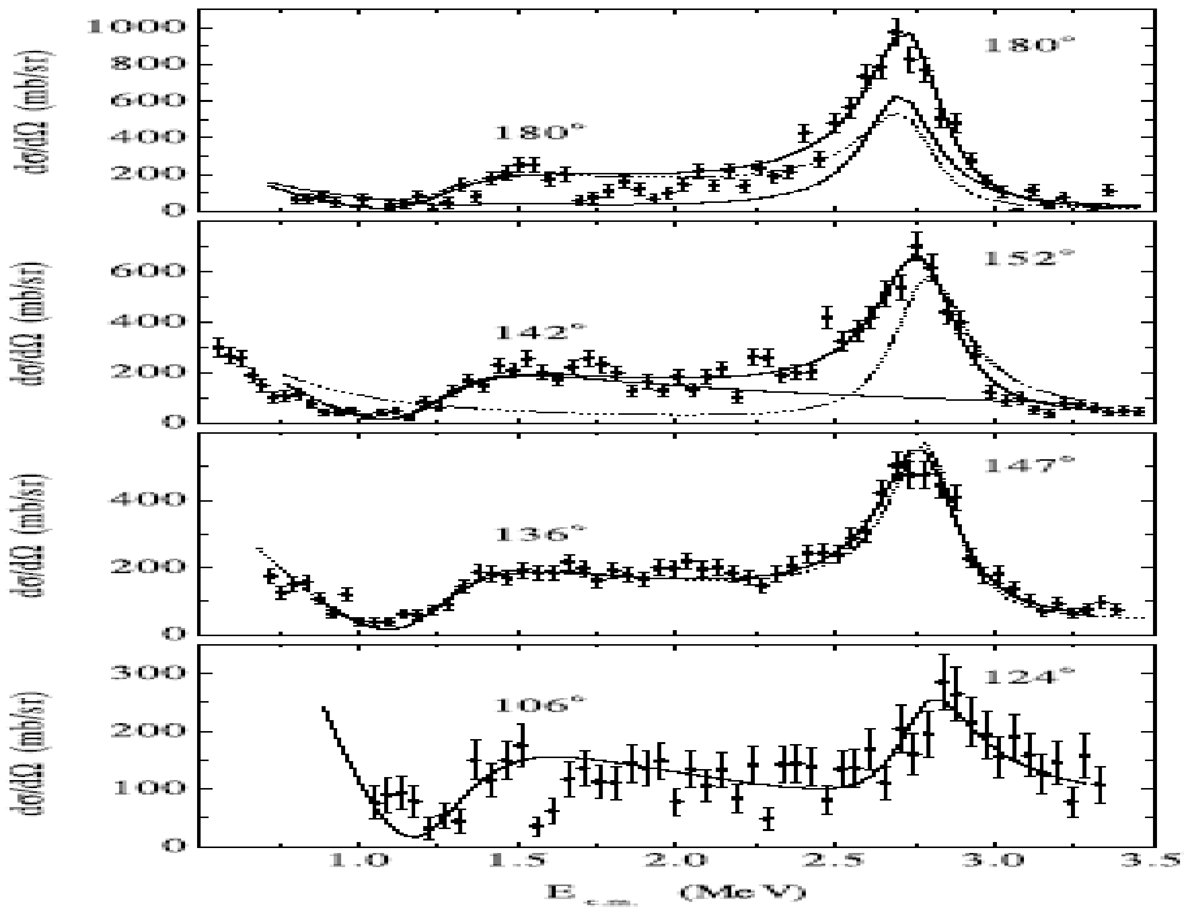

The solid lines are the final fits. The dotted curve in the upper panel shows the fit assuming a $1/2^+$ ground state and 3/2+ excited state. The dash-dotted curve shows the fit assuming a $1/2^+$ ground state and $5/2^+$ excited state. The second panel shows the separate contributions of s wave (dot-dashed line) and d wave (dotted line). The dashed line in the third panel shows the best fit which has a diffuseness parameter of 0.64 fm.

$^{18}Ne+p$, $\theta=180^0$ c.m.

Eur. Phys. J. A **24, 237 (2005)**

F. de Oliveira Santos *et al.*: Study of ^{19}Na at SPIRAL

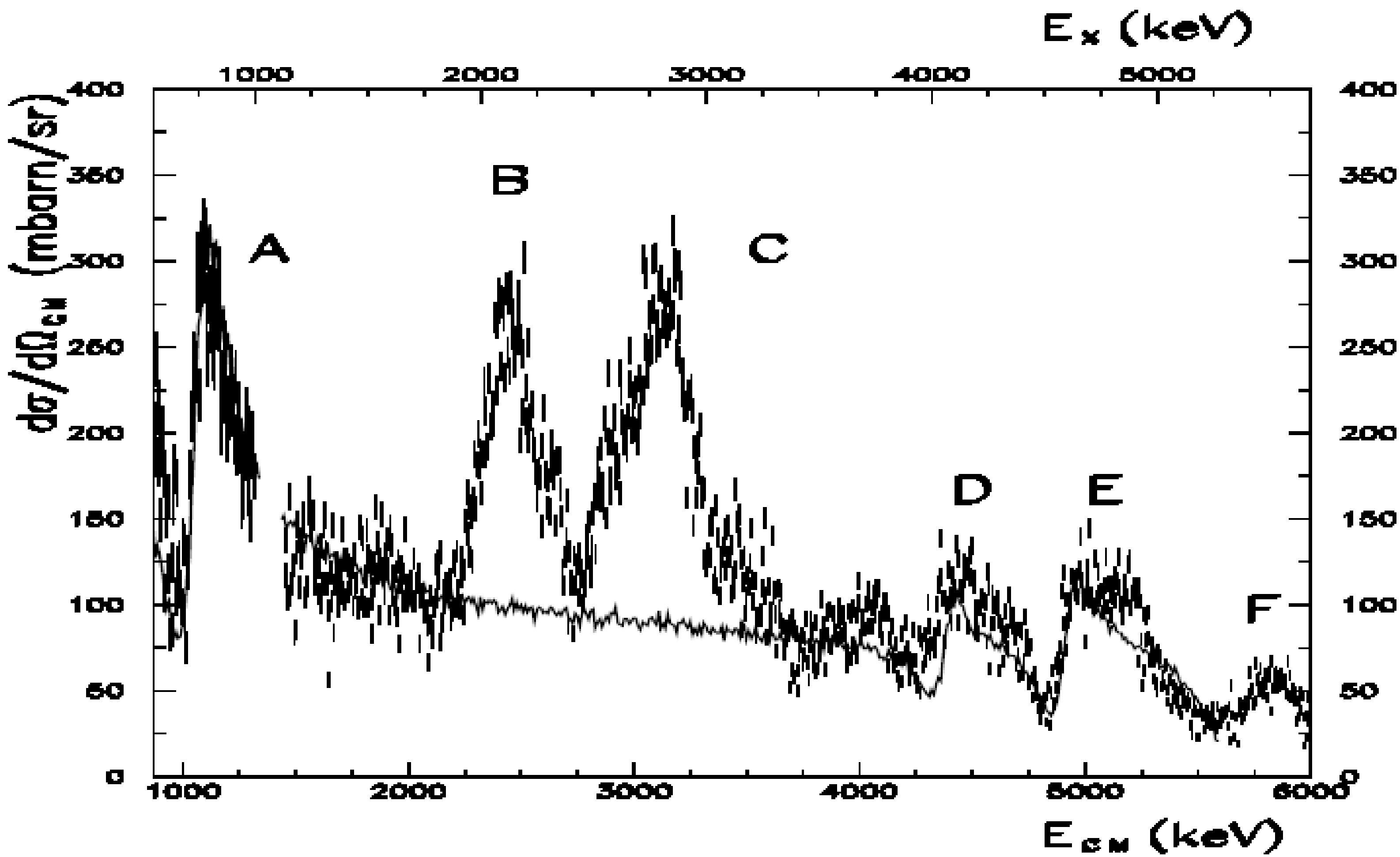

$^{14}O(\alpha,p)$

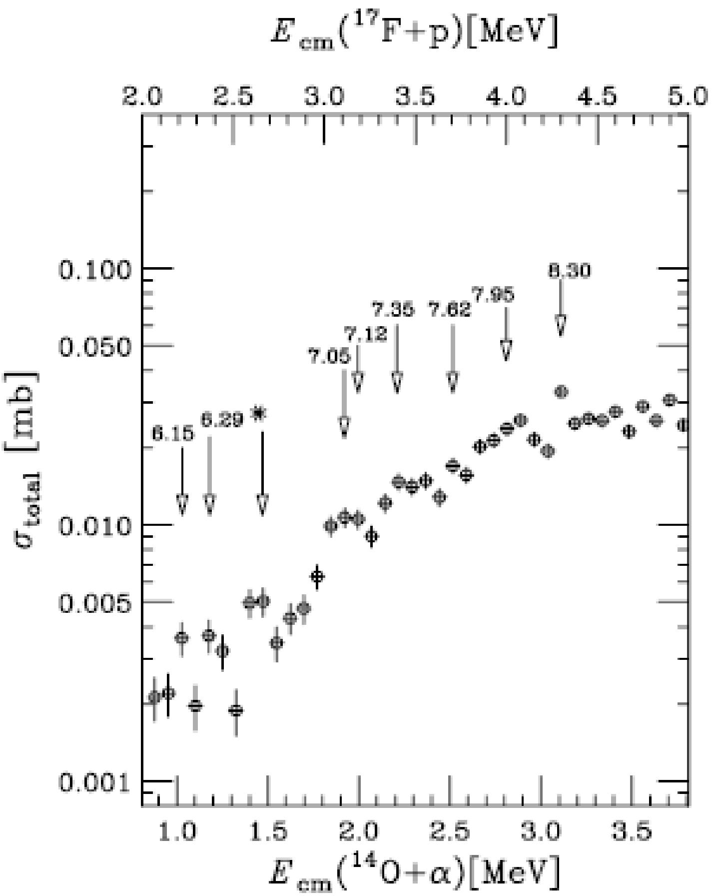

Figure 2. Measured cross sections for the $^{14}O(\alpha,p)^{17}F$ reaction. The asterisk mark is the new observation.

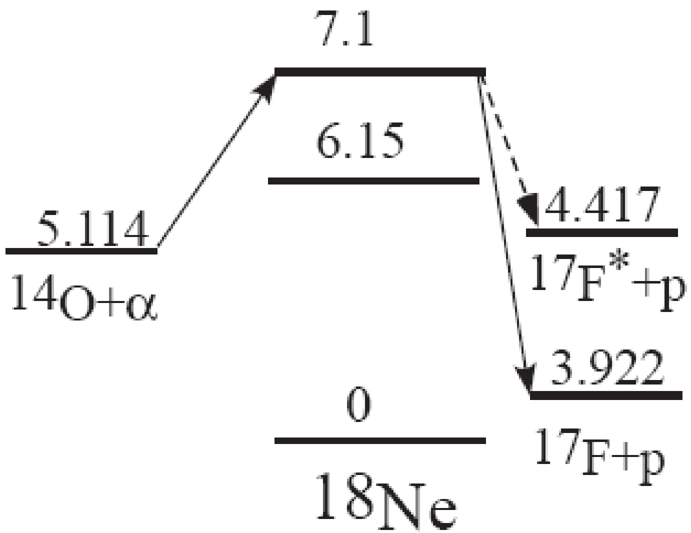

Figure 3. Level Scheme of ^{18}Ne. The dashed line arrow shows a transition to the excited state of ^{17}F.

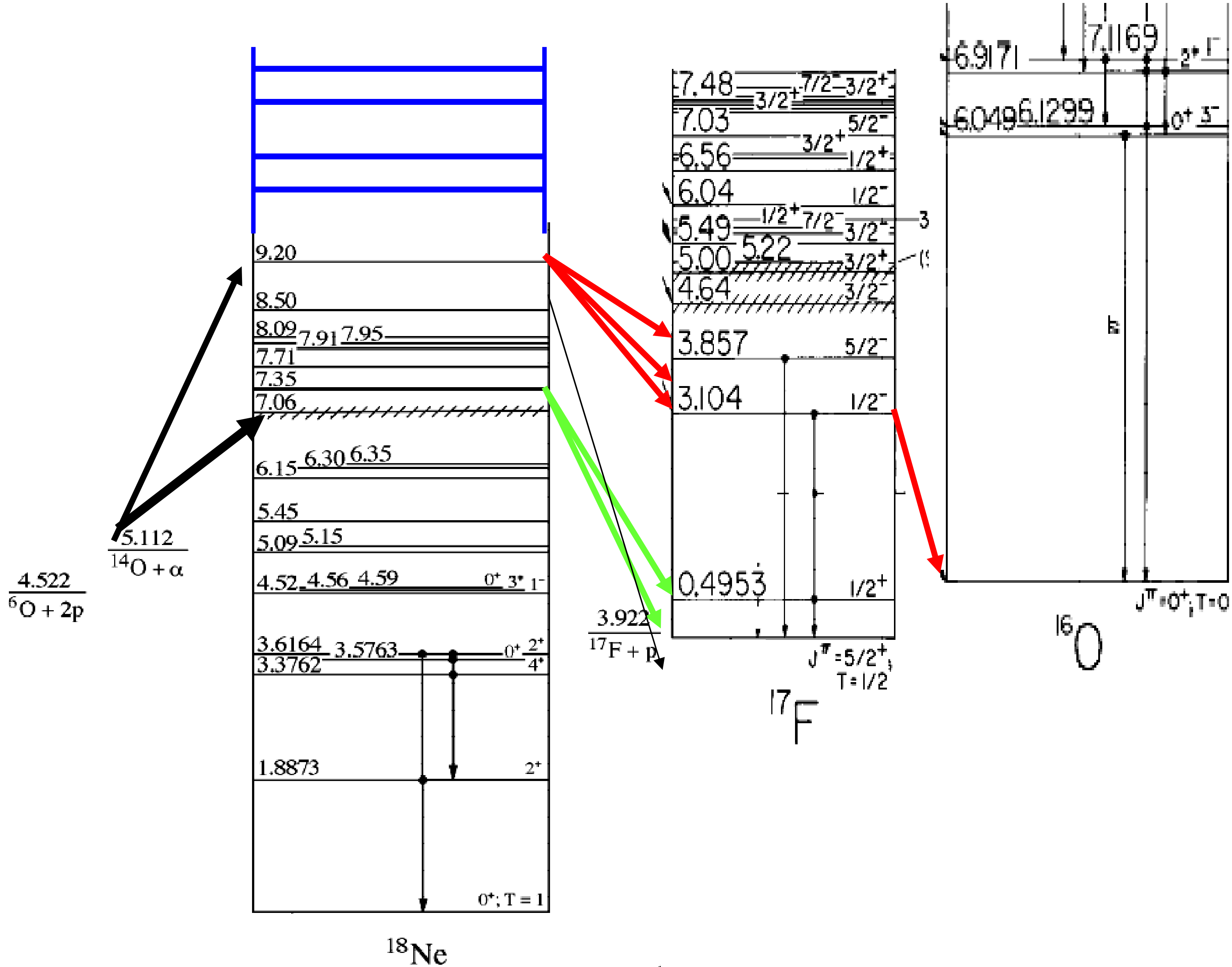

9.20
8.50
8.09 7.91 7.95
7.71
7.35
7.06
6.15 6.30 6.35
5.45
5.09 5.15
4.52 4.56 4.59 0+ 3+ 1−
3.6164 3.5763 0+ 2+
3.3762 4+
1.8873 2+
0+; T = 1
18Ne
5.112
14O + α
4.522
6O + 2p
3.922
17F + p
7.48 3/2+ 7/2− 3/2+
7.03 5/2−
6.56 3/2+ 1/2+
6.04 1/2−
5.49 1/2+ 7/2− 3/2+
5.00 5.22 3/2+
4.64 3/2−
3.857 5/2−
3.104 1/2−
0.4953 1/2+
Jπ=5/2+; T=1/2
17F
6.9171 7.1169 2+ 1−
6.049 6.1299 0+ 3−
Jπ=0+; T=0
16O

Excitation function for the $^{14}O(\alpha,2p)$ reaction

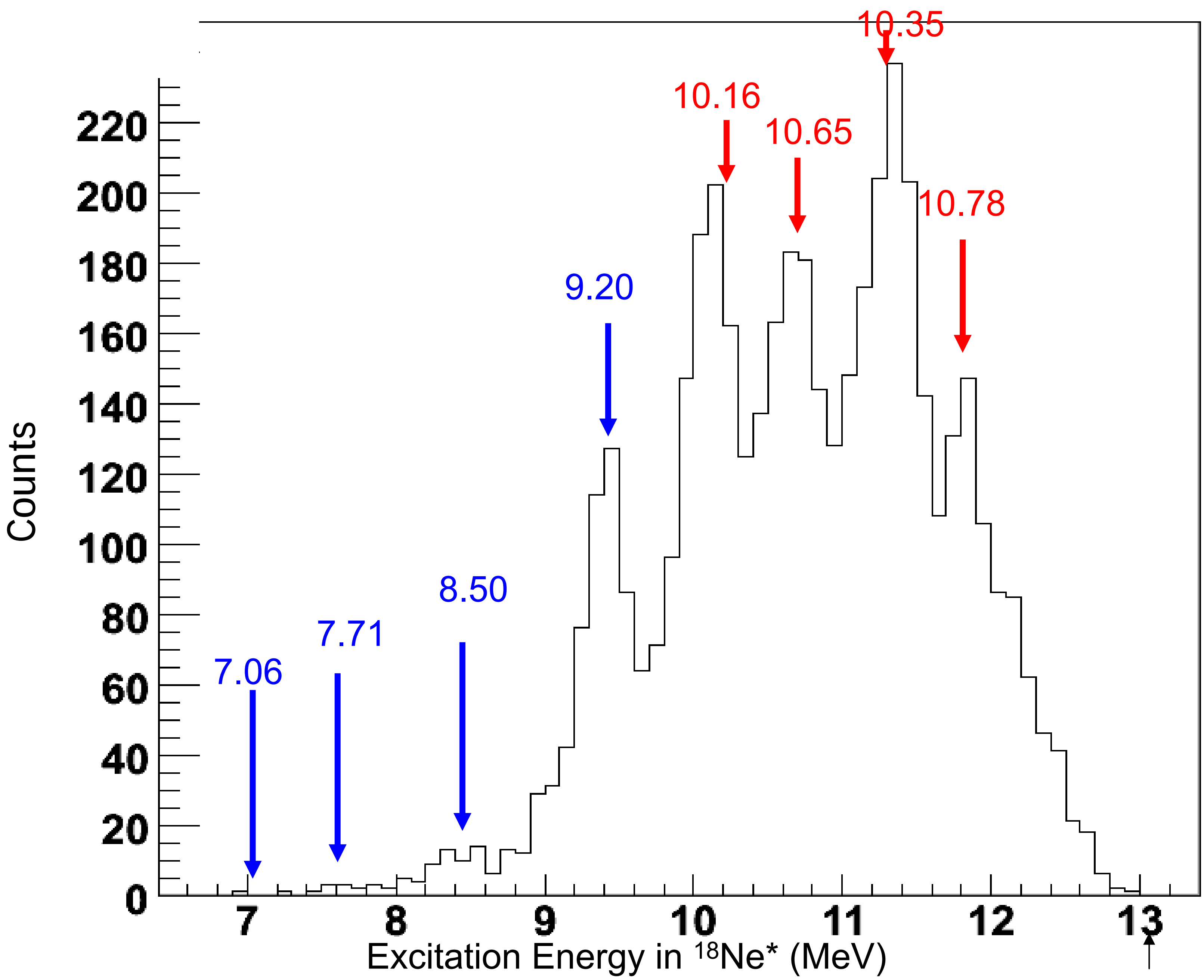

Bad News T=3/2 and T=1/2 states can be populated

$$^{12}B+p \rightarrow {}^{13}C \;<\; \begin{array}{ll} T=3/2 & 1 \\ T=1/2 & 2 \end{array}$$

(isobaranalogs of ^{13}O and ^{13}B)

T= 1 1/2

Good News More than 10 decay channels are open for the T=1/2 states.

If everything OK, how to take into account the T=1/2 channel? By using classical R-matrix?

$$\sigma=(A_{\text{hard sphere}}+A_{\text{Resonance}})^2 \quad ??$$

A= 13 isobar diagram

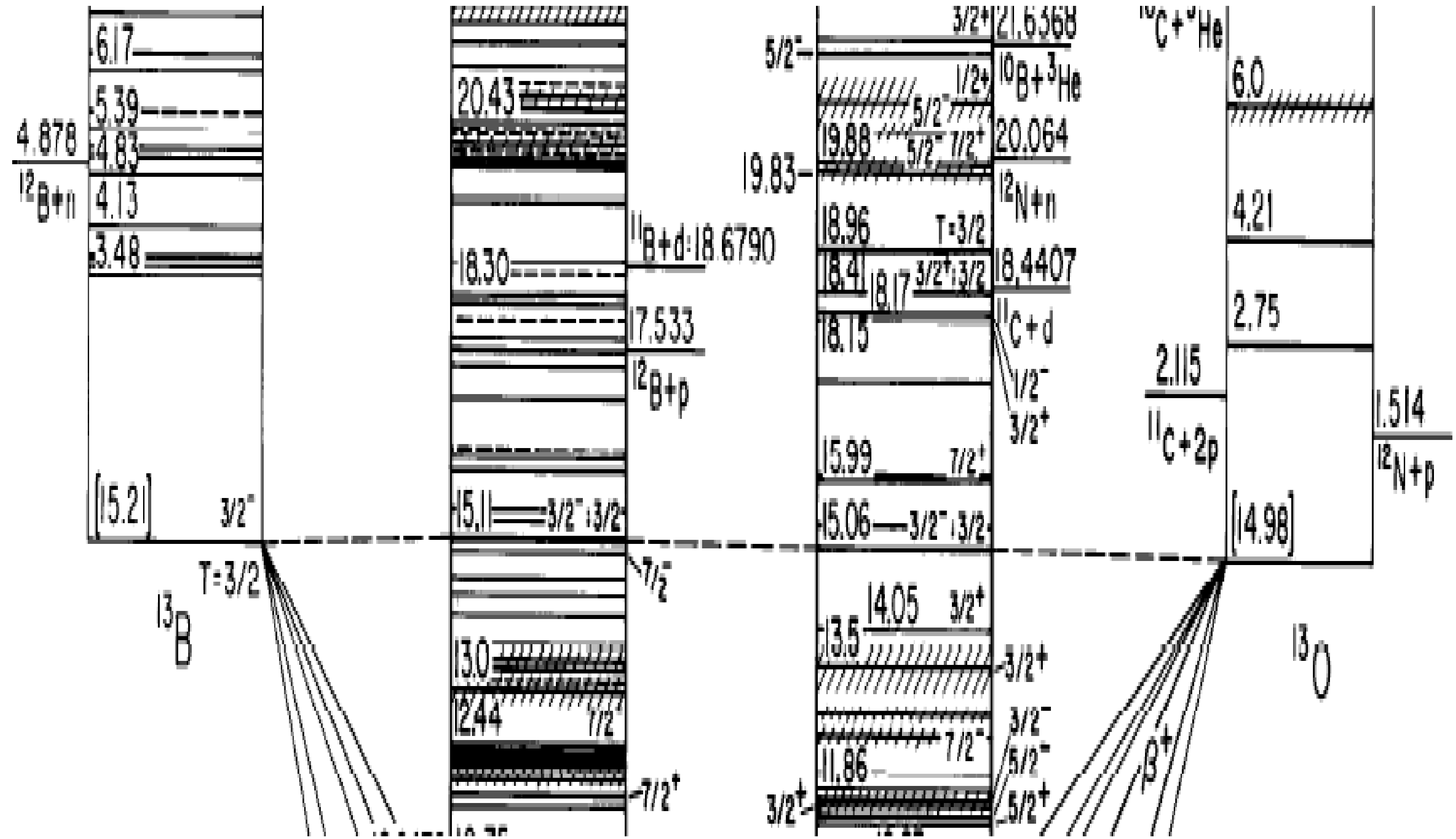

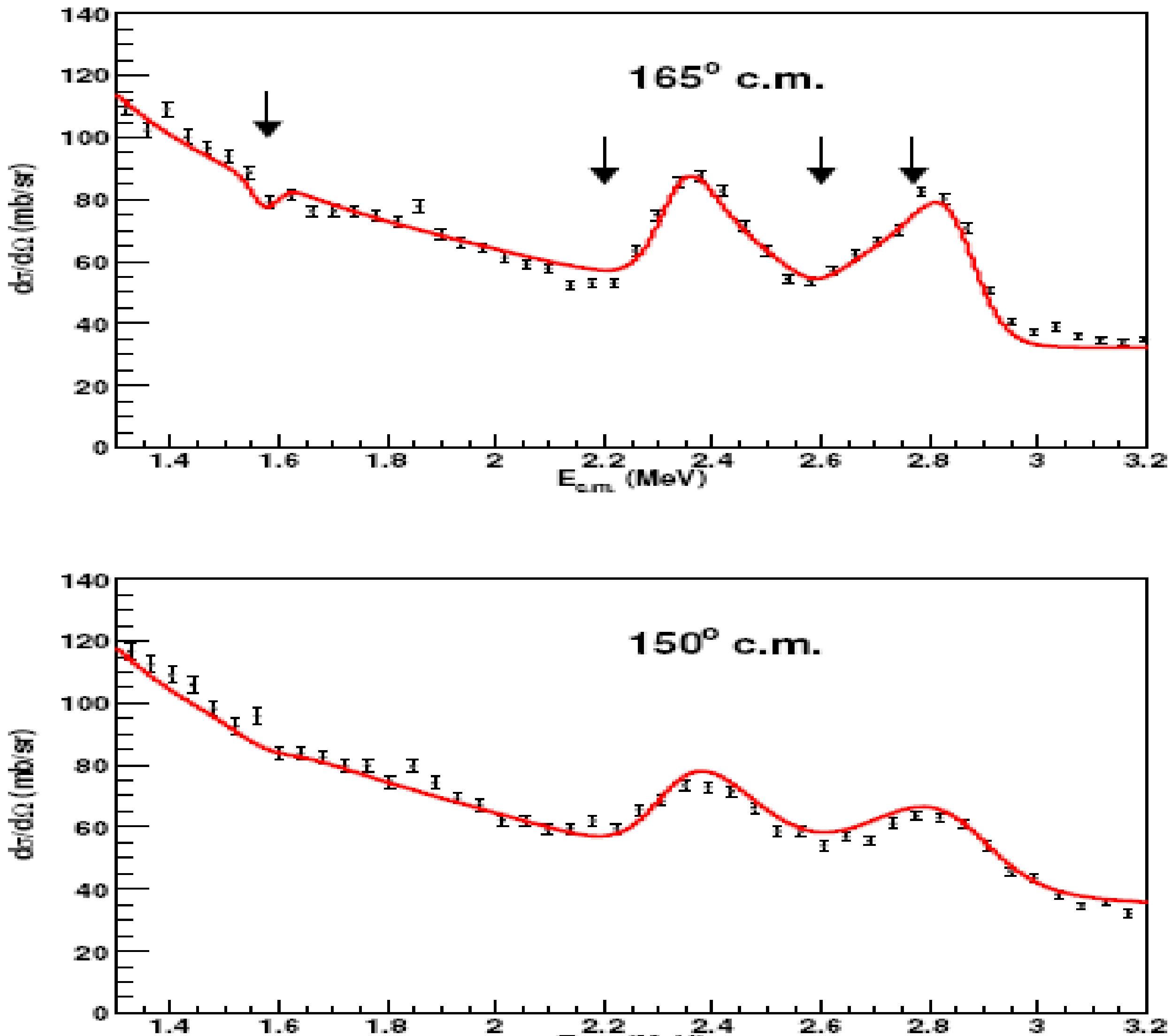

Figure 6: Excitation functions for ^{12}B+p elastic scattering measured at 165° and 150°in (c.m.). The solid line represents the best R-matrix fit which includes six T=3/2 resonances and the absorption phase shift (see text). Arrows on the top figure indicate excitation energies of the high-lying resonances. The R-matrix fit was convoluted with the experimental resolution function.

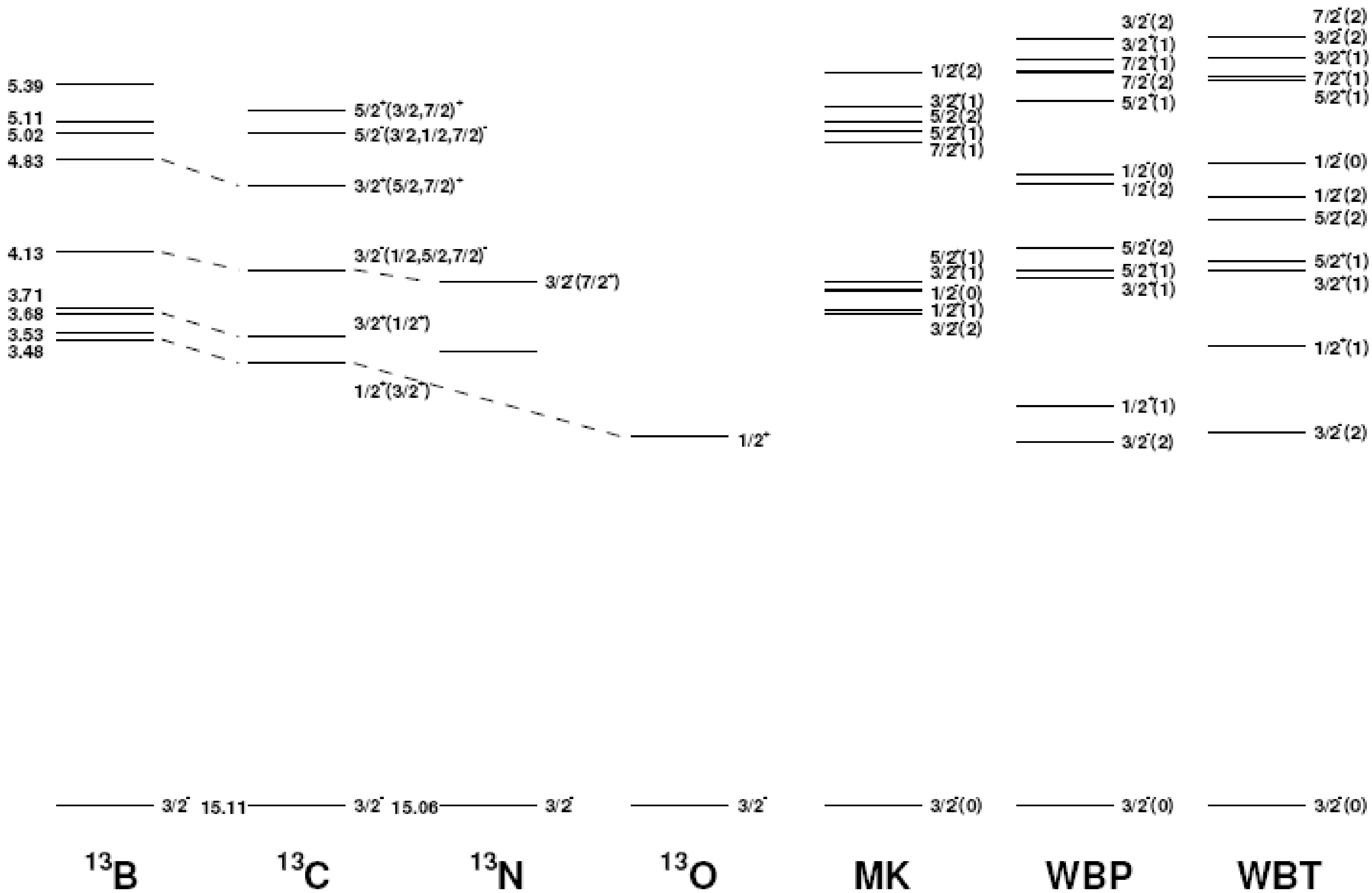

Figure 7: The T=3/2, A=13 isobaric chain. Numbers shown in parentheses after the spins in the shell-model calculations are $\hbar\omega$. Only those T=3/2 states that were observed in the present work are shown for ^{13}C.

α-cluster structure in light N≠Z nuclei

Historically the α-particle (nucleus of helium atom) model of the atomic nucleus was the first leading model of nuclear structure

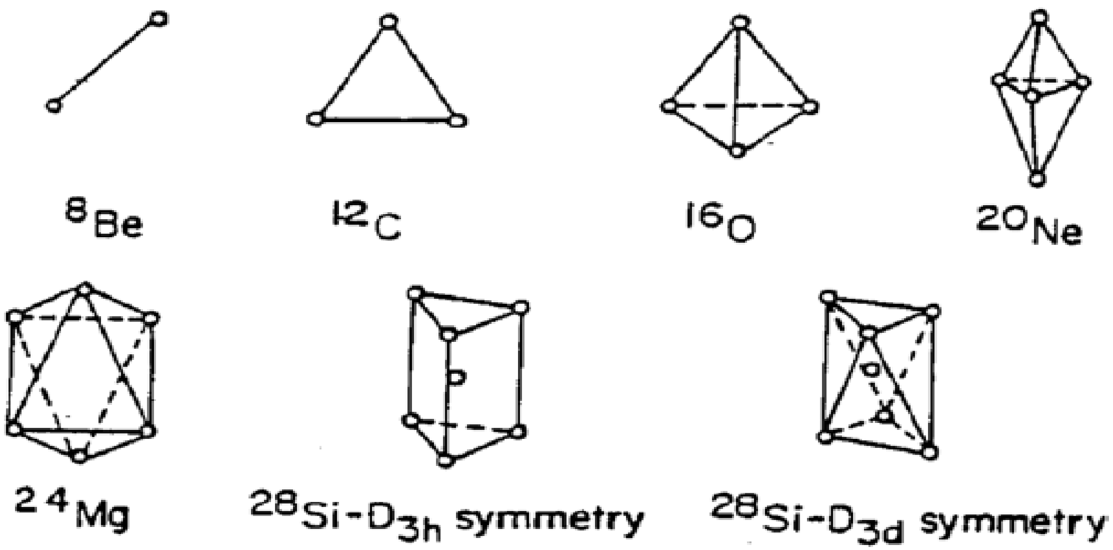

Figure 5. Geometric α-particle structures predicted by Brink [63]. Note that the arrangements reflect the number of possible bonds between α-particles predicted by Hafstad and Teller [5].

Martin Freer
Rep. Prog. Phys. **70** (2007) 2149

Later the α clusters (correlated motion of two protons and two neutrons with zero spin) were introduced…

α-cluster structure in light N=Z nuclei

The single particle limit for the resonance width, $\Gamma_w \sim \hbar^2/\mu R^2$ represents the maximum single particle reduced width (without antisymmetrization) for a particle (with reduced mass, μ.) in a nuclear potential with radius R.

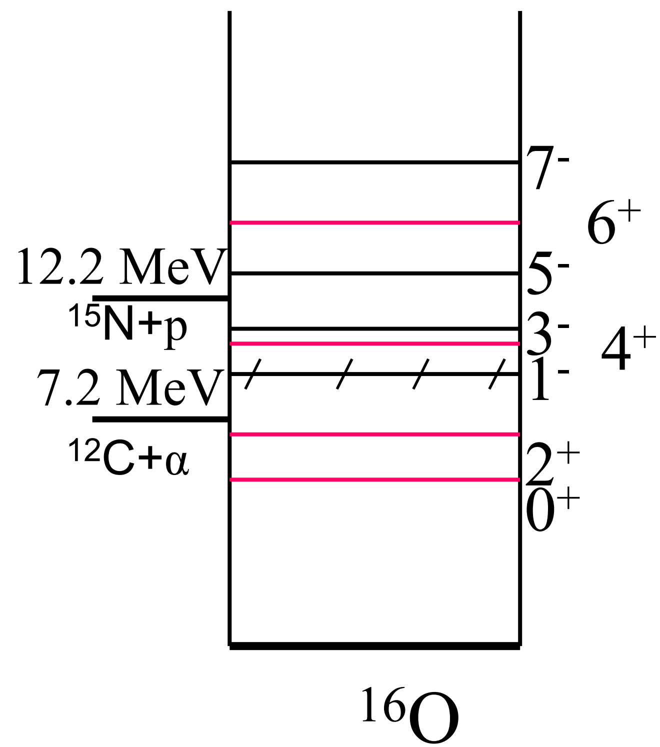

The Wigner Limit, $\sim\hbar^2/\mu R^2$, is an estimation of the maximum reduced width a particle (with reduced mass μ) can have (without antisymmetrysation) in a potential of radius R.

W. L. ~ 1 MeV for the α widths in the light nuclei

W. L. ~ 4 MeV for the nucleon widths in the light nuclei

Time of flight of 1 MeV n through a nucleus corresponds to ~ 6 MeV

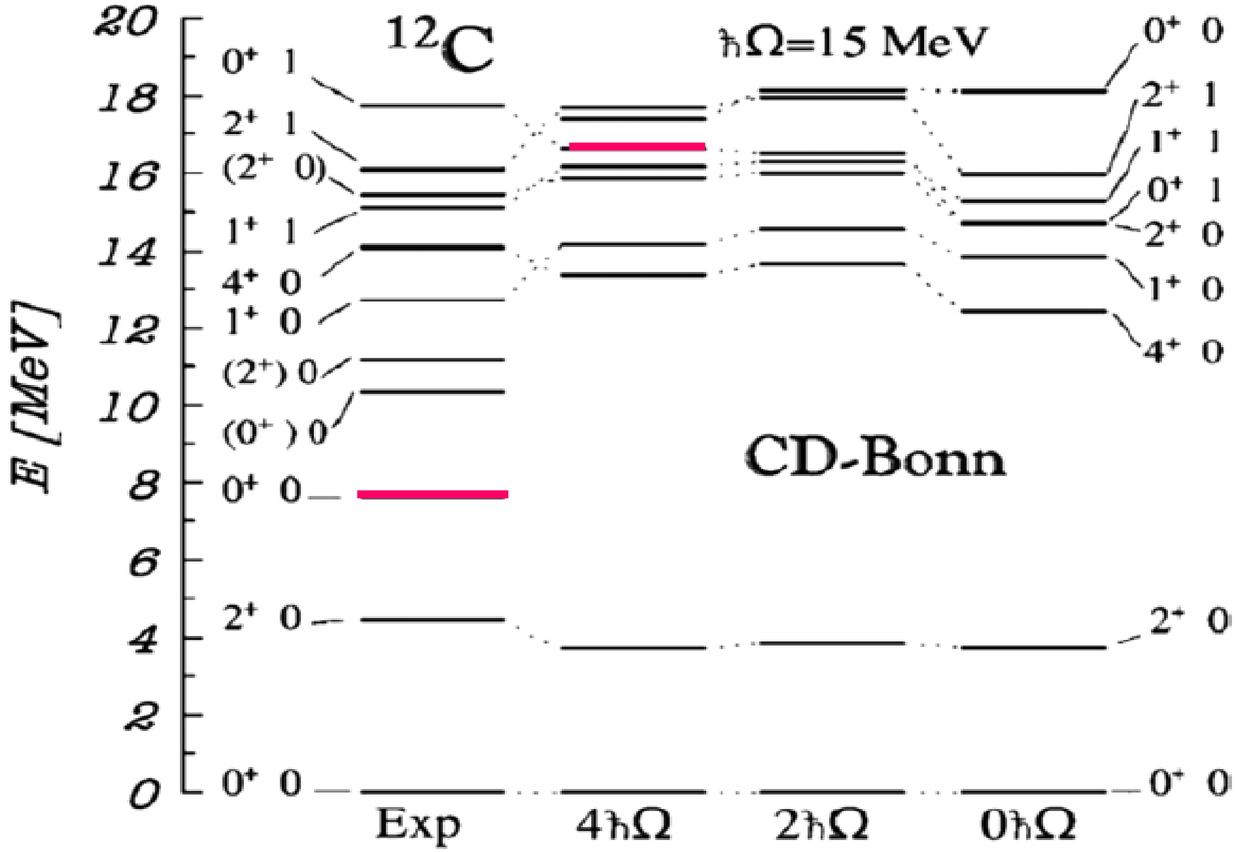

The no core shell-model calculations for the nucleus ^{12}C. The left hand part of the figure shows the experimental results. The calculations using the CD Bonn *N–N* interaction with increasing numbers of oscillator orbits are shown on the right.

1. THE SURFACE POTENTIAL MODEL

The simplest way to analyze the principal consequences of a surface potential model is to consider a potential that satisfies the boundary conditions $\Psi_\alpha(R) = 0$ and $\Psi_\alpha(R - \Delta R) = 0$, where R is the radius of the nucleus and ΔR is the thickness of the surface layer, i.e., a potential that confines the particle to a spherical surface layer of thickness ΔR.

The energy eigenvalues for the case $\Delta R \ll R$ can be easily found:

$$E = \frac{n^2 \pi^2 \hbar^2}{2\mu(\Delta R)^2} + \frac{\hbar^2 l(l+1)}{2\mu R^2}, \qquad (1)$$

where μ is the reduced mass. Of course it is the 0^+

V. Z. Gol'dberg, V. P. Rudakov, and V. A. Timofeev
I. V. Kurchatov Atomic Energy Institute
(Submitted June 19, 1973)
Yad. Fiz. 19, 503–515 (March 1974)

What is inside ?

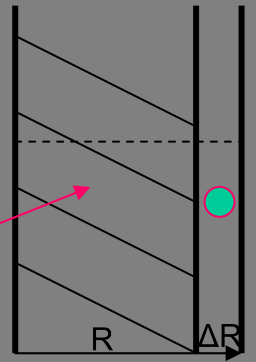

The number of nodes N for the radial wave functions are calculated by the harmonic-oscillator relations as
2N + L = Σ(2ni+ li),
where L is the angular momentum of the cluster, while ni and li the corresponding shell model numbers for nucleons

^{10}Be (α+^{6}He)

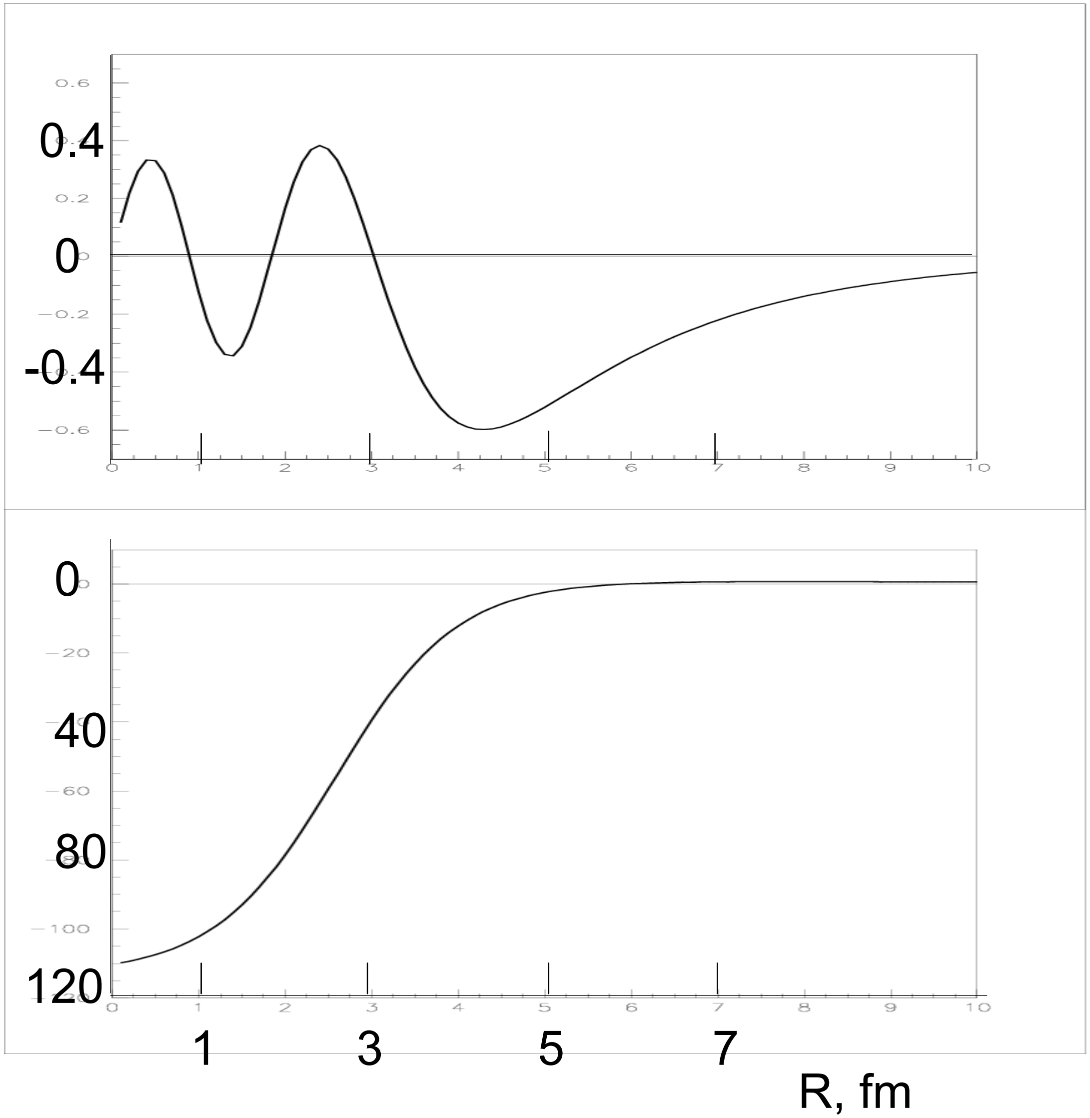

α+^{6}He wave function in a potential well with forbidden states

Potential parameters
R=2.58 fm; a=0.7 fm; V_0=-116.8 MeV

How to obtain from experiment data on the shell/cluster degree of freedom relationship

1. Single nucleon transfer reactions- relatively difficult, small cross section [^{15}N(d,n) Bohne et al., NP A196, 41 (1973)]
2. Nucleon decay of the α-cluster states in N=Z nuclei-very difficult

Are there α-cluster states in N≠Z nuclei?
What is interplay between the shell model (nucleon) and α-cluster structure ?

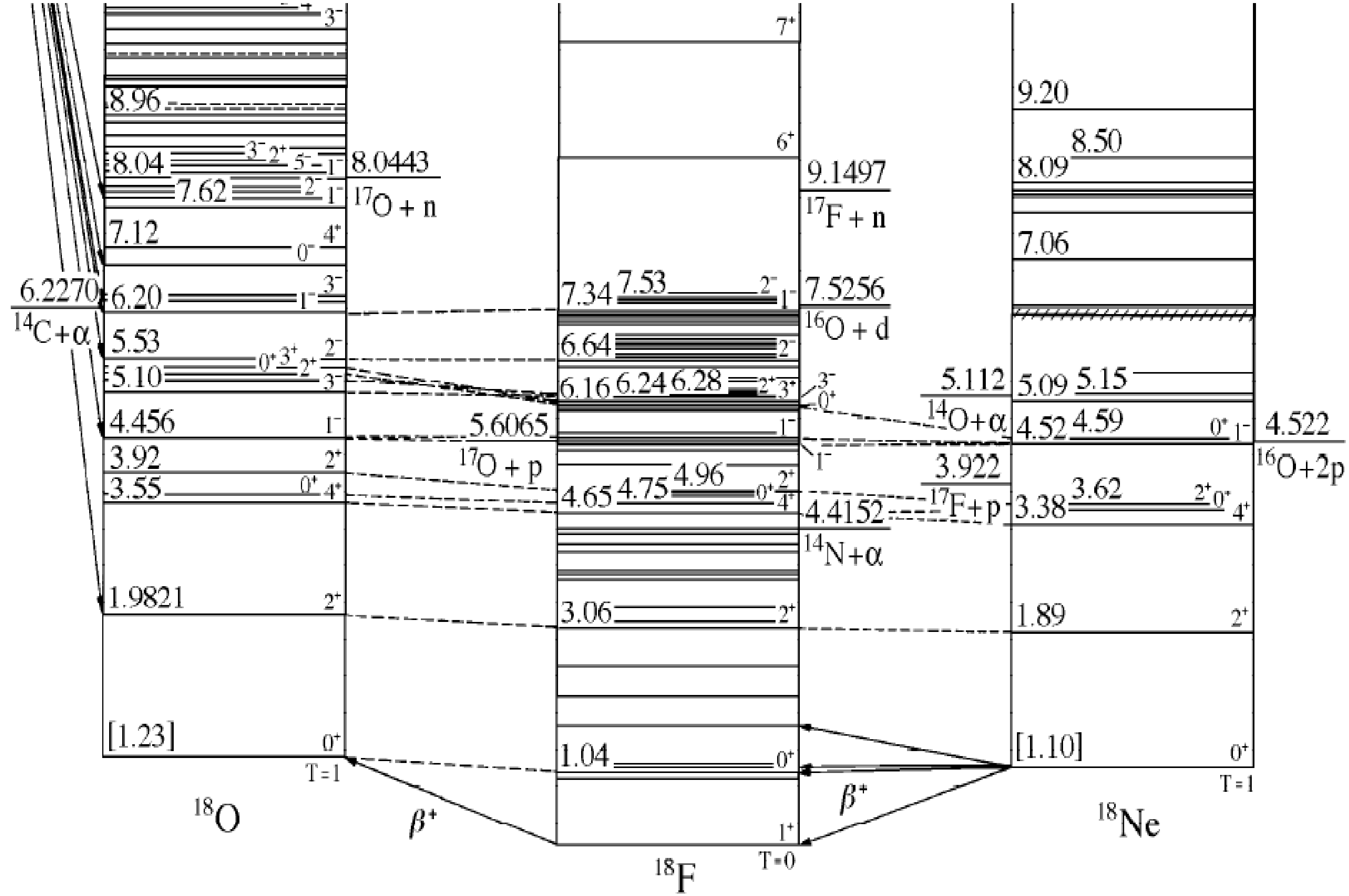

Isobar diagram for A=18

Excitation functions for the $^{14}C+\alpha$ and $^{14}O+\alpha$ elastic scattering

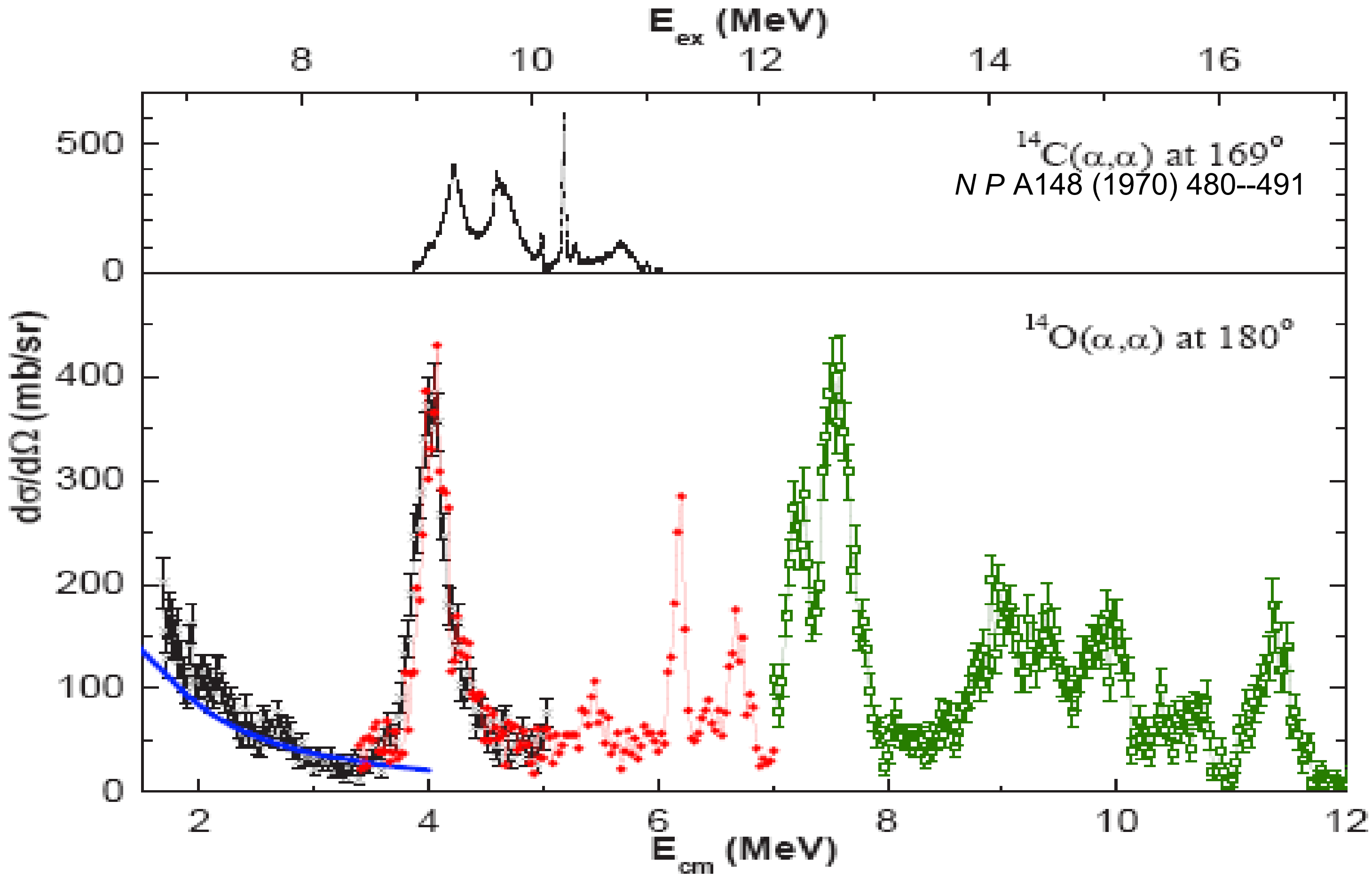

The excitation functions of the α+^{14}C elastic scattering at various angles

Excitation function at 90^o degrees in c.m. was taken from the literature18. Red curve is the best R-matrix fit, blue dashdotted curve is the best fit without very broad 0+ state at 3.7 MeV.

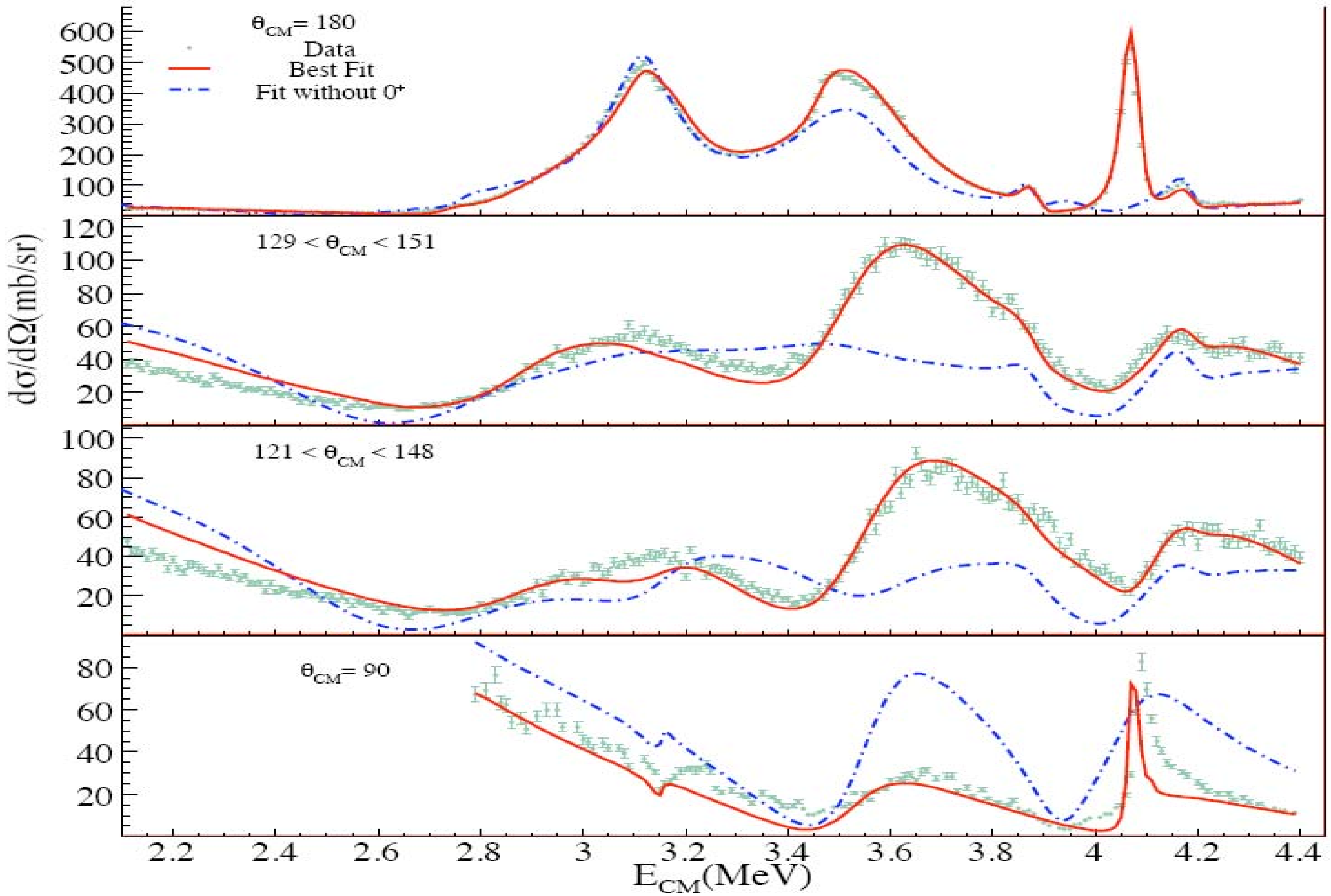

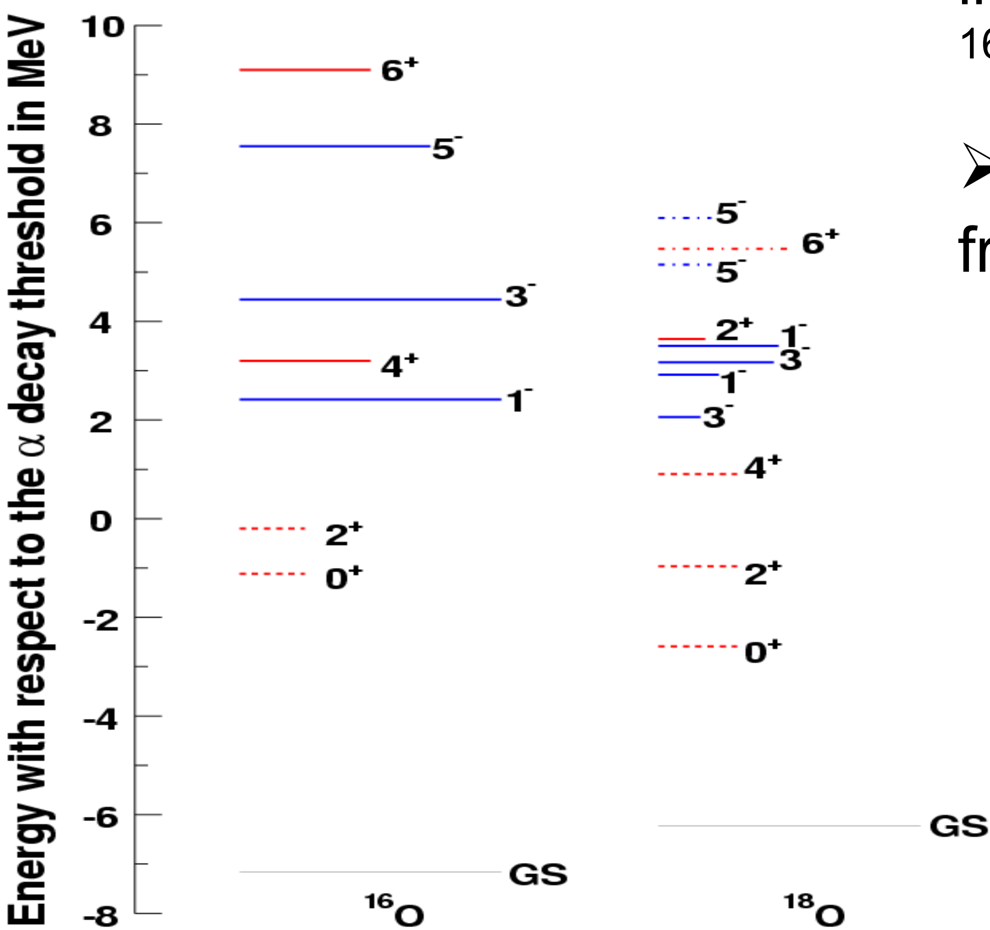

- Moment of inertia in ^{18}O is increased with respect to ^{16}O.
- Cluster states are more fragmented in ^{18}O.

Strong splitting was not predited in either N.Furutachi et al., Prog.Theor.Phys.(Kyoto) 119, 403 (2008) or in D.Baye, P.Descouvemont Phys.Lett. 146B, 285 (1984)

Resonances in the elastic α+^{14}C channel.

Very broad Γ≈3-5 MeV 0^+ state at 3.8+/-0.5 MeV above the α decay threshold was observed.

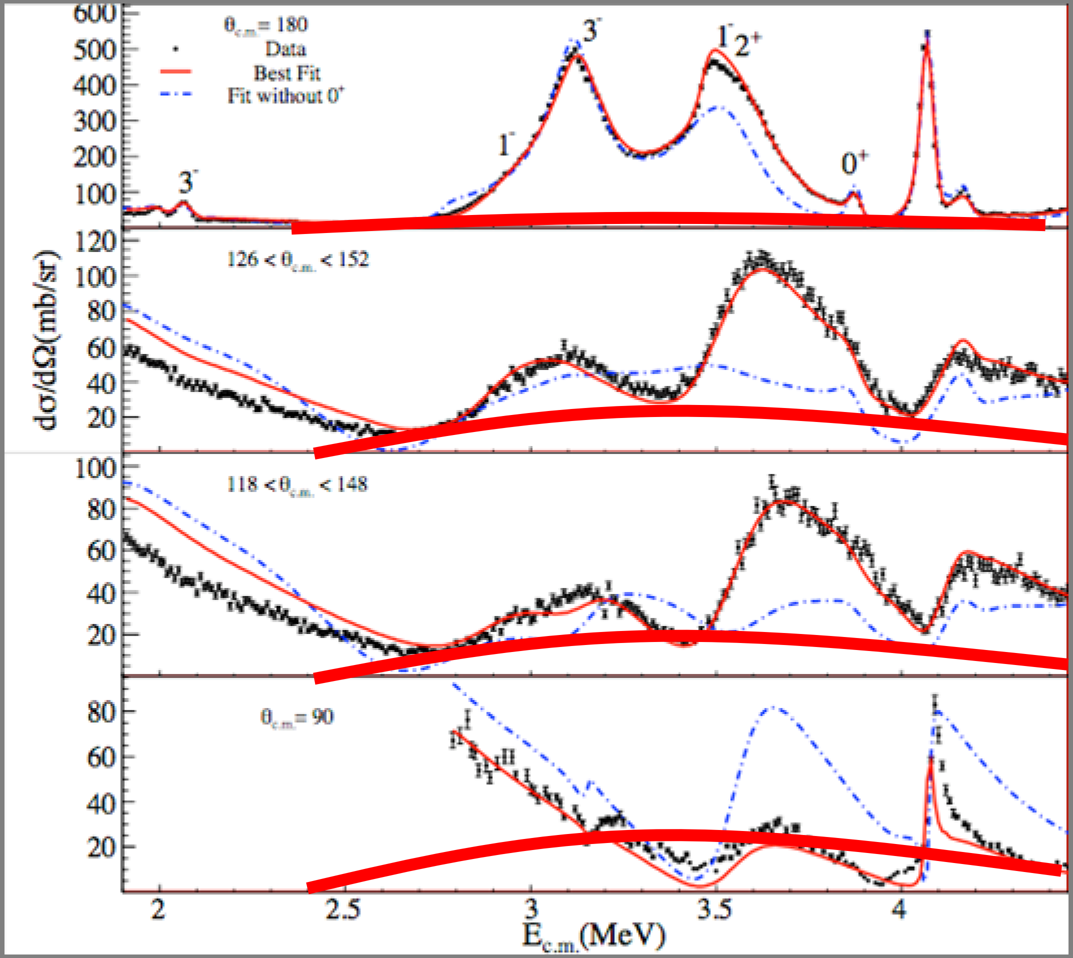

α halo state in ^{18}O

0^+ at 3.8+/-0.5 MeV (~10.0 MeV ^{18}O excitation energy) with width of ~3-5 MeV is necessary to fit the α+^{14}C data.
This width corresponds to a pure α particle state.

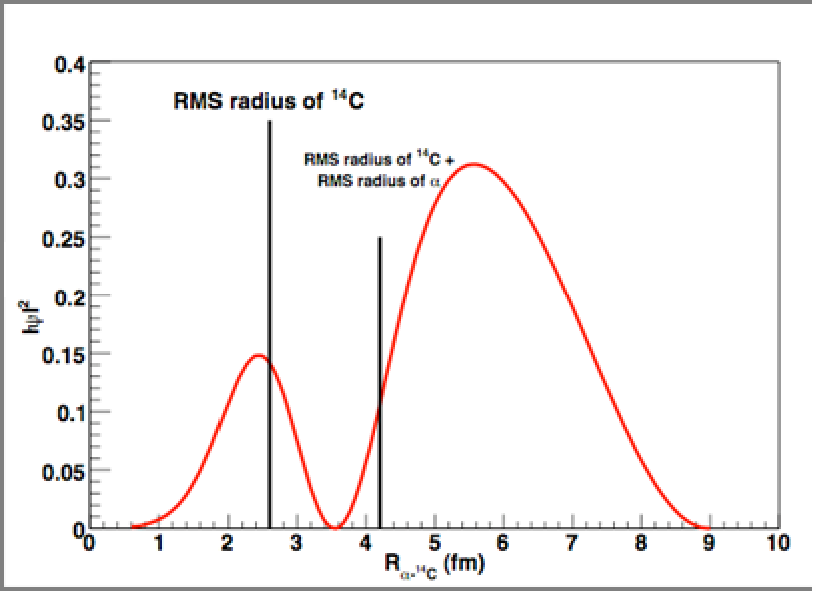

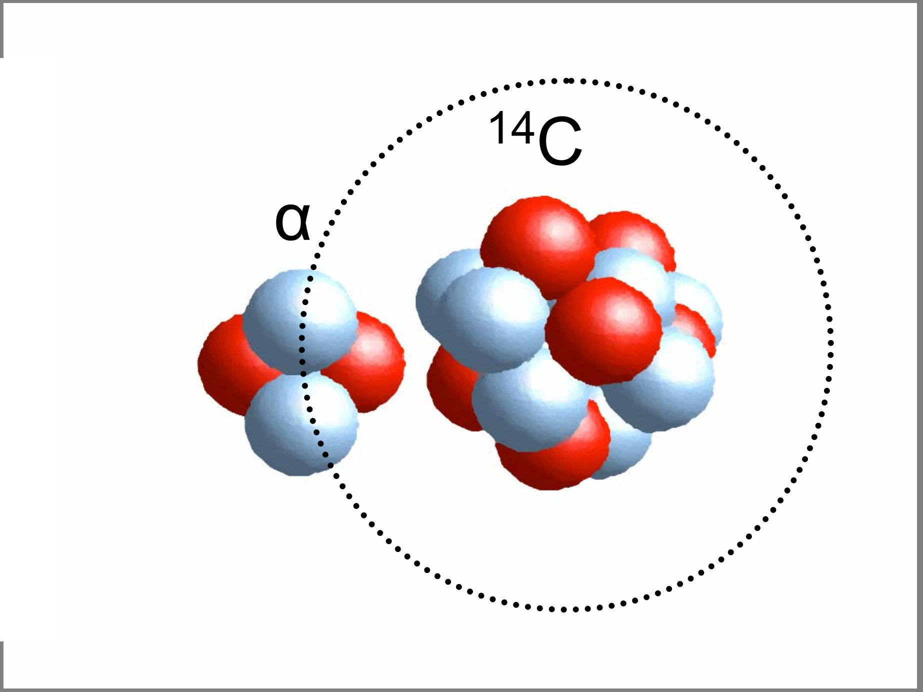

α halo states

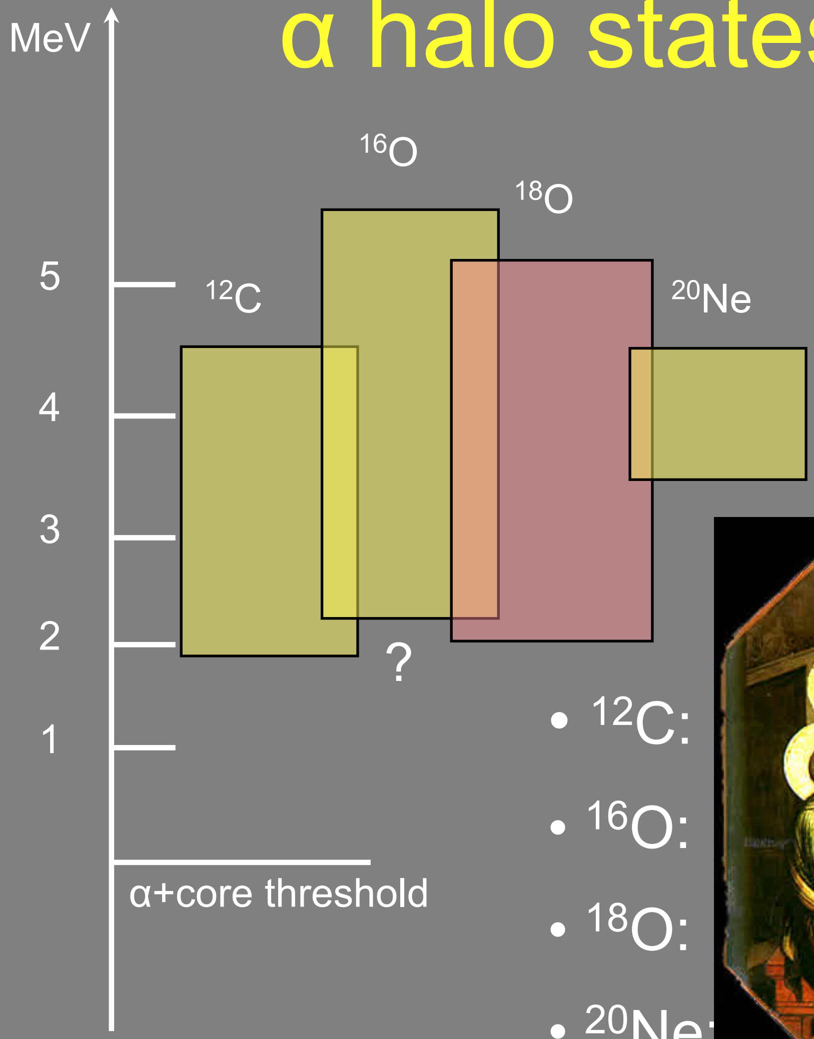

- ^{12}C:
- ^{16}O:
- ^{18}O:
- ^{20}Ne:

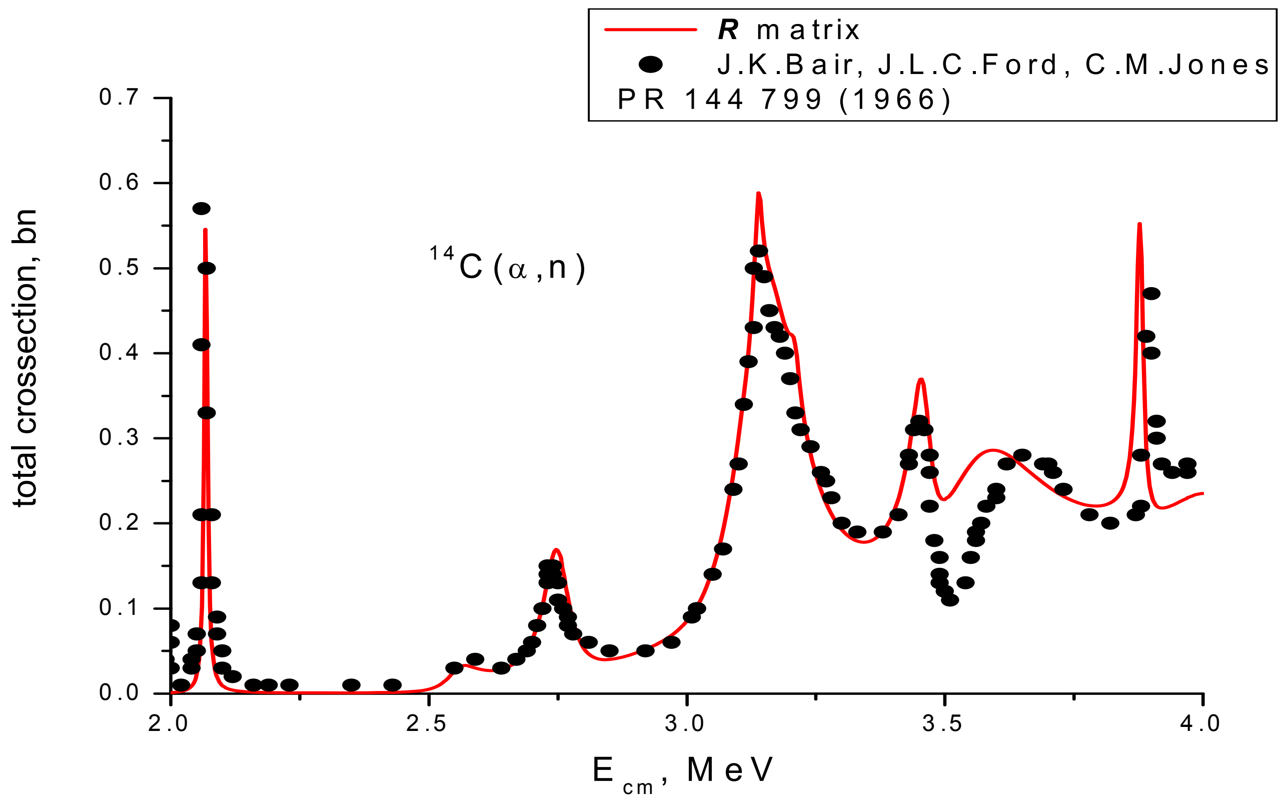

R matrix
J.K.Bair, J.L.C.Ford, C.M.Jones
PR 144 799 (1966)
14C (α,n)
total crossection, bn
E cm, MeV
0.0
0.1
0.2
0.3
0.4
0.5
0.6
0.7
2.0
2.5
3.0
3.5
4.0

Thank ya'll

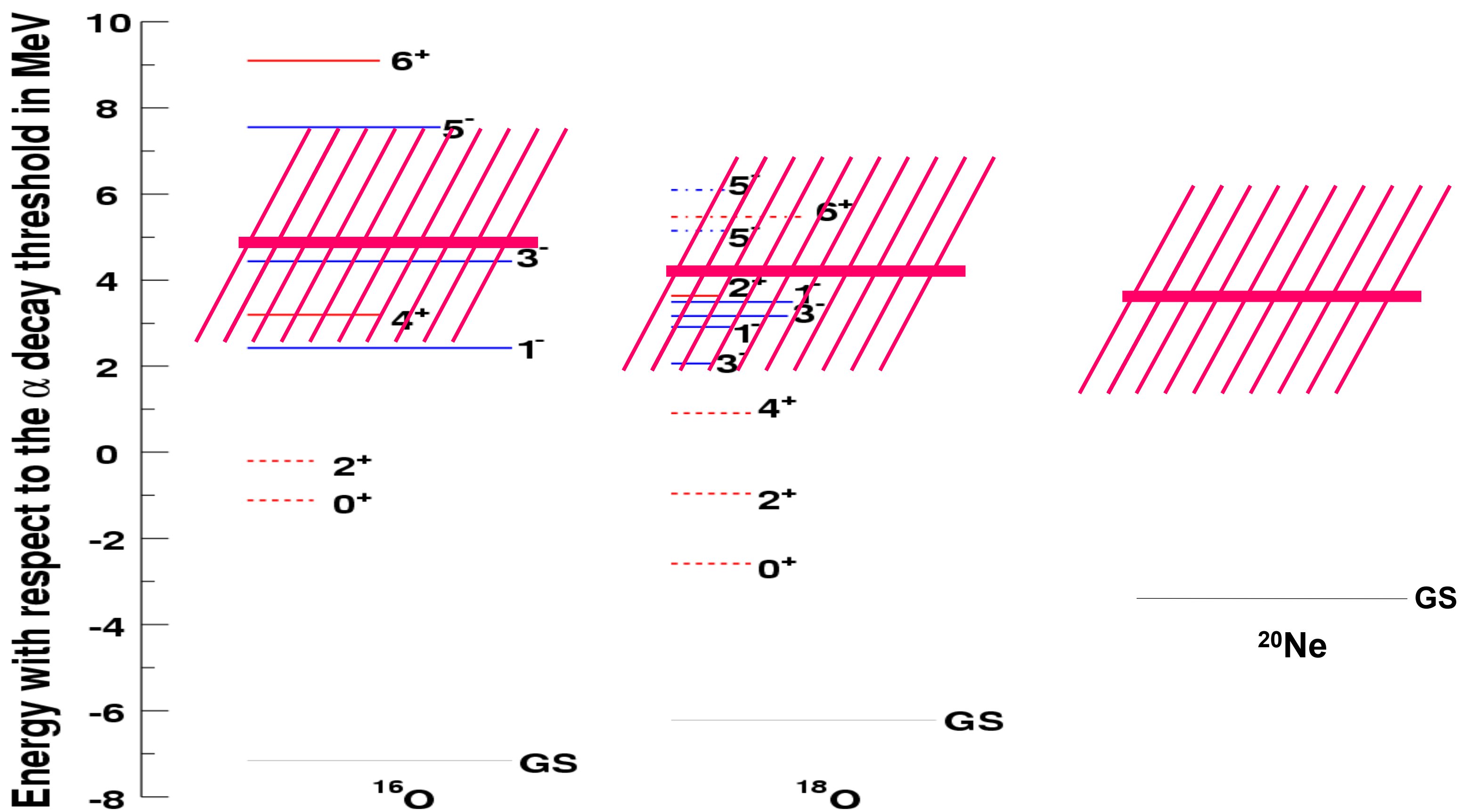
Energy with respect to the α decay threshold in MeV
10
8
6
4
2
0
-2
-4
-6
-8
6+
5-
3-
4+
1-
2+
0+
GS
16O
5-
6+
5-
2+
1-
3-
1-
3-
4+
2+
0+
GS
18O
GS
20Ne

Plan of the talk

- **Introduction**

New renaissance of resonance reactions studies is feed by astrophysics as well as by the structure of exotic nuclei

- **Technique**

Thick target inverse kinematics method

- **Examples**

$^{14}O+\alpha$ identification spectrum

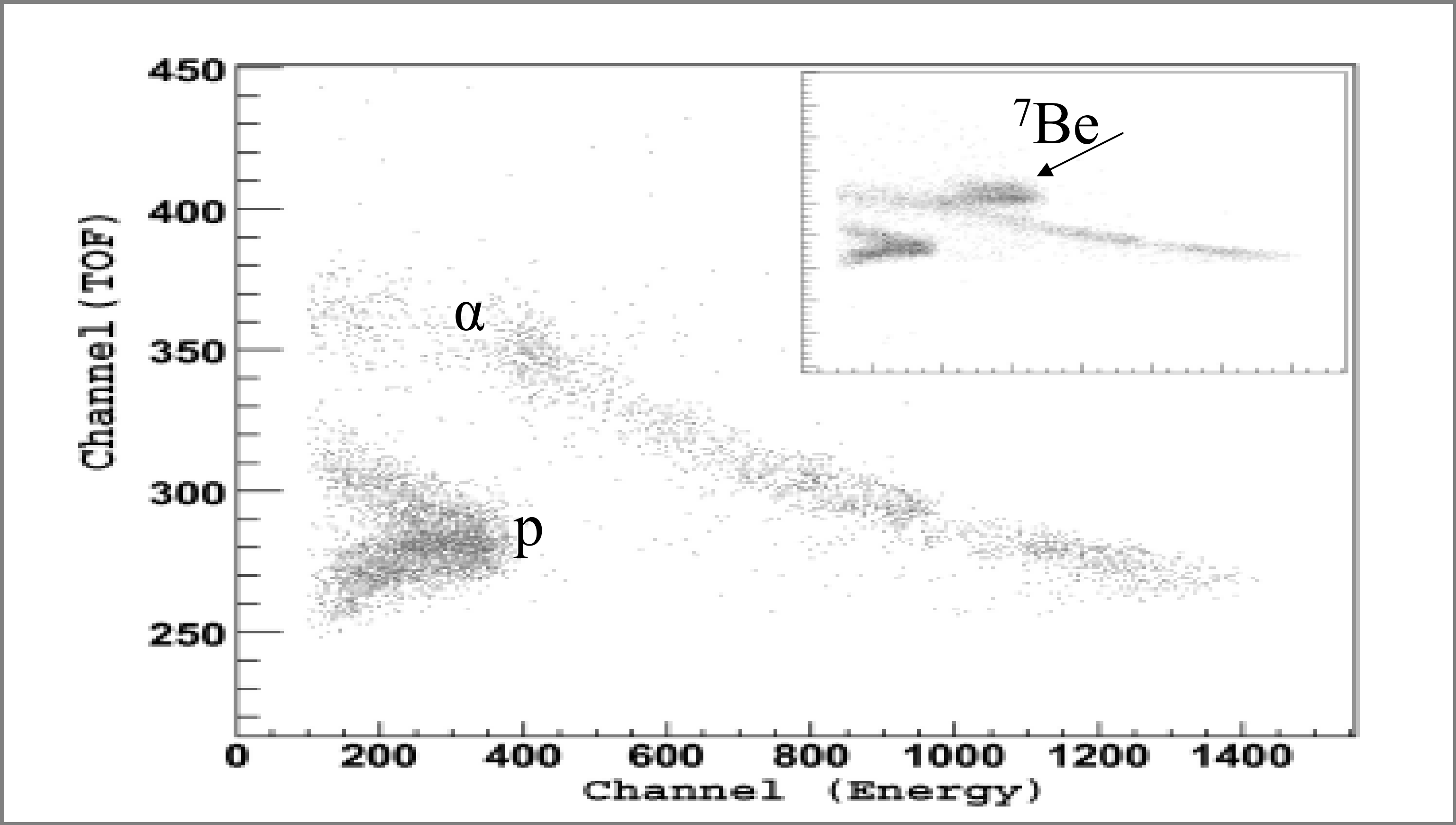

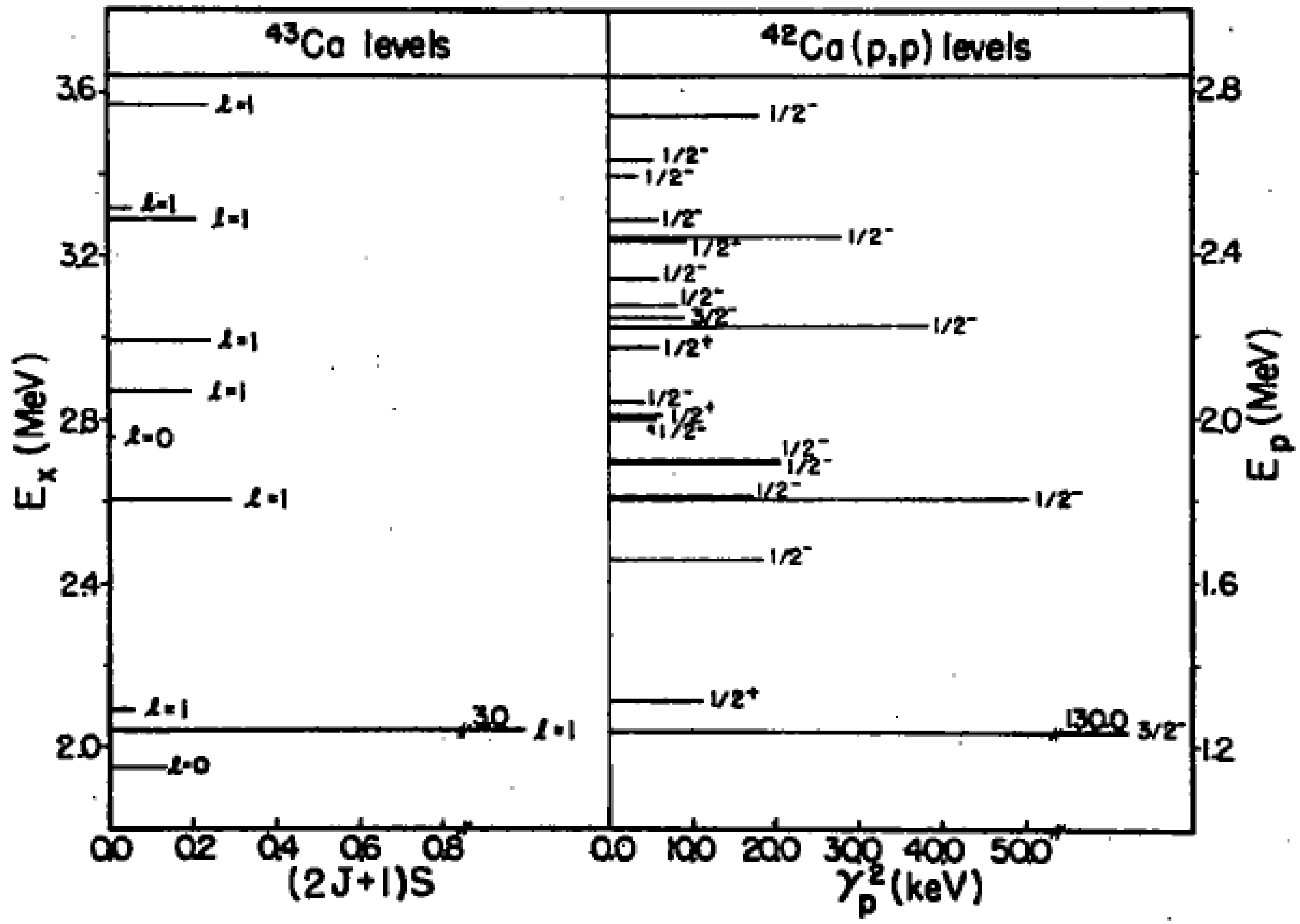

Fig. 3. Comparison of the largest s- and p-wave resonances observed in ^{42}Ca(p, p) with the levels (and their strengths) observed in the ^{42}Ca(d, p) reaction. The energy scales are matched by aligning the strong $\frac{1}{2}^-$ analogue and parent states. Despite the apparent correlation between the largest $\frac{1}{2}^-$ resonances and the $l = 1$ parent states, attempts to match the analogues and/or analogue fragments with the appropriate parent states proved futile (see discussion in text).

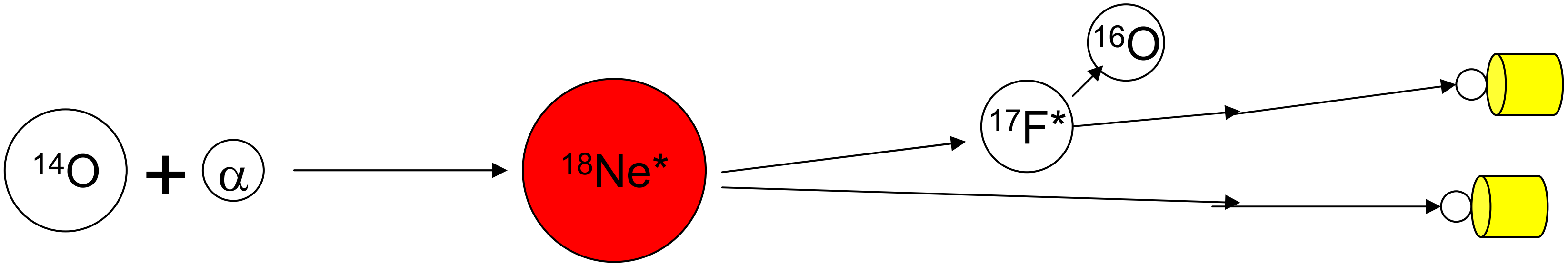

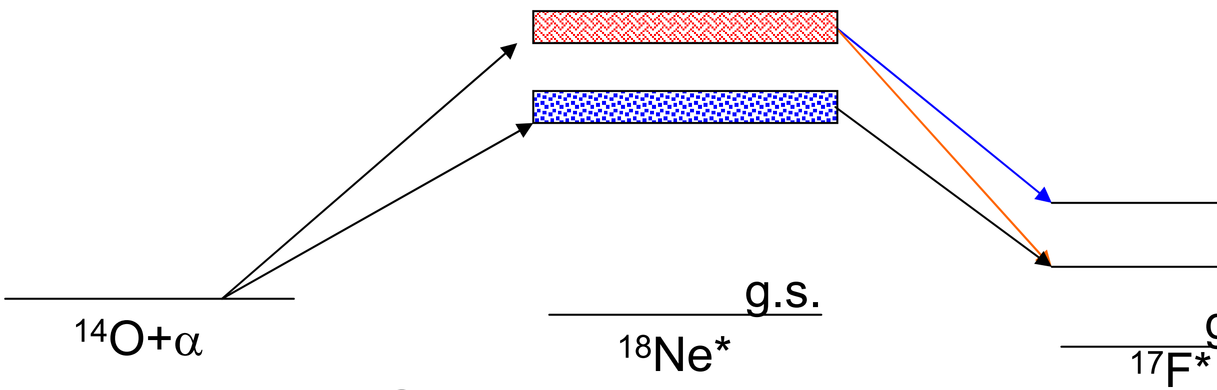

$$\vec{P}_0 = \vec{P}_1 + \vec{P}_2 + \vec{P}_3$$

$$E_0 = E_1 + E_2 + E_3$$

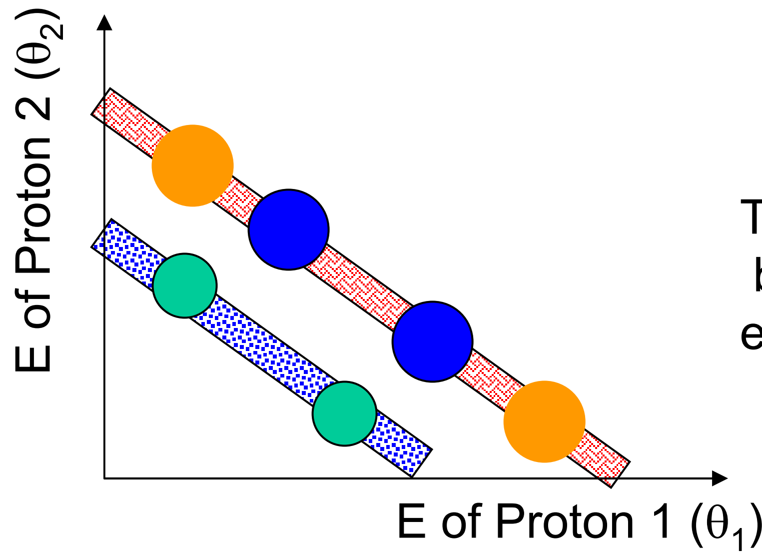

Three particle kinematics for the broad range of the ion incident energy

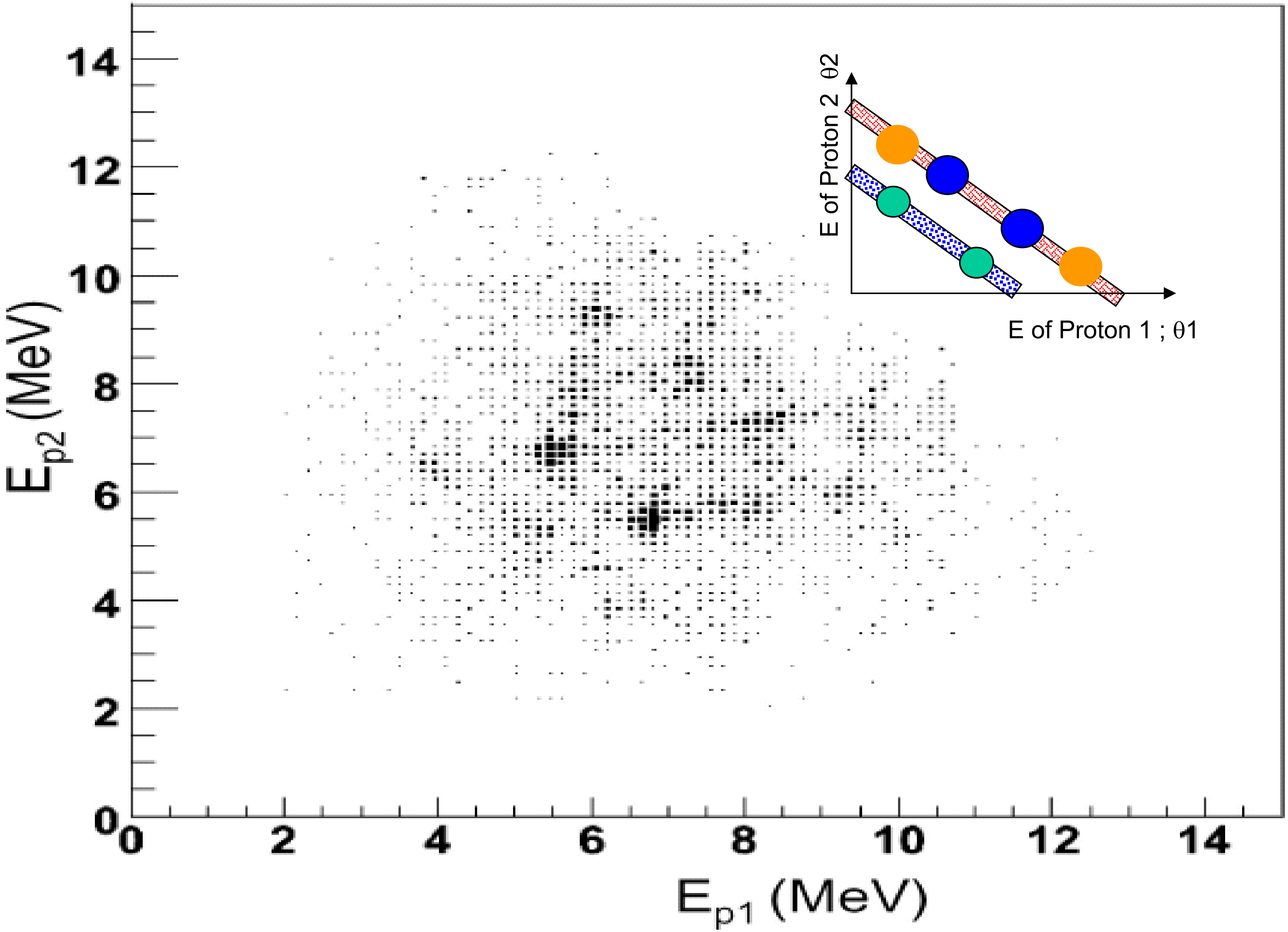

Fig. 6. the Dalitz plot of the coincident protons from the reaction $^{14}O(^4He,2p)^{16}O$. The energy of protons are given in lab system.

$^{12}C(T=0)+p(T=1/2)$
$\rightarrow {}^{13}N(T=3/2)$

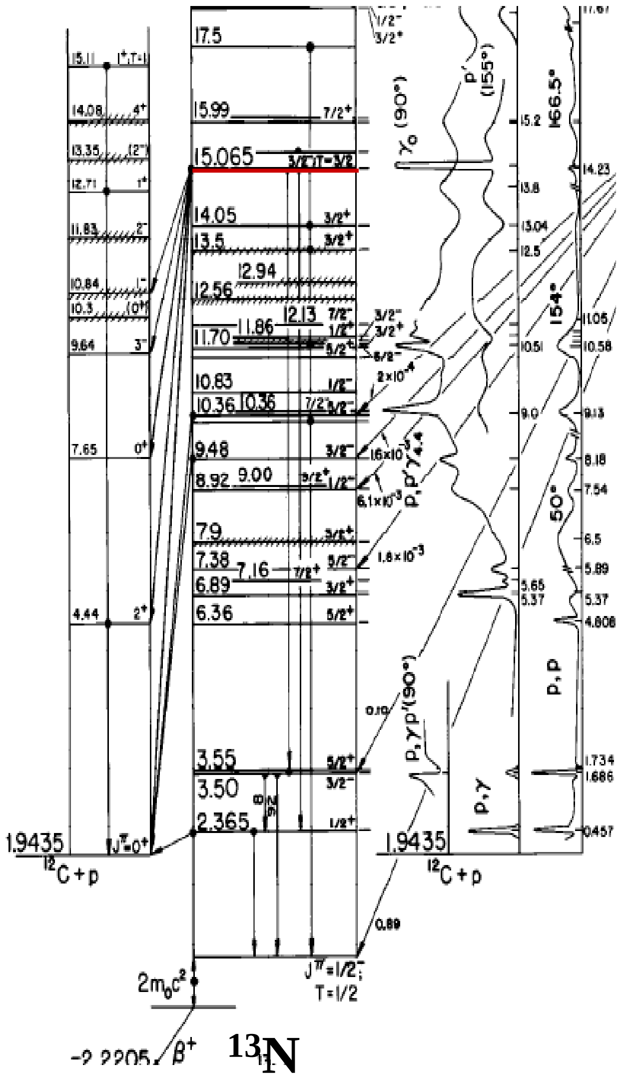

^{13}N

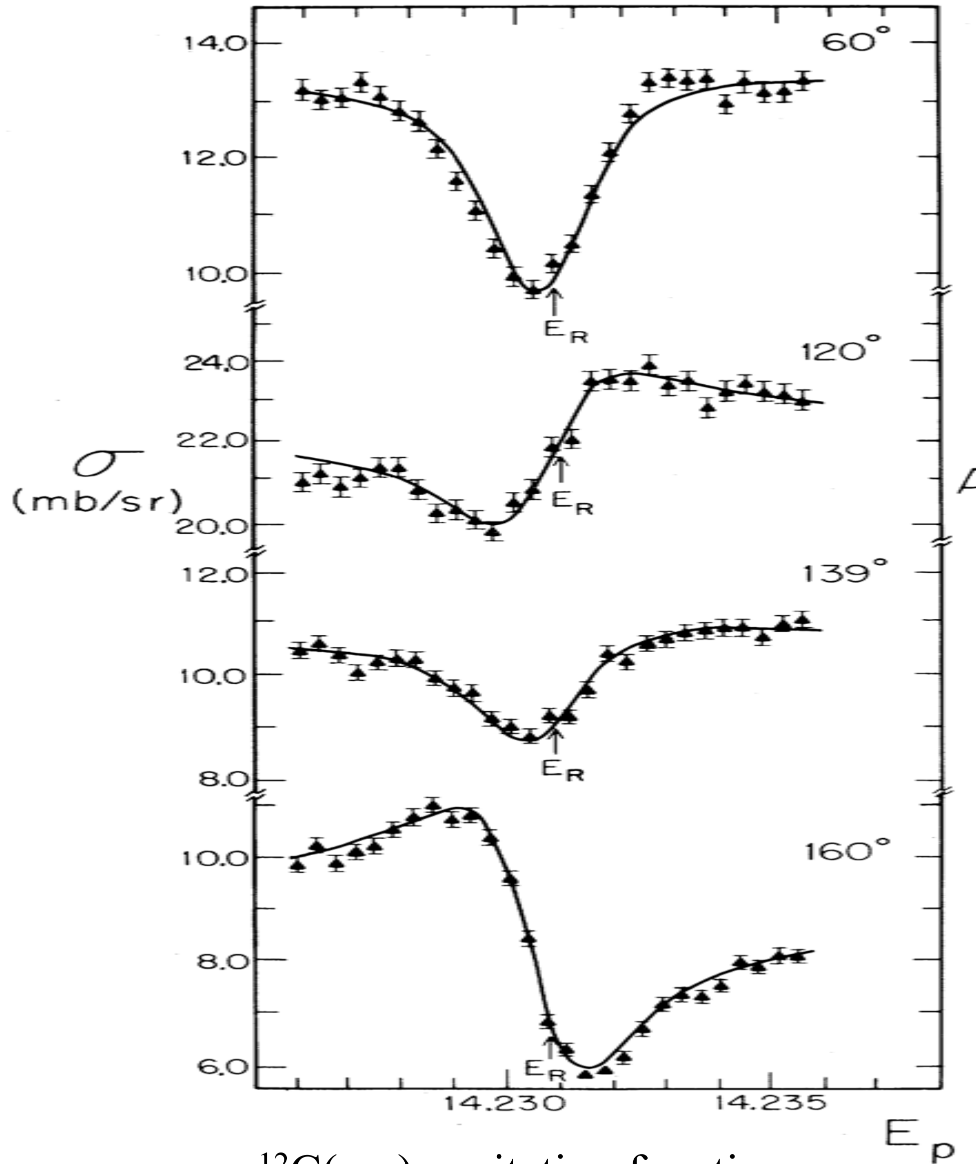

$^{12}C(p,p)$ excitation functions

W.J. Thompson et al., P.R.L 45, 703 (1980)

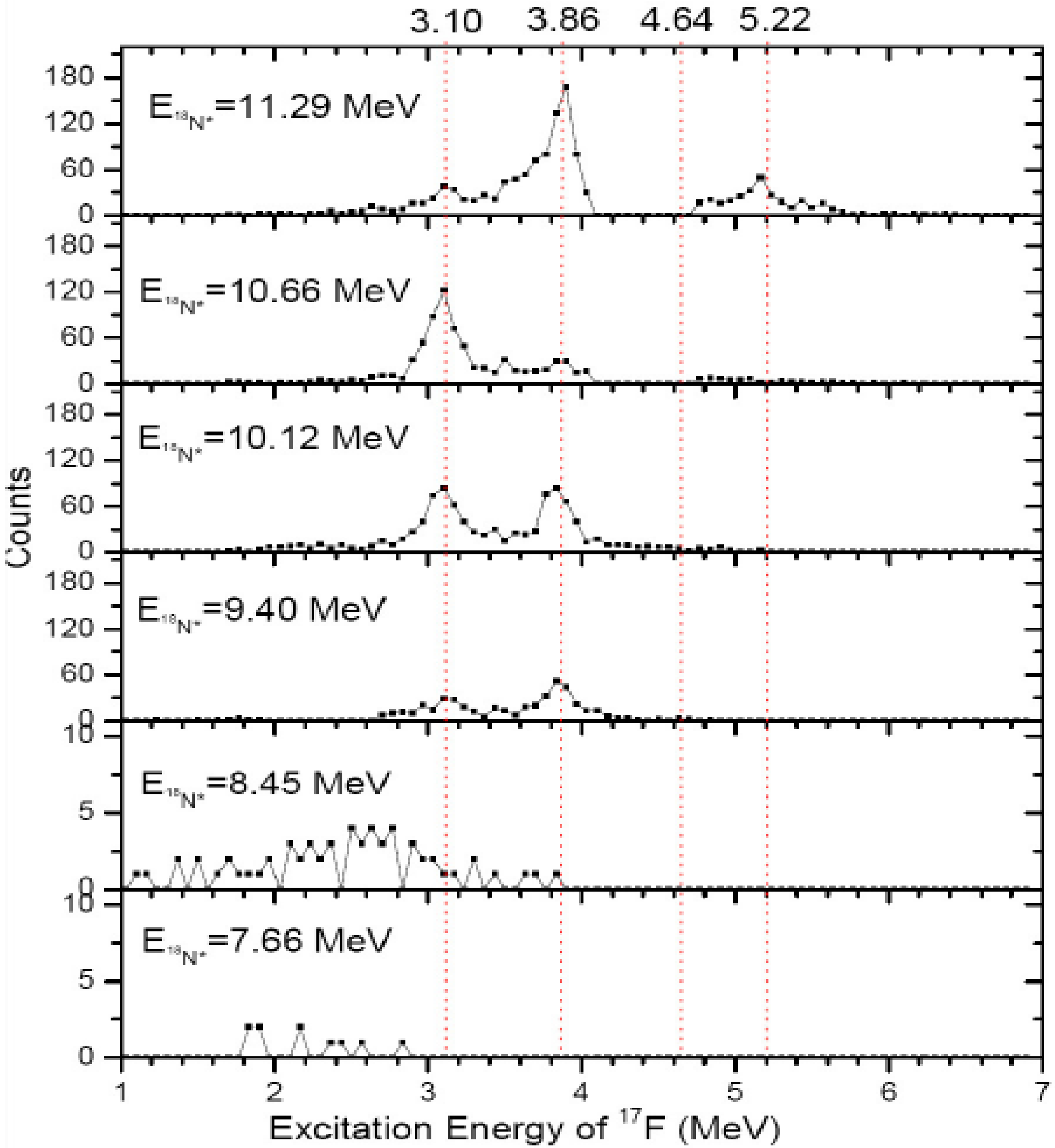

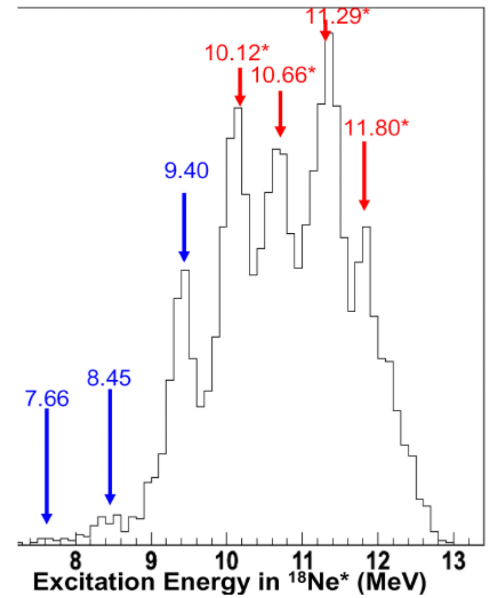

^{8}Ne* states which decay through 2-proton emission.The cros
MeV is about 0.045 mb, and 11.29 MeV peak is about 3.9 mb

proton decay modes of the ^{18}Ne states

Excitation function for the ^{12}B+p elastic scattering at 165^0.

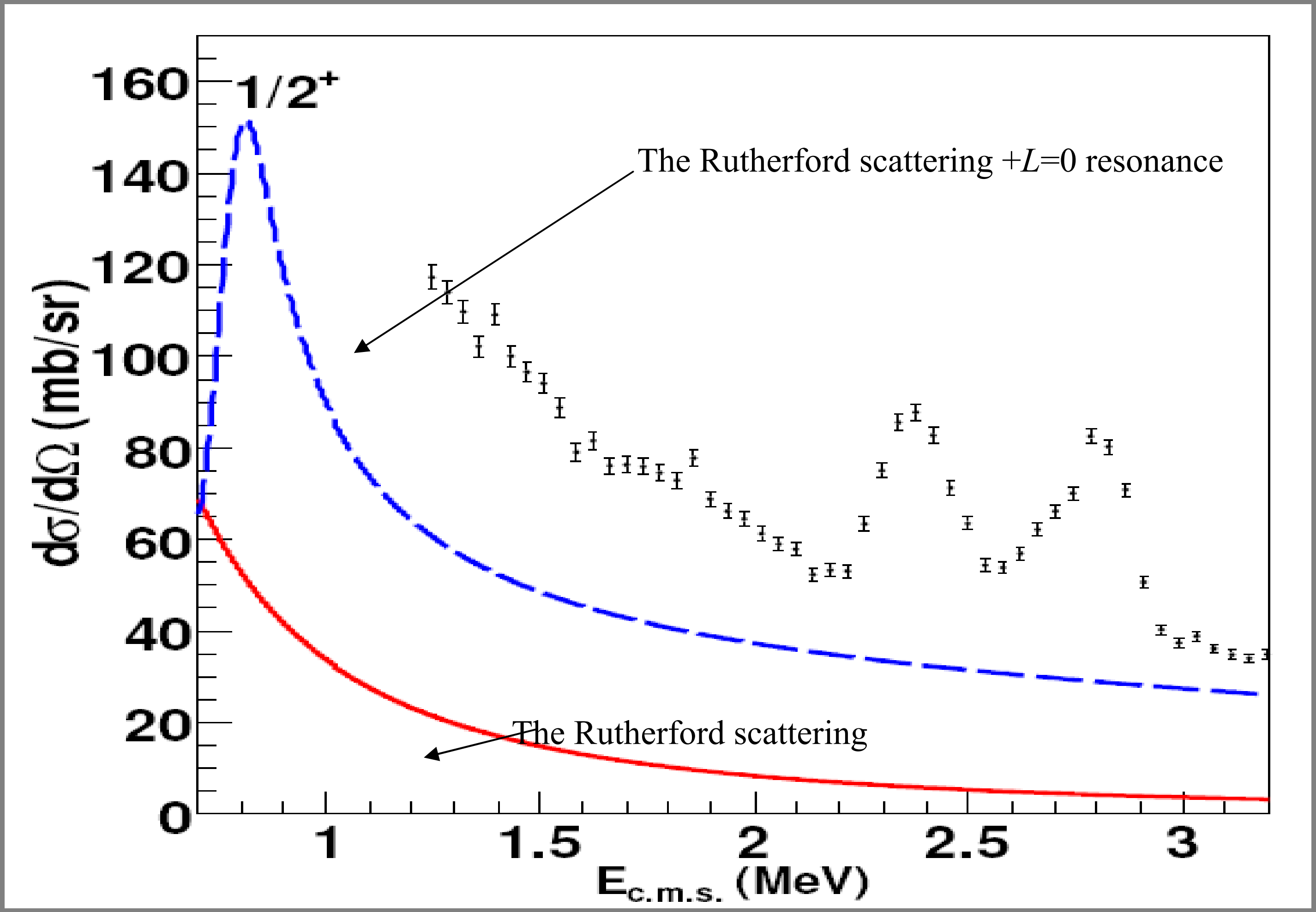

2p decay of 8.45 MeV state in ^{18}Ne

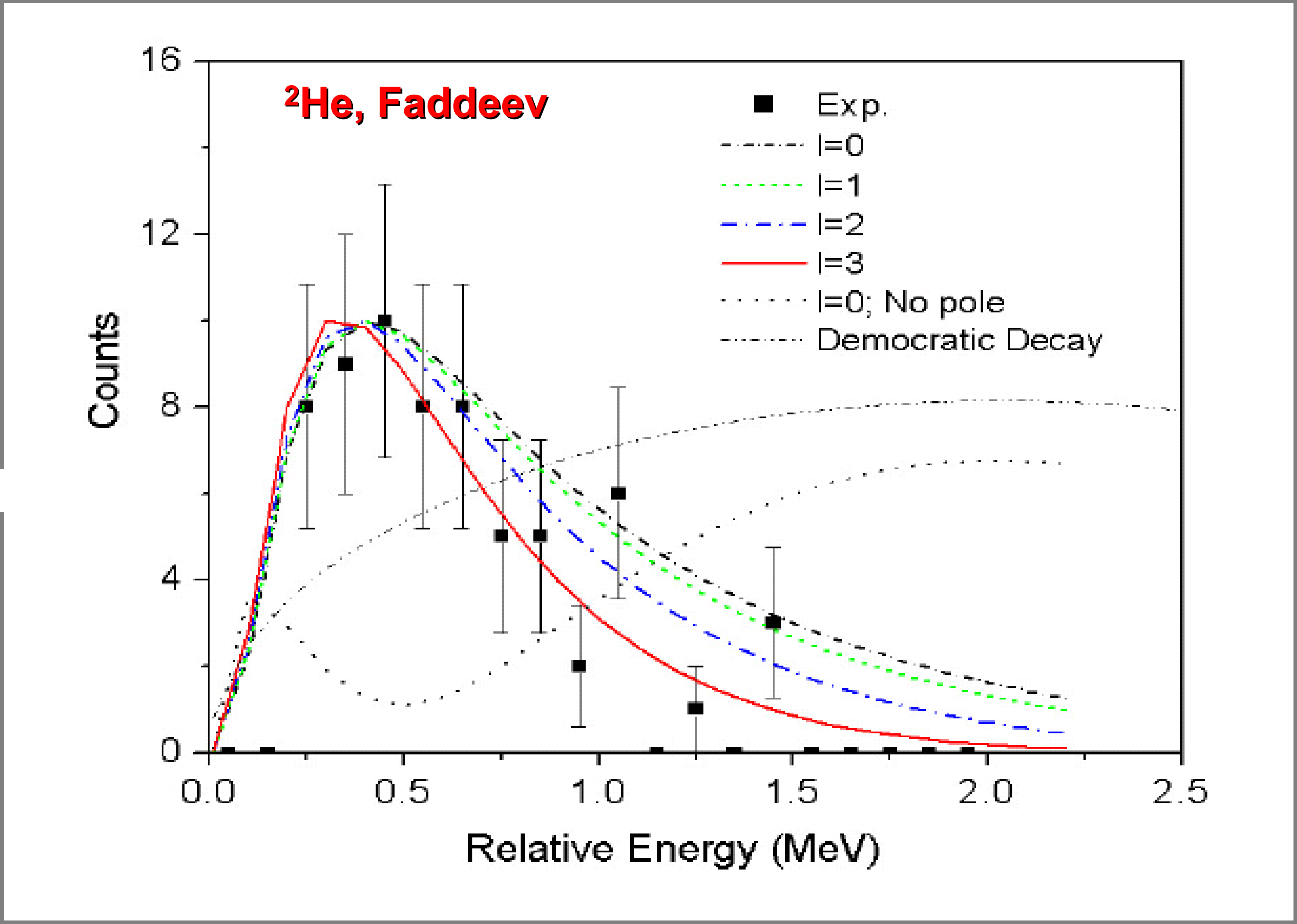

Changbo Fu, V.Z.Goldberg, A.Mukhamedzhanov et al,
Phys. Rev. C, 76, 021603(R) (2007)

Reaction place identification trough time of flight

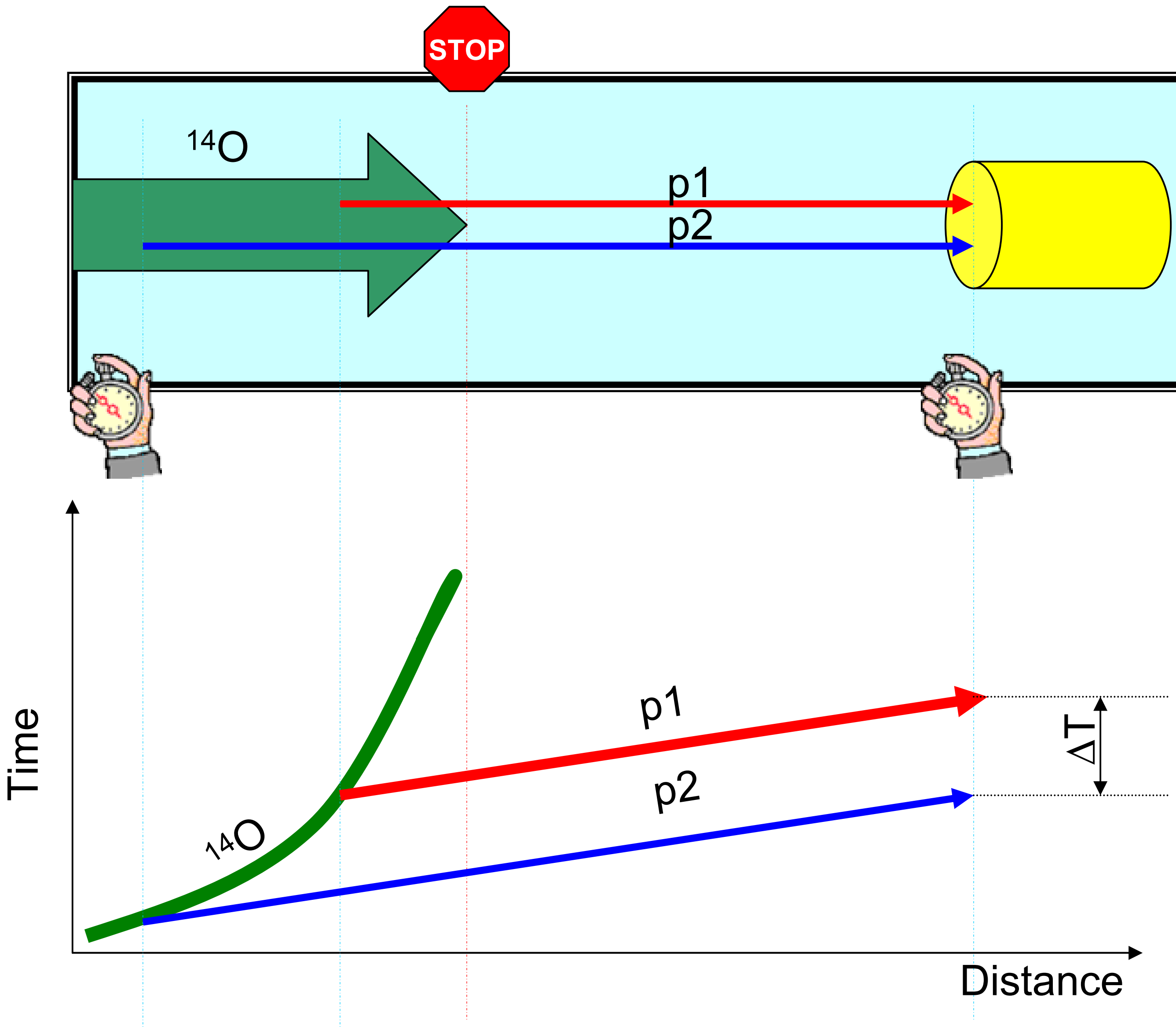

$$^{14}O + \alpha \rightarrow {}^{18}Ne^* \rightarrow \begin{cases} {}^{14}O + \alpha \\ {}^{17}F + p \\ p + {}^{17}F^* \rightarrow p + {}^{16}O + p \end{cases}$$

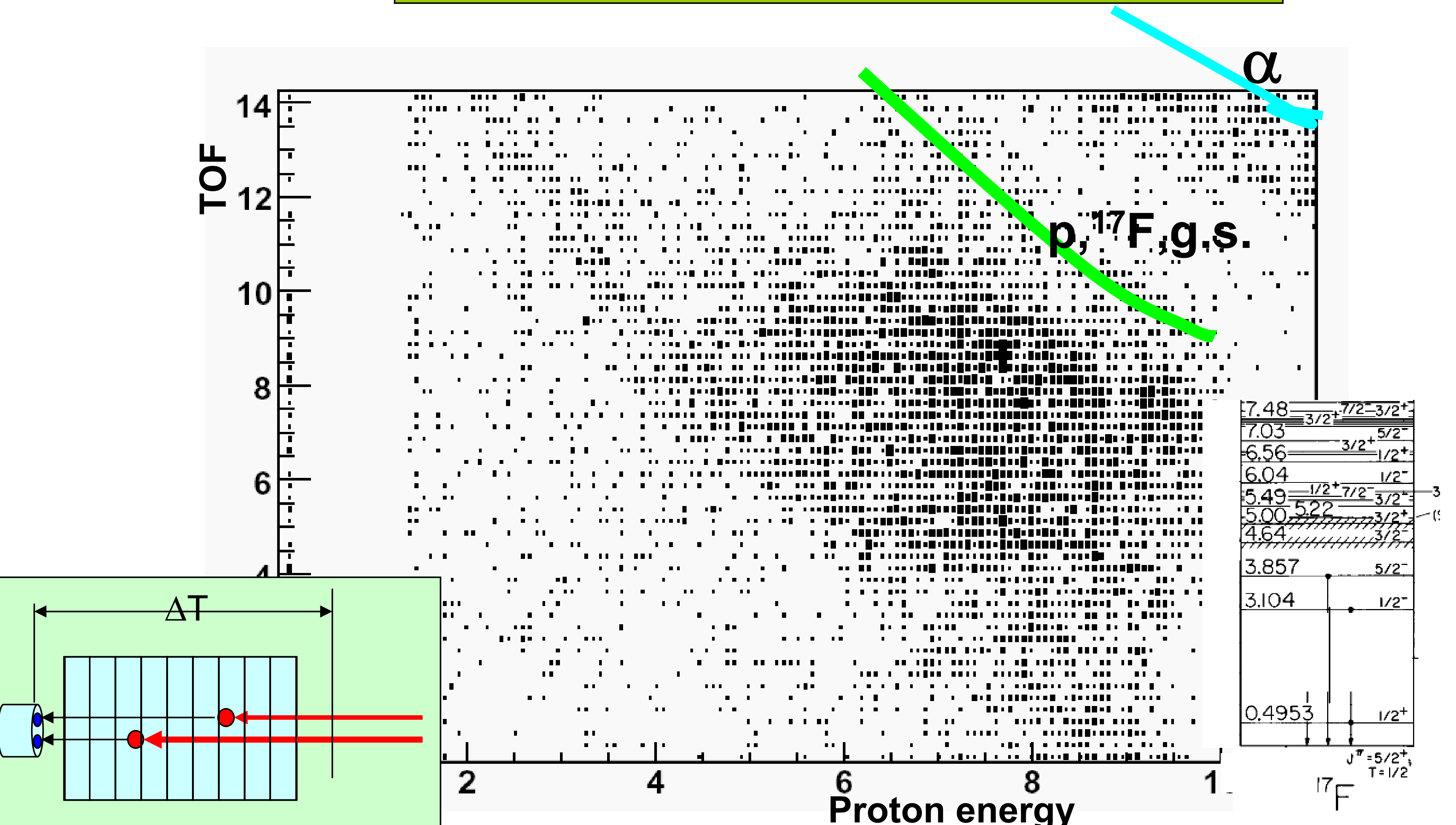

Nucleosynthesis in Cosmos

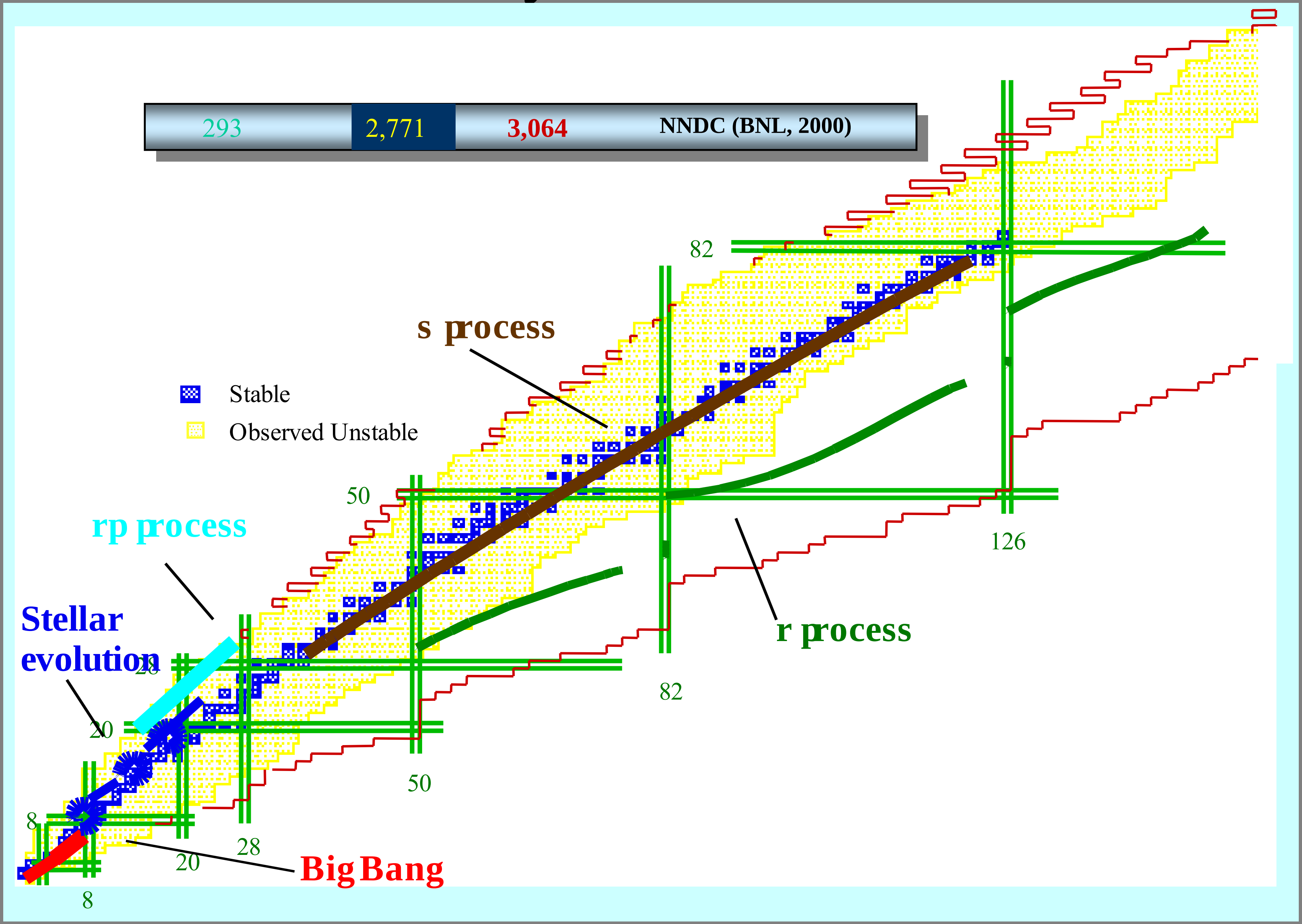

Phys.Rev. C 75, 024607 (2007)
B.B.Skorodumov et al.

$^{12}N+p$

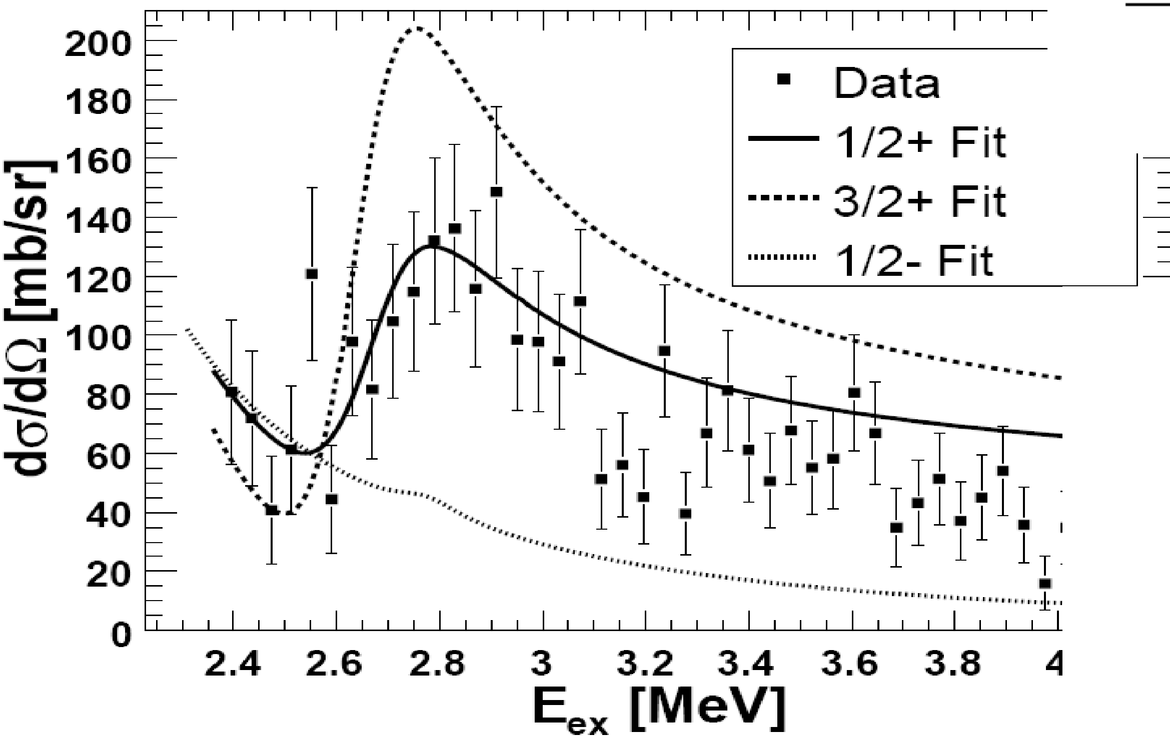

Figure 4.5. Single resonance R-matrix fits for the experimental dat from the detector at 7.5^0. The solid line shows the fit with the assumption of a single $1/2^+$ resonance. A $3/2^+$ assignment would lea the fit shown by the dashed line. A $1/2^-$ assignment would lead to the fit shown by dotted curve.

POTENTIAL-MODEL RESULTS FOR THE $1/2^+$ STATE IN ^{13}O.

V_0 MeV	r_0[1] fm	a fm	Γ_{sp} MeV	Δ[2] keV	ε (MeV) Isotopic Shift	SF[3]
-56.60	1.22	0.600	525	0.16	0.65	0.77
-56.65	1.17	0.735	717	0.29	0.74	0.60

[1] $r_{Coul.}$ = 1.21 fm
[2] $\Delta = E_{res} - E_{sp}$
[3] $SF = 1 - \Delta/\varepsilon$

RESONANCE PARAMETERS FOR LEVELS IN ^{13}O

N	J^π	E_{ex} MeV	Γ MeV
1	$1/2^+$	2.69±0.05	0.45±0.1
2	$(1/2,3/2)^-$	3.29±0.05	0.08±0.03
3	$(3/2^-)$[1]	(4.55)	(0.24)
4	$(3/2^+)$[1]	(5.00)	(0.78)
5	$(3/2^+)$[1]	(5.70)	(2.00)

[1] Distant resonances used in the R-matrix fit.

***R*-matrix fit. $^{14}O+\alpha$ excitation functions.**

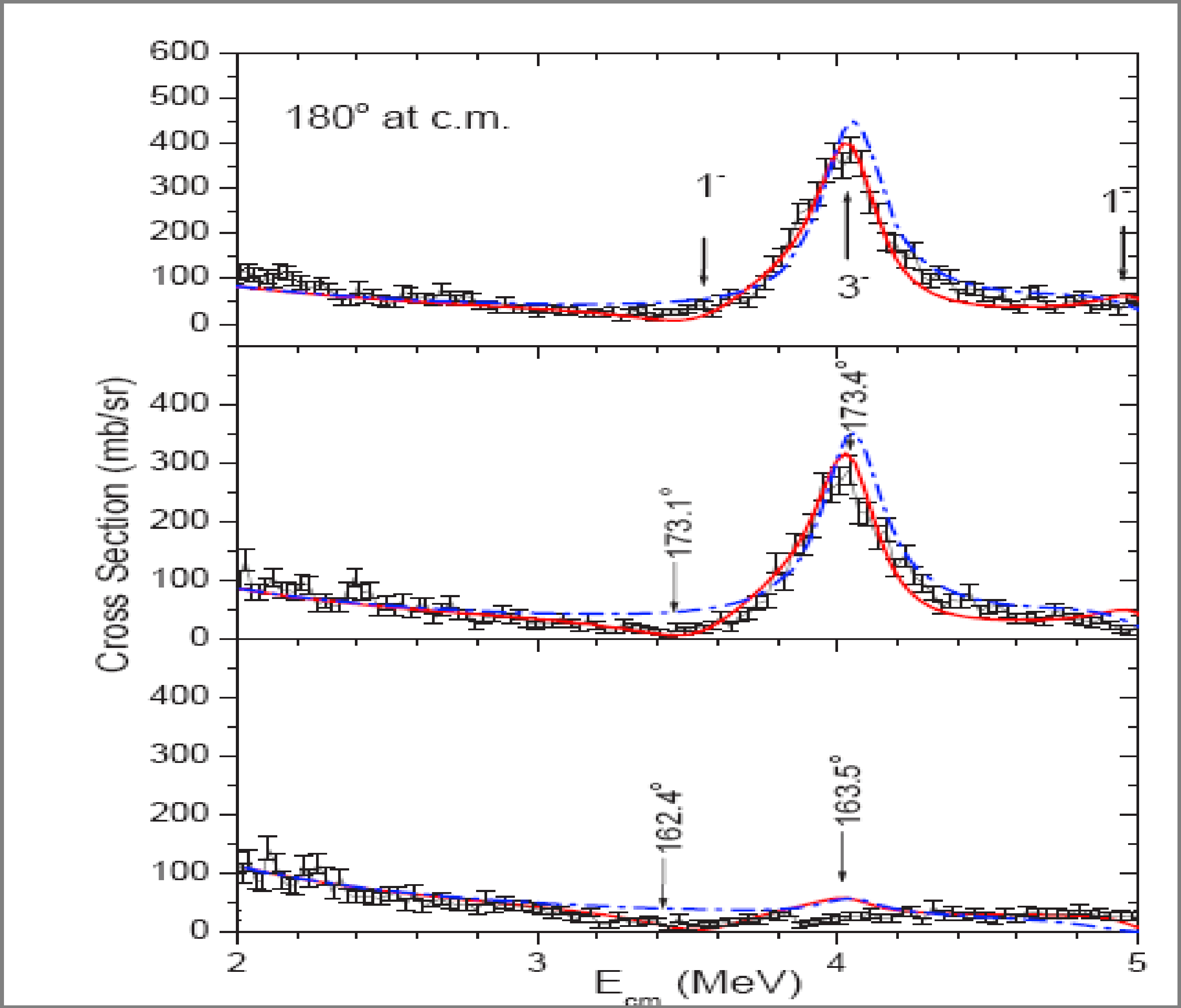

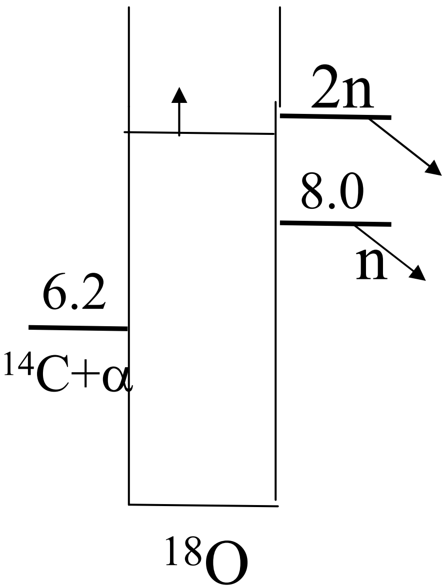
2n
8.0
n
6.2
$^{14}C+\alpha$
^{18}O

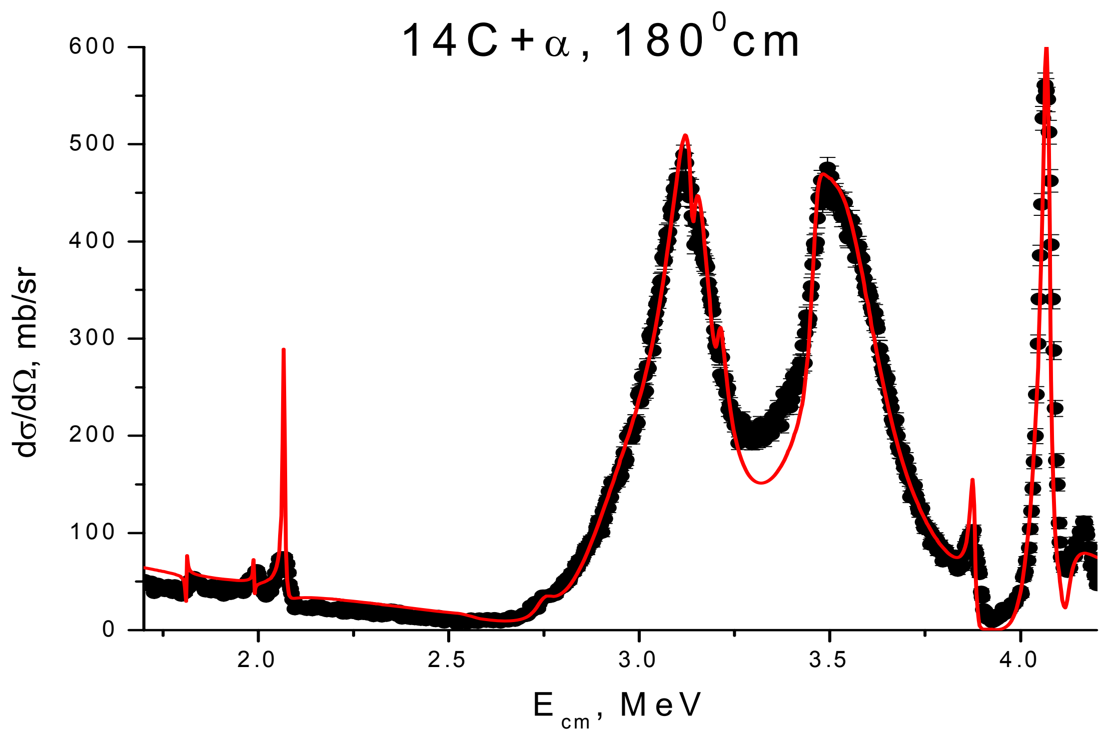
14C+α, 180⁰cm
dσ/dΩ, mb/sr
E cm, MeV
600
500
400
300
200
100
0
2.0
2.5
3.0
3.5
4.0

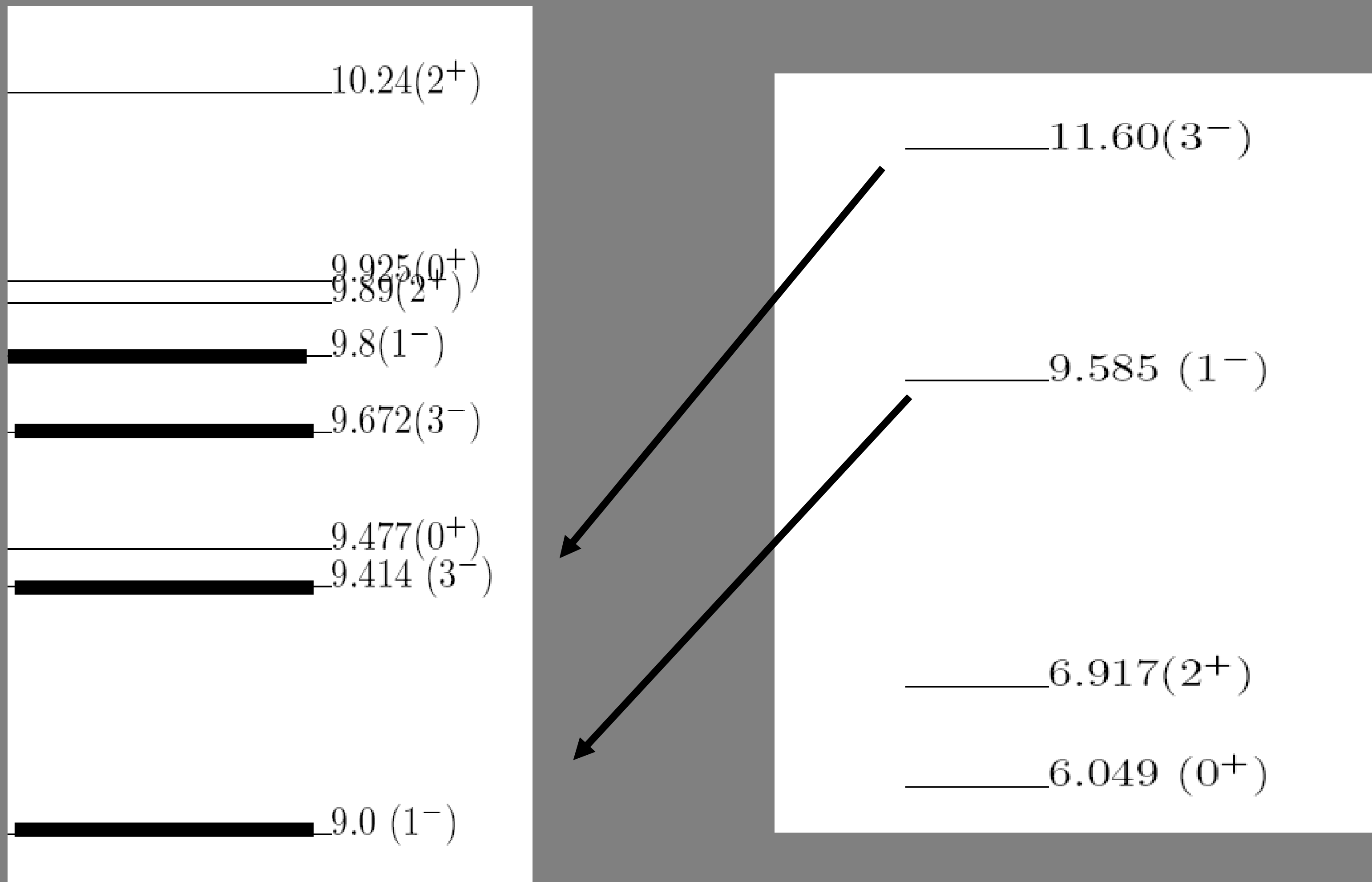

^{18}O Alpha cluster structure

^{16}O Alpha cluster structure

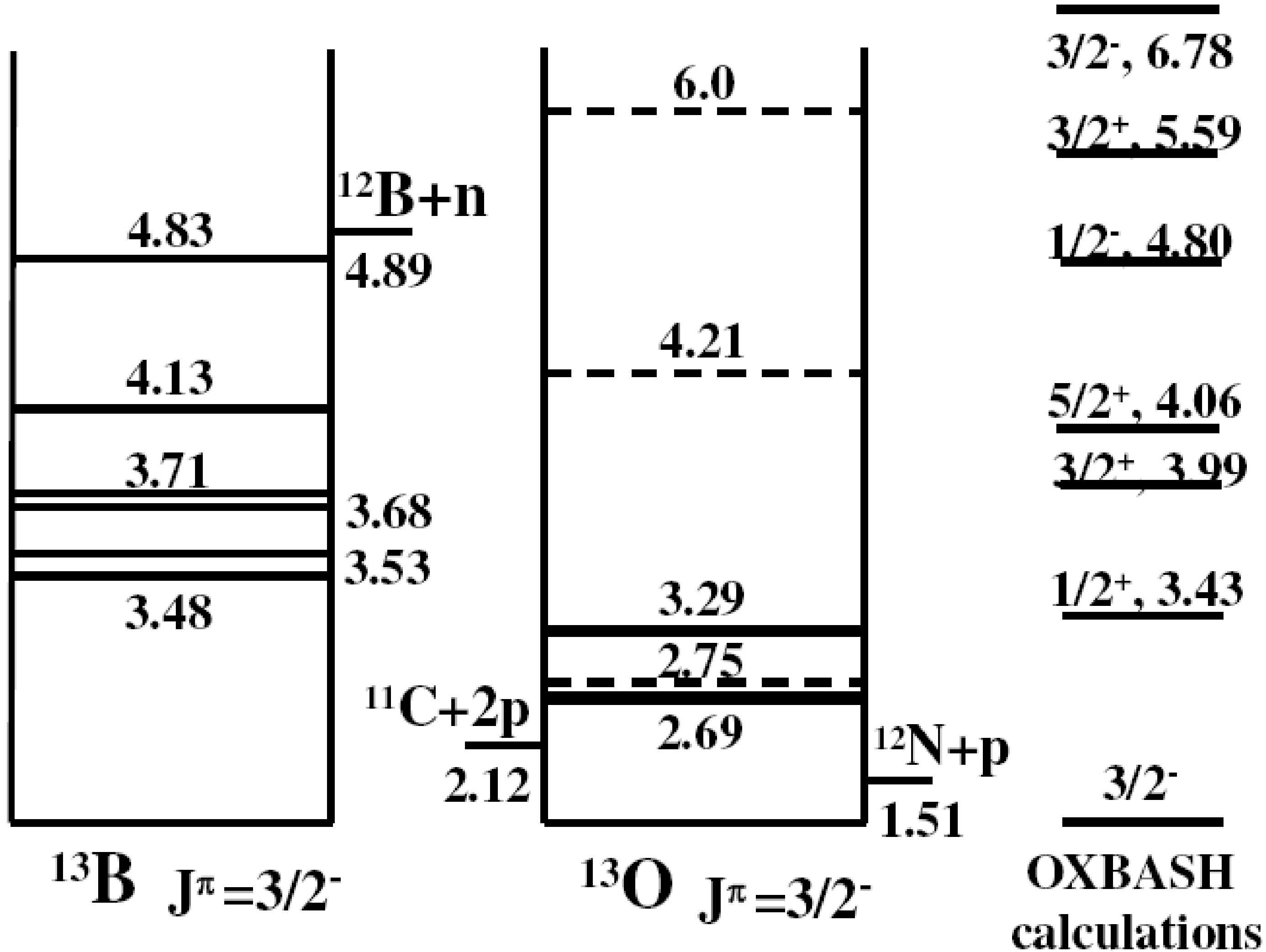

Figure 4.1. Level scheme of the mirror nuclei ^{13}B and ^{13}O. The dashed lines in the ^{13}O level scheme represent levels from Ref. [1]. The solid lines are the present results. On the right side of the figure, OXBASH calculations [18] with the WBT [67] interaction are presented.

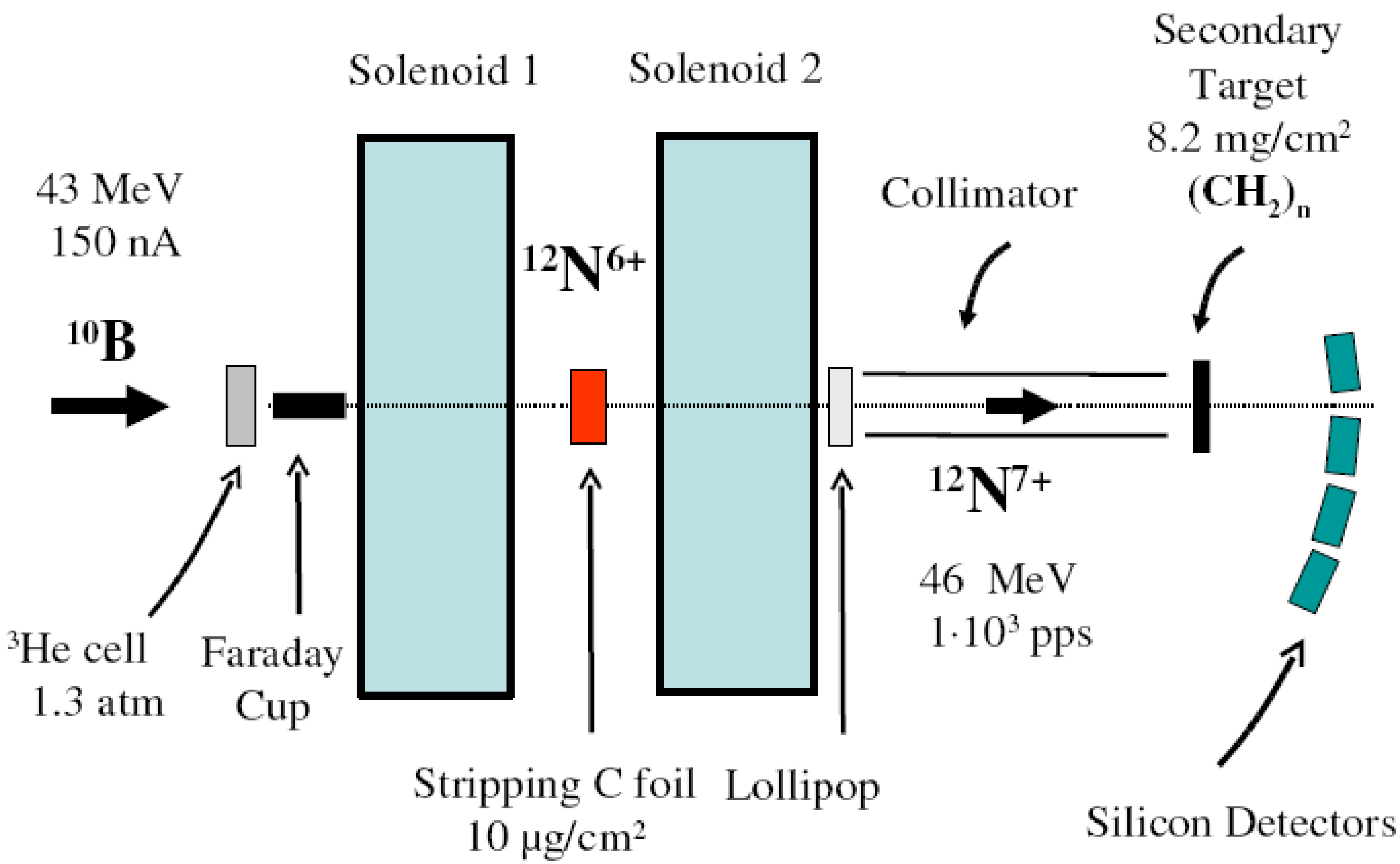

Figure 4.2. The schematic experimental setup of *TwinSol*. The "lollipop" reduces contamination of the beam by intercepting ions that focus at a different location relative to the ^{12}N beam.

RESONANCE PARAMETERS FOR LEVELS IN ^{13}O

N	J^{π}	E_{ex} MeV	Γ MeV
1	$1/2^{+}$	2.69 ± 0.05	0.45 ± 0.1
2	$(1/2,3/2)^{-}$	3.29 ± 0.05	0.08 ± 0.03
3	$(3/2^{-})$[1]	(4.55)	(0.24)
4	$(3/2^{+})$[1]	(5.00)	(0.78)
5	$(3/2^{+})$[1]	(5.70)	(2.00)

[1]Distant resonances used in the R-matrix fit.

Energy Resolution for IKTT Method
^{11}C(50 MeV)+p, zero degree

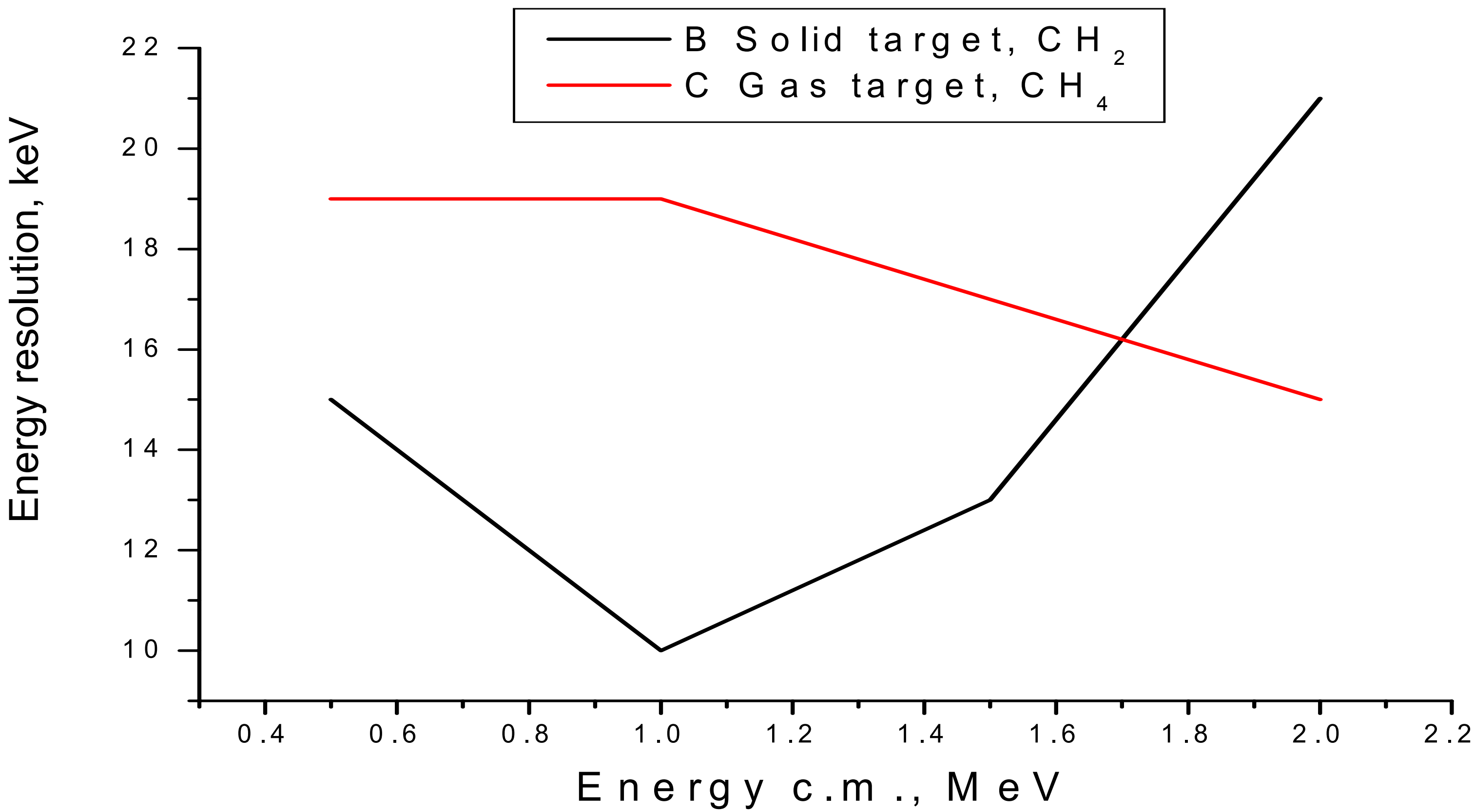

Changbo Fu, V.Z.Goldberg, G.V. Rogachev et al,
Phys. Rev. C, 76, 021603(R) (2007)

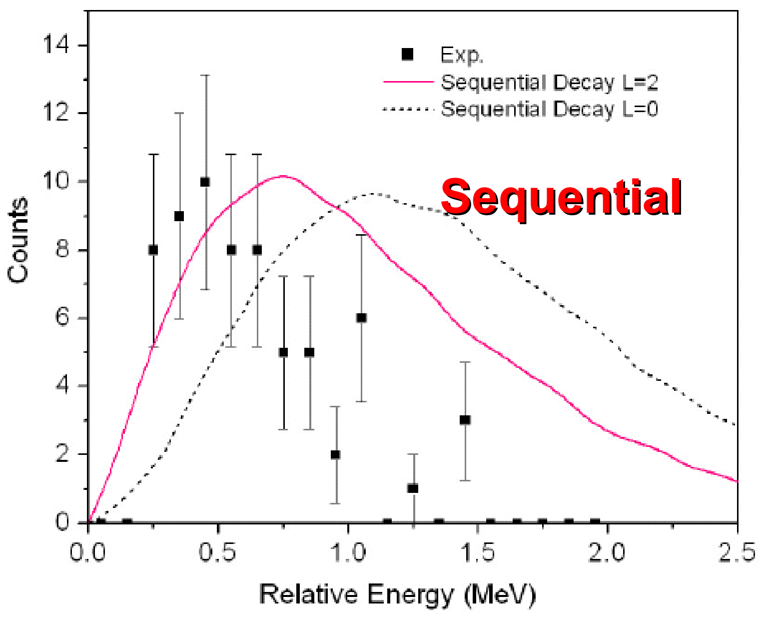

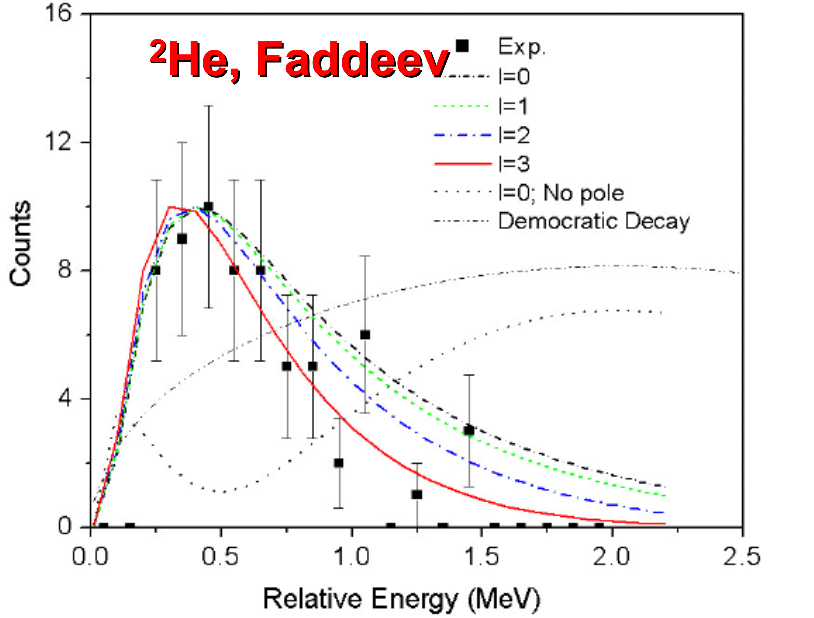

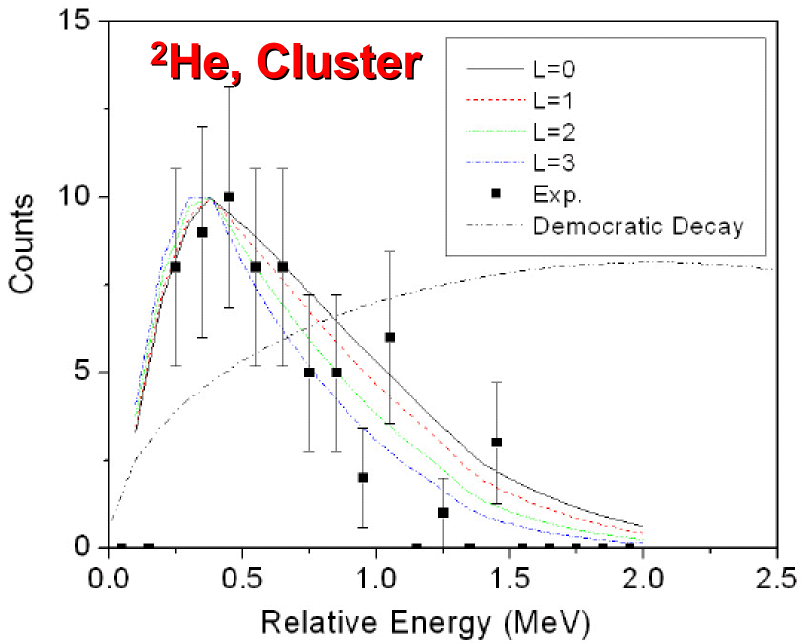

l=0 resonance in ^{37}Cl

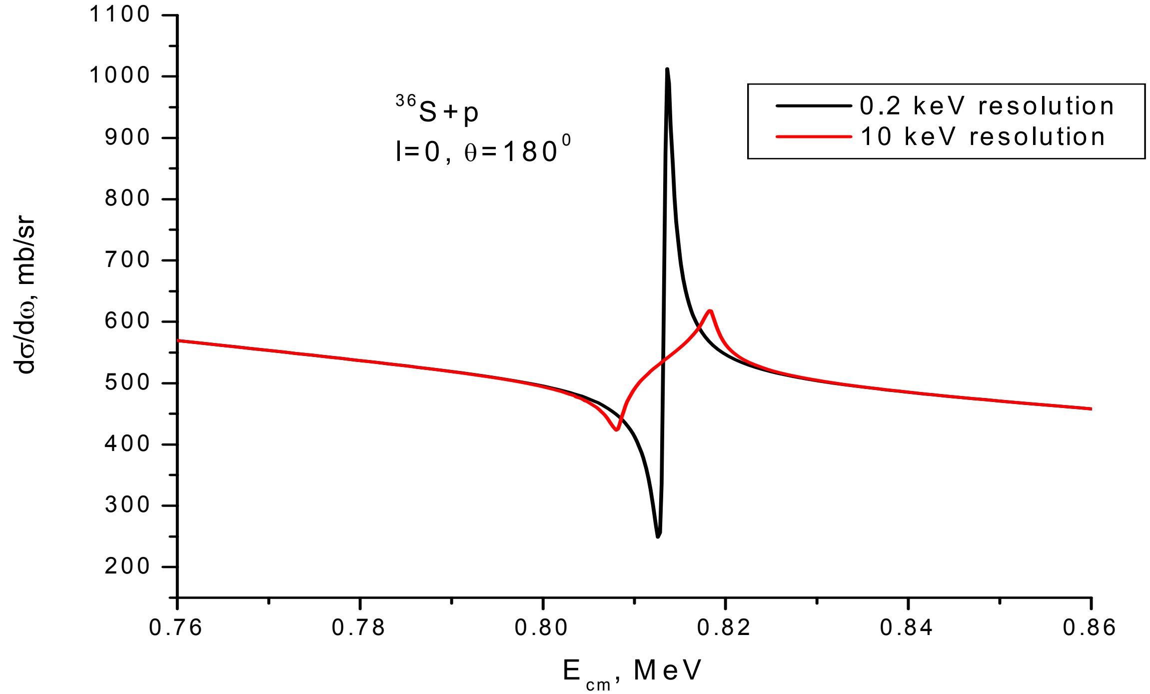

l=0 resonance in ^{15}N

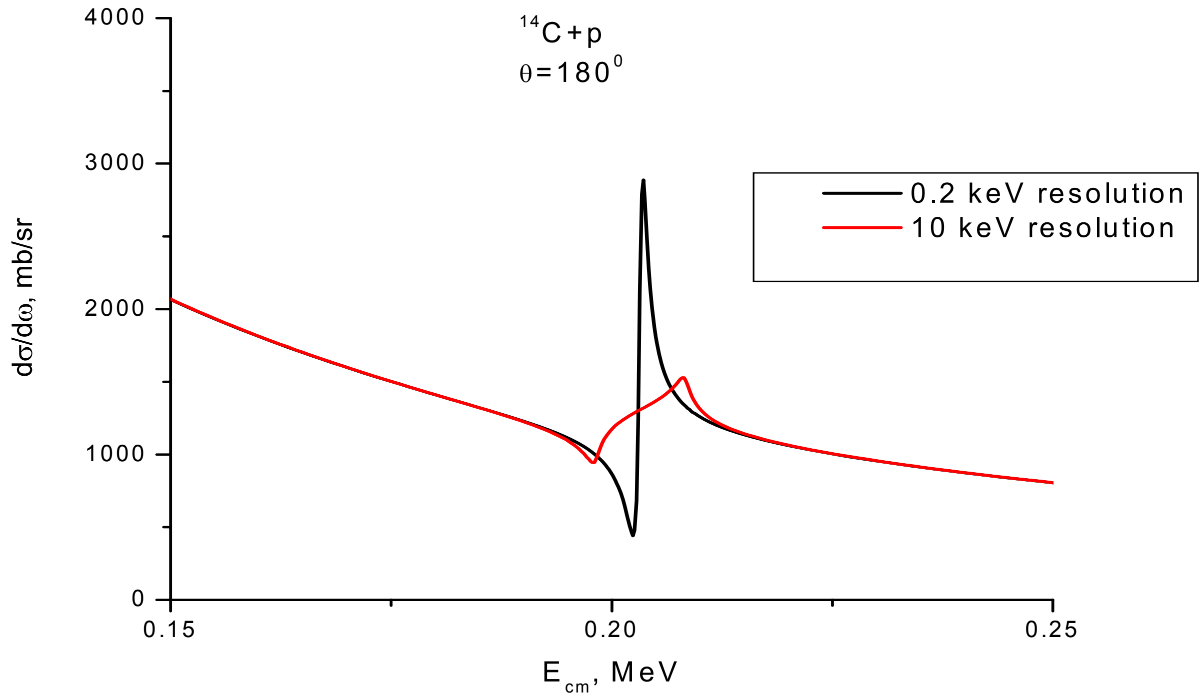

Lower Limit for observation is about 1keV

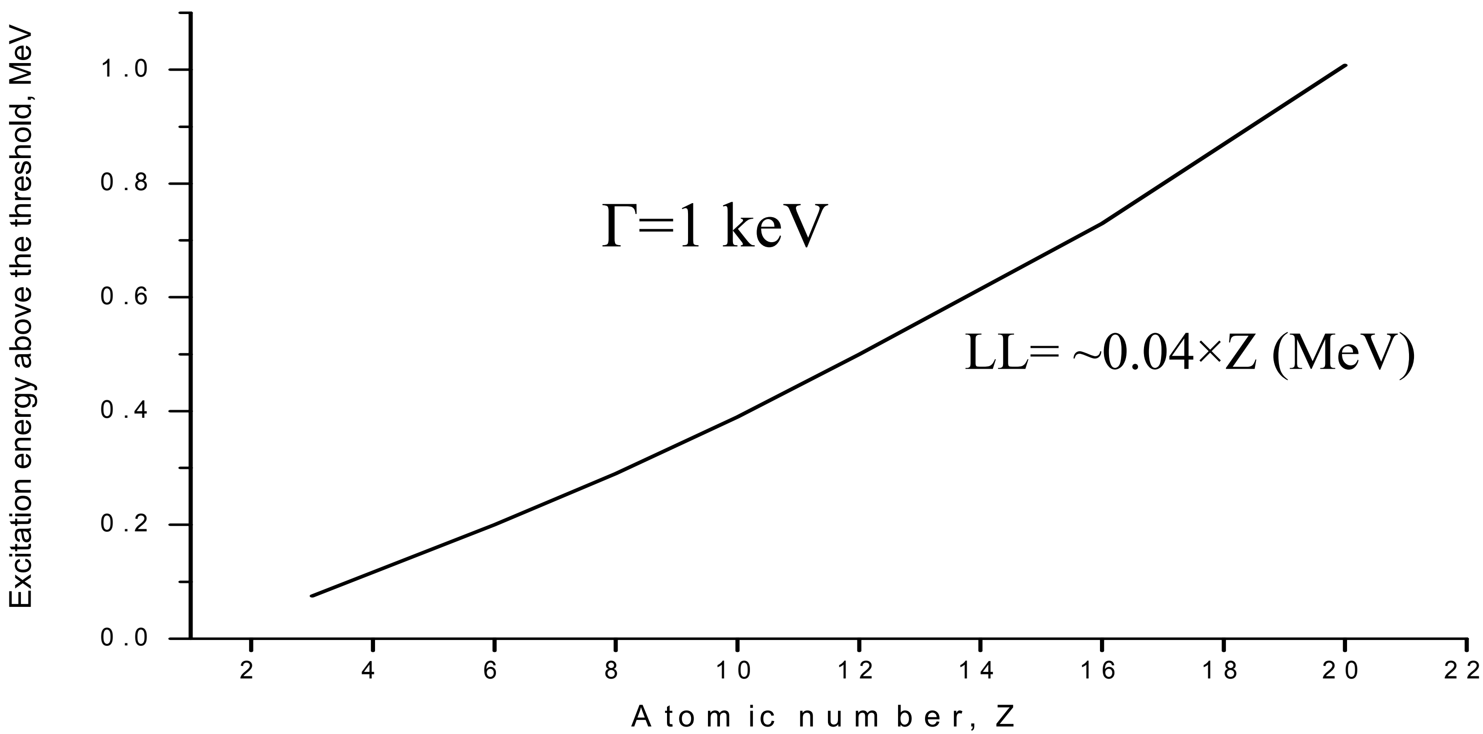

Are inelastic resonances dangerous? ^{11}C(36 MeV) + p

Elastic M>m

$$E_m \approx 4\frac{mM}{(M+m)^2}\left(E_0 - \frac{E^*}{2}\frac{M+m}{m}\right).$$

Inelastic M>m (θ_{lab}=0)

$$E_m = E_0\frac{4mM}{(M+m)^2}\cos^2\theta_{\text{lab}}.$$

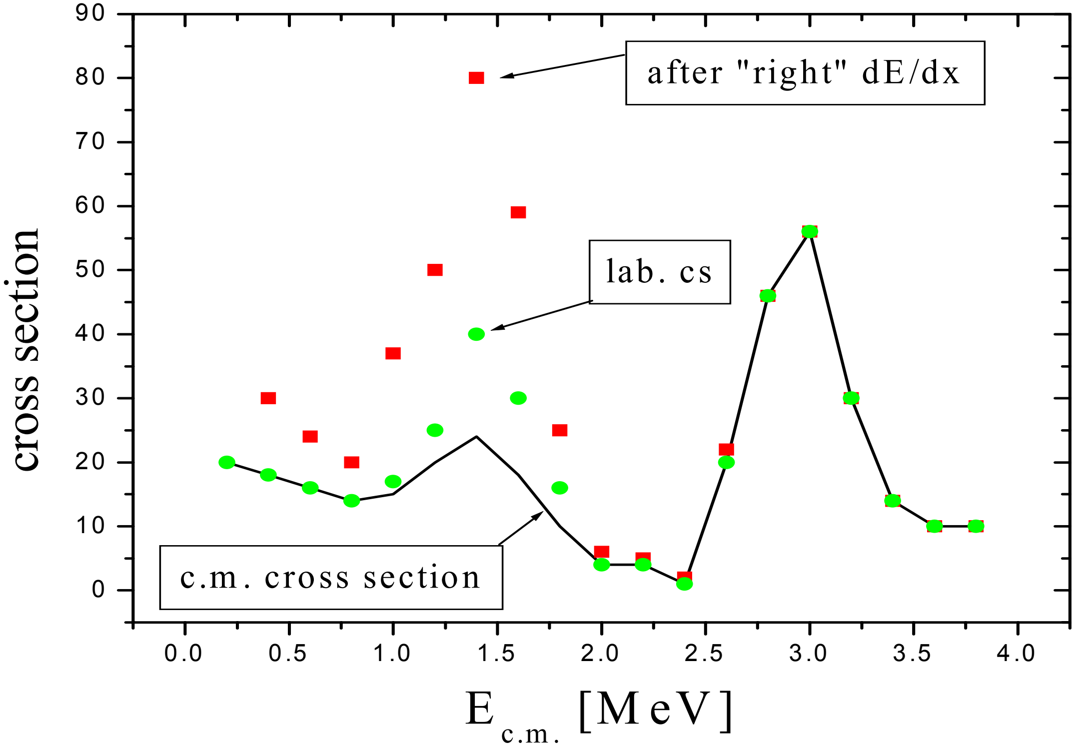

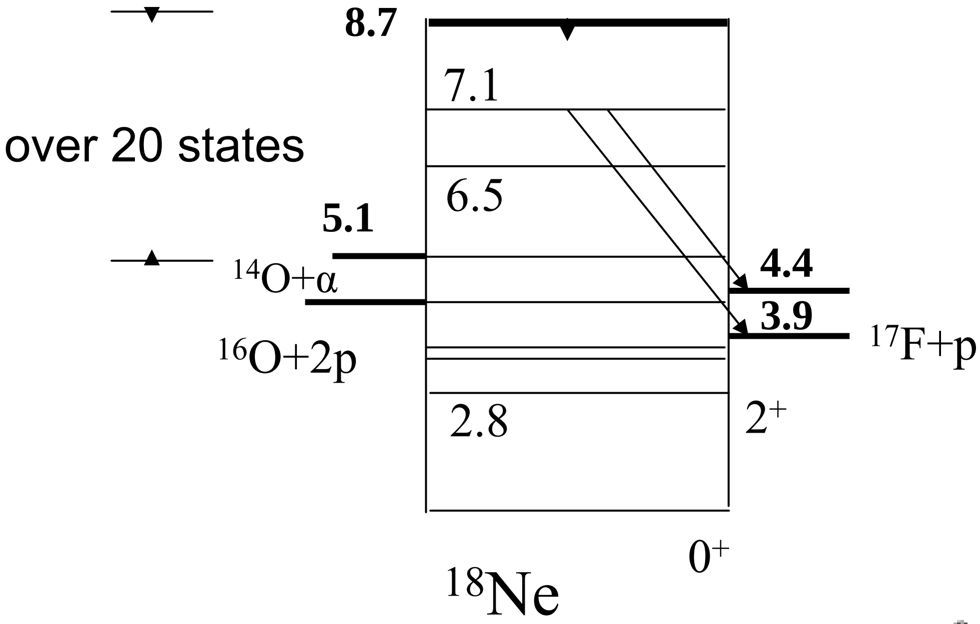

N. Notani, S. Kubono, T. Teranishi et al.,Nucl. Phys. A738, 411 (2004)

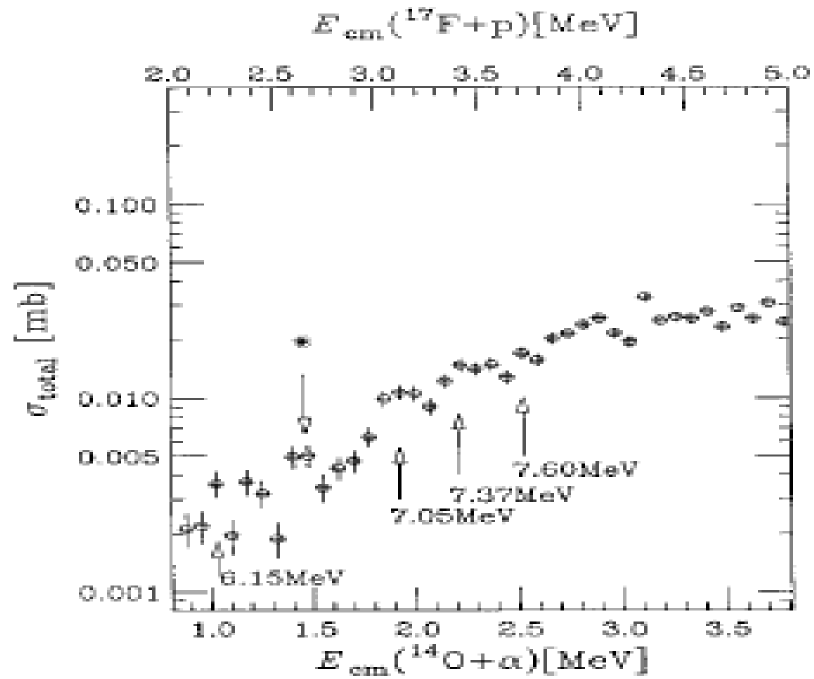

Figure 2. Measured cross sections for the $^{14}O(\alpha,p)^{17}F$ reaction. The asterisk mark is the new peak.

Spectroscopy of ^{12}N in the ^{11}C ($3/2^-$) +p elastic scattering

(no simplifications)

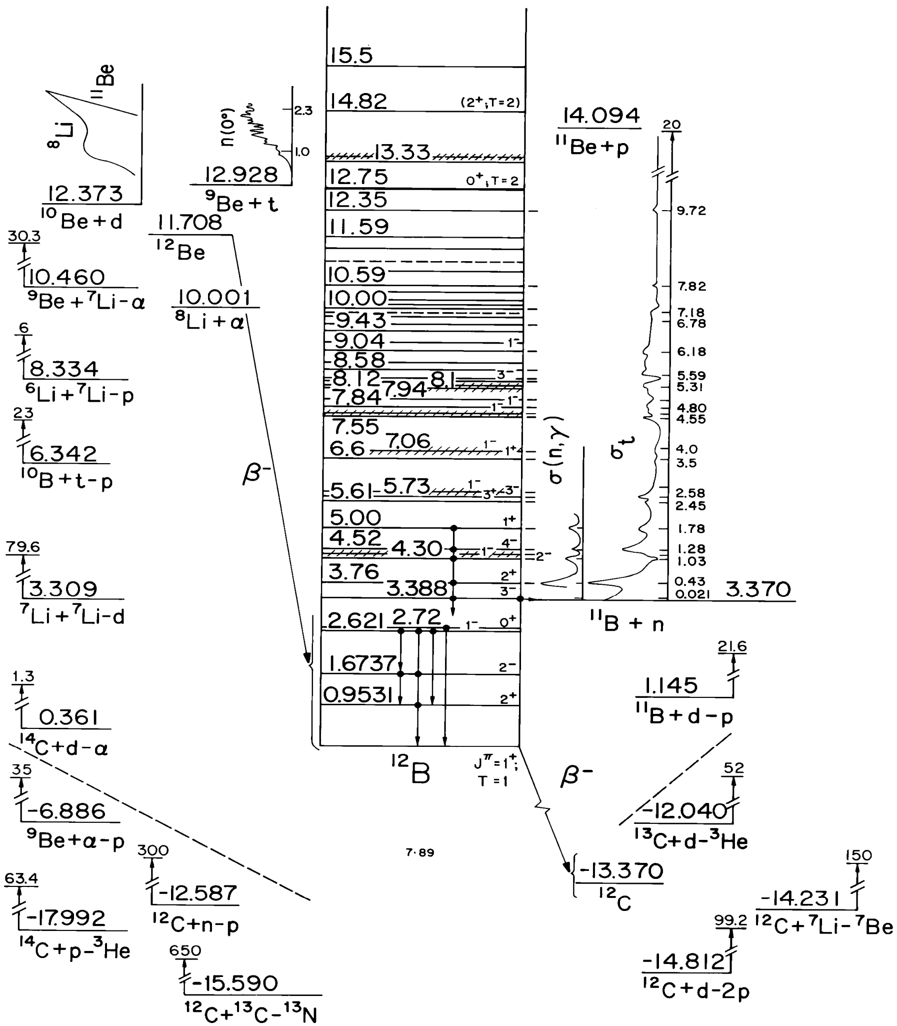

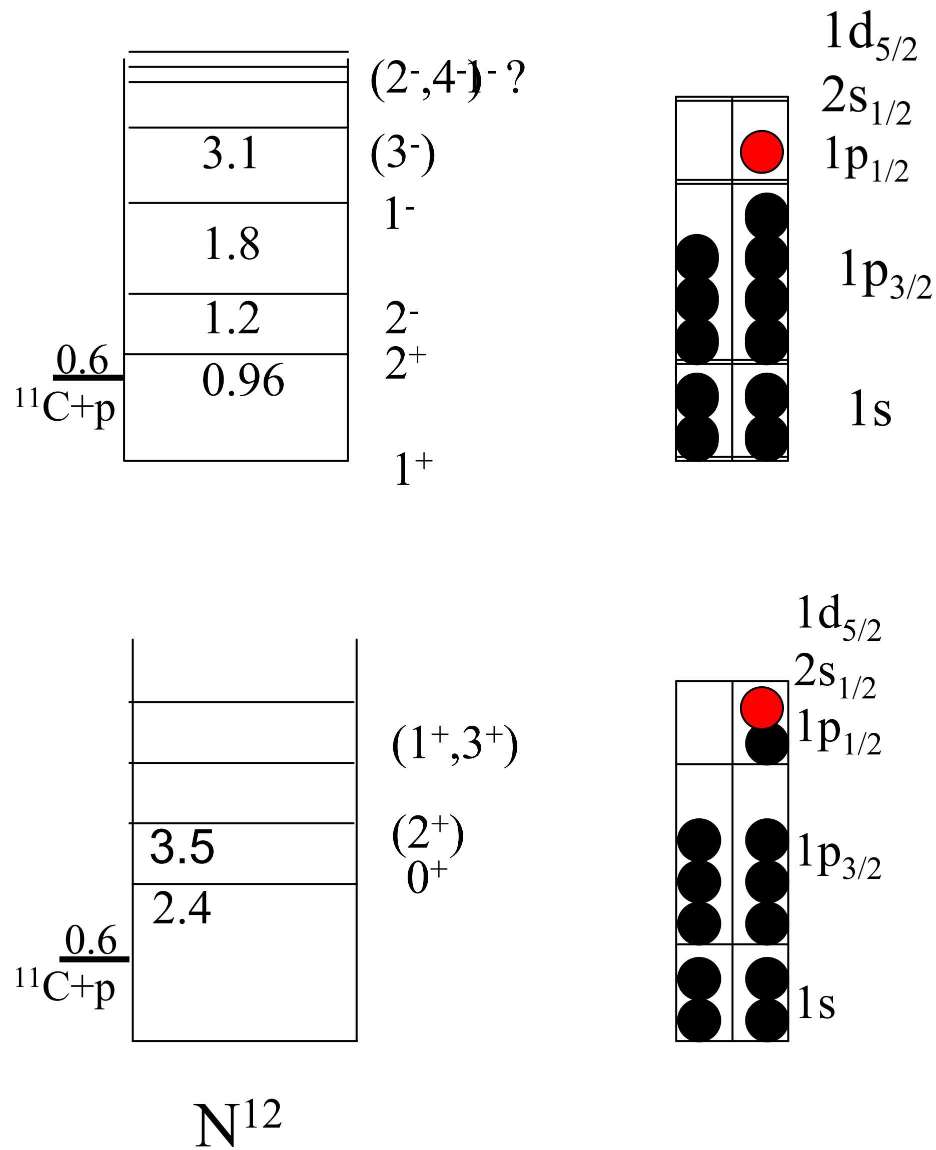

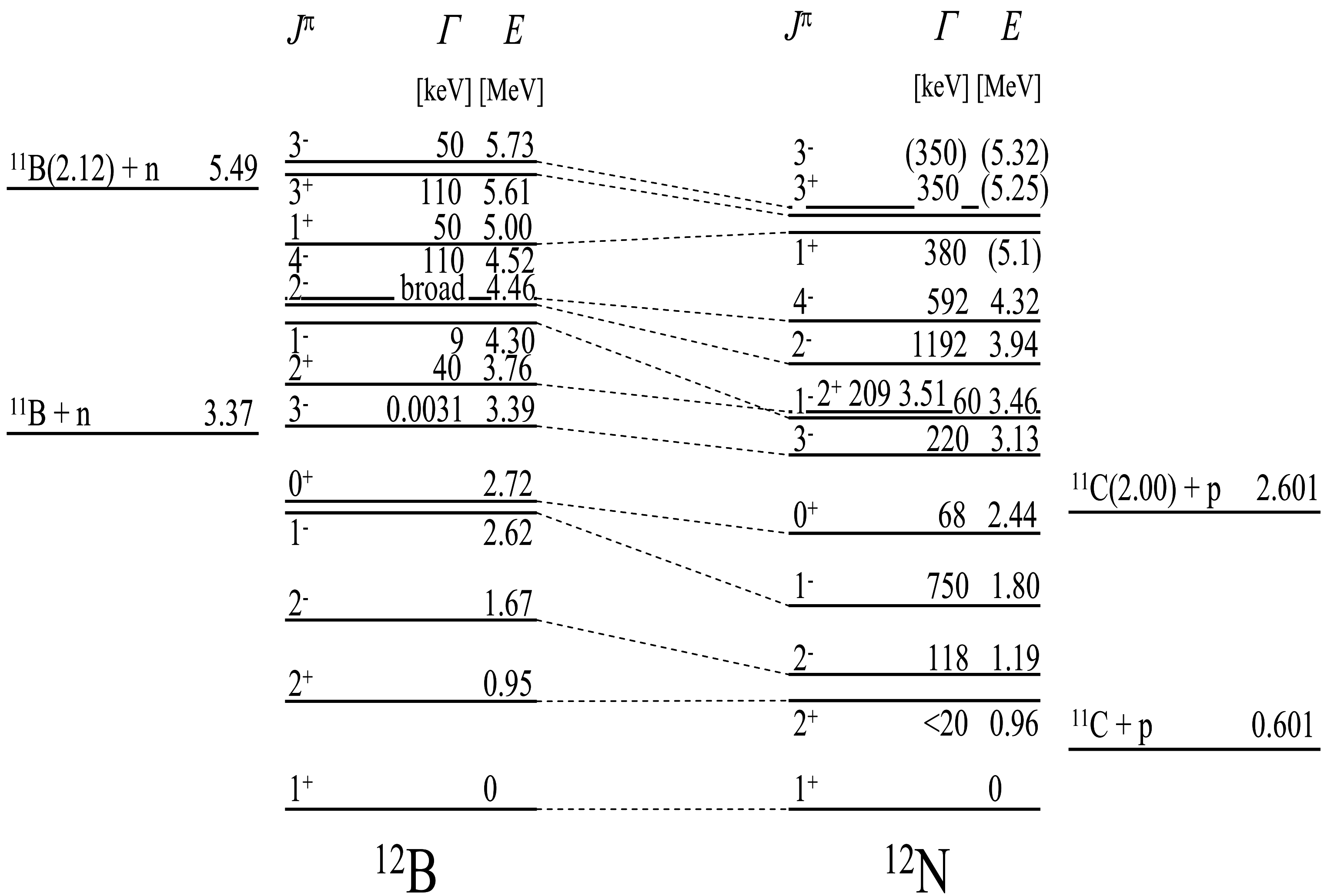

Jπ Γ E
[keV] [MeV]
3- 50 5.73
3+ 110 5.61
1+ 50 5.00
4- 110 4.52
2- broad 4.46
1- 9 4.30
2+ 40 3.76
3- 0.0031 3.39
0+ 2.72
1- 2.62
2- 1.67
2+ 0.95
1+ 0
11B(2.12) + n 5.49
11B + n 3.37
12B
Jπ Γ E
[keV] [MeV]
3- (350) (5.32)
3+ 350 (5.25)
1+ 380 (5.1)
4- 592 4.32
2- 1192 3.94
1- 2+ 209 3.51 60 3.46
3- 220 3.13
0+ 68 2.44
1- 750 1.80
2- 118 1.19
2+ <20 0.96
1+ 0
11C(2.00) + p 2.601
11C + p 0.601
12N

TABLE I: Parameters of the Woods-Saxon Potential

Parameters	^{17}O/^{17}F	^{15}C	^{15}F
V_o	-58.9	-54.15	-53.67[a]
V_{sl}	6.4	6.4	6.4
r_o	1.17	1.17	1.17
$r_o(sl)$	1.17	1.17	1.17
r_o(Coulomb)	1.21	1.21	1.21
a	0.64	0.71	0.735
a_{sl}	0.64	0.64	0.64
	Nucleon binding energy (MeV)		
$1/2^+$	3.270/0.105	1.218	-1.290
$5/2^+$	4.140/0.600	0.478	-2.795

[a]For the s state V_o=-53.27.

Energy relationship for (p, n) reactions

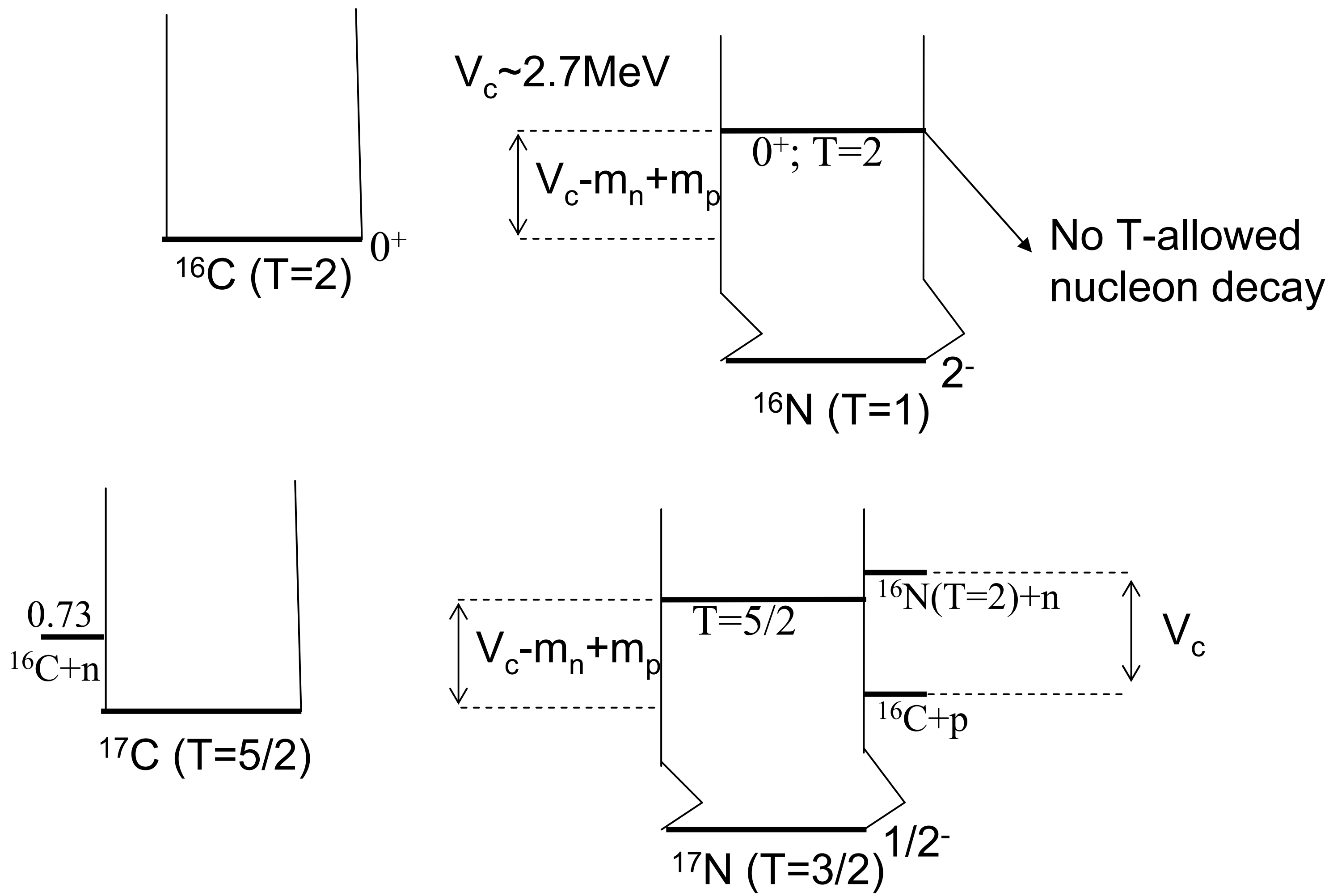

Isobaric analogs of ^{9}He in ^{9}Li.

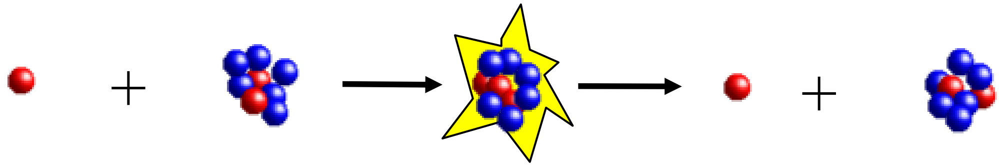

p	^{8}He	^{9}Li
T=1/2	T=2	$T_>=5/2$
		$T_<=3/2$

Decay of T=3/2 states back to elastic channel is hindered due to the presence of the other channels.

There are only two isospin allowed decay channels for T=5/2 states

$$\Psi_{^9\mathrm{Li}(T=5/2)} = \frac{1}{\sqrt{5}}\Psi_{^8\mathrm{He}+p} + \frac{2}{\sqrt{5}}\Psi_{^8\mathrm{Li}(T=2)+n}$$

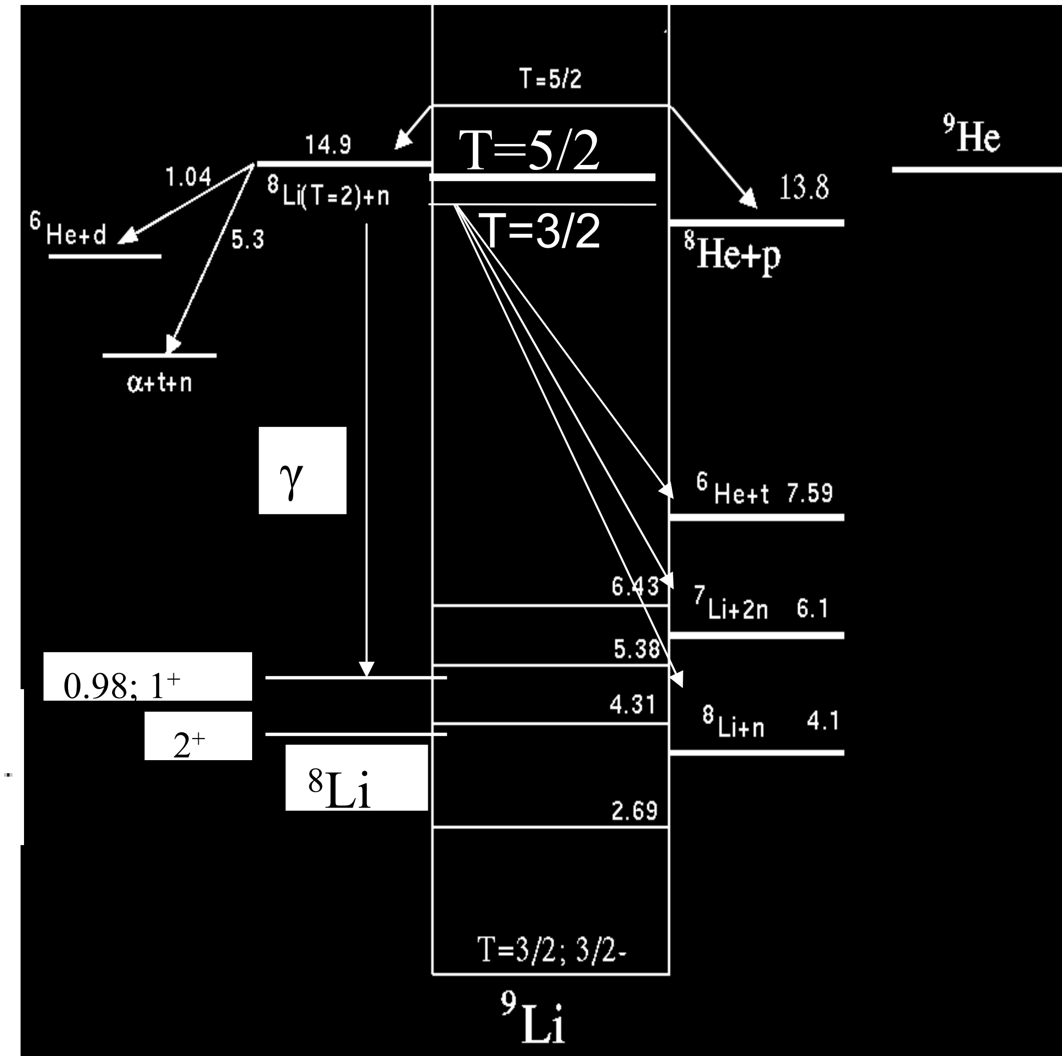

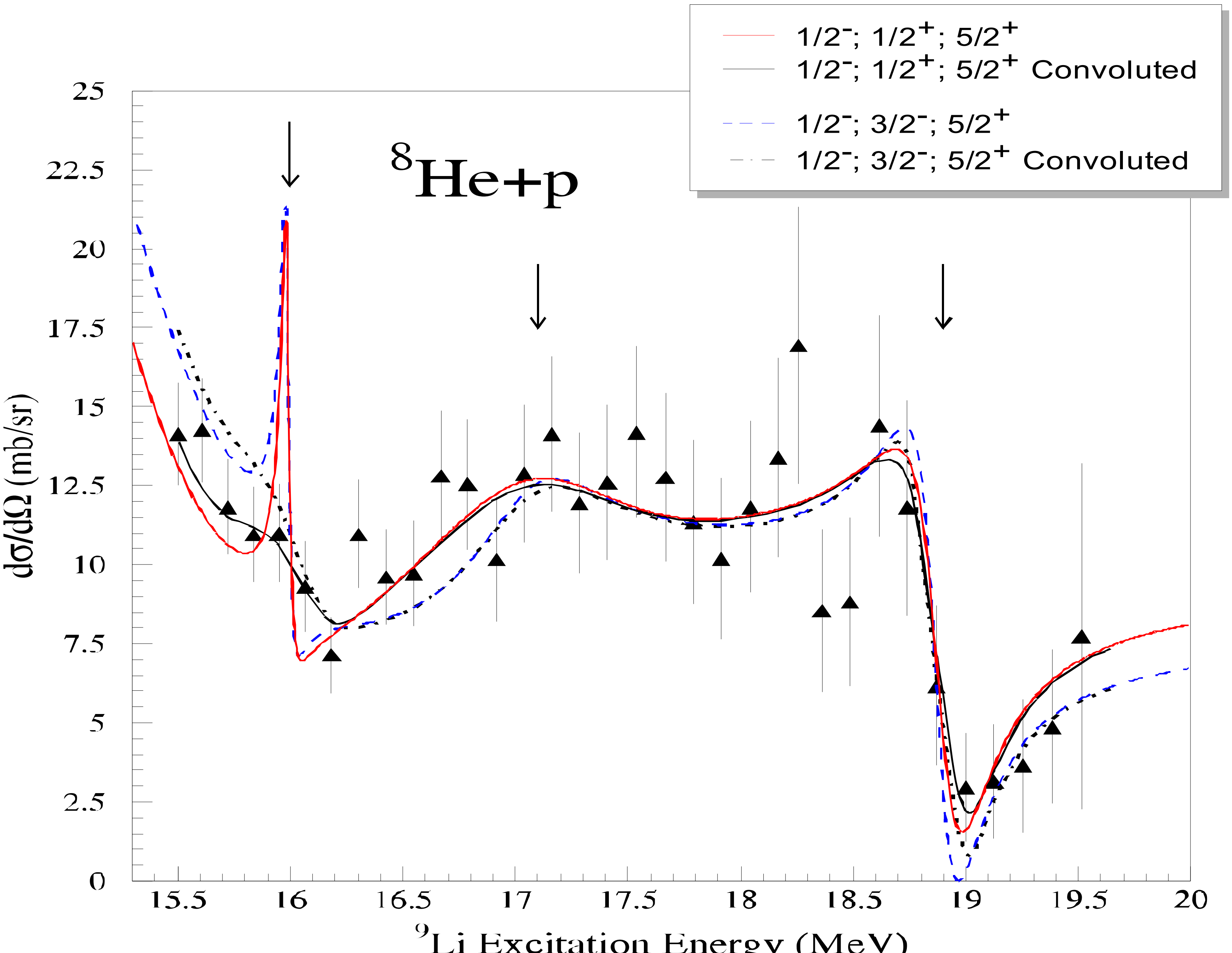
1/2⁻; 1/2⁺; 5/2⁺
1/2⁻; 1/2⁺; 5/2⁺ Convoluted
1/2⁻; 3/2⁻; 5/2⁺
1/2⁻; 3/2⁻; 5/2⁺ Convoluted
^{8}He+p
dσ/dΩ (mb/sr)
^{9}Li Excitation Energy (MeV)
25
22.5
20
17.5
15
12.5
10
7.5
5
2.5
0
15.5
16
16.5
17
17.5
18
18.5
19
19.5
20

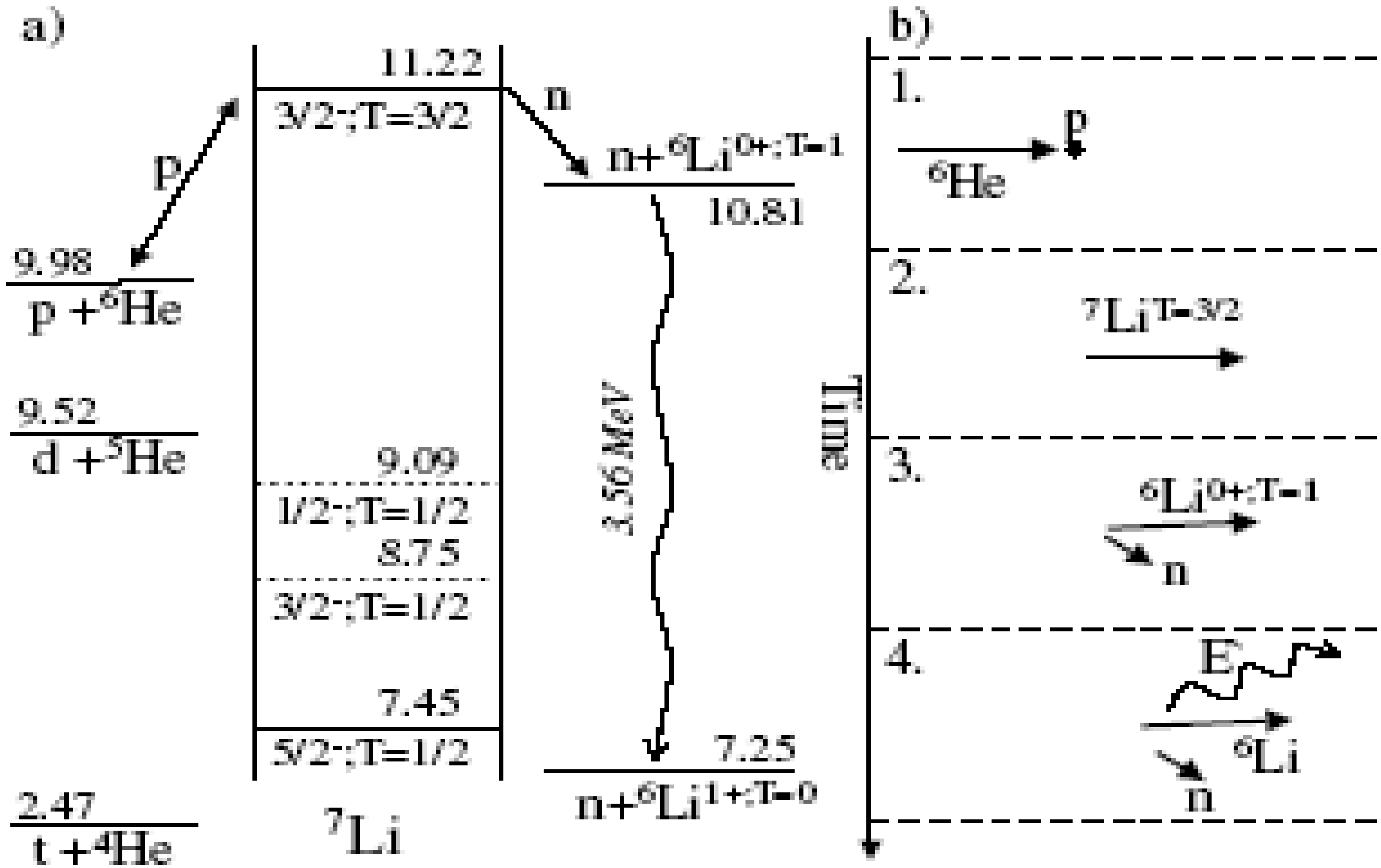

Figure 1: a) Decay pathways for the T=3/2 resonance in ^{7}Li , and b) the successive kinematics stages of the studied reaction.

TWINSOL RNB, University of Notre Dame

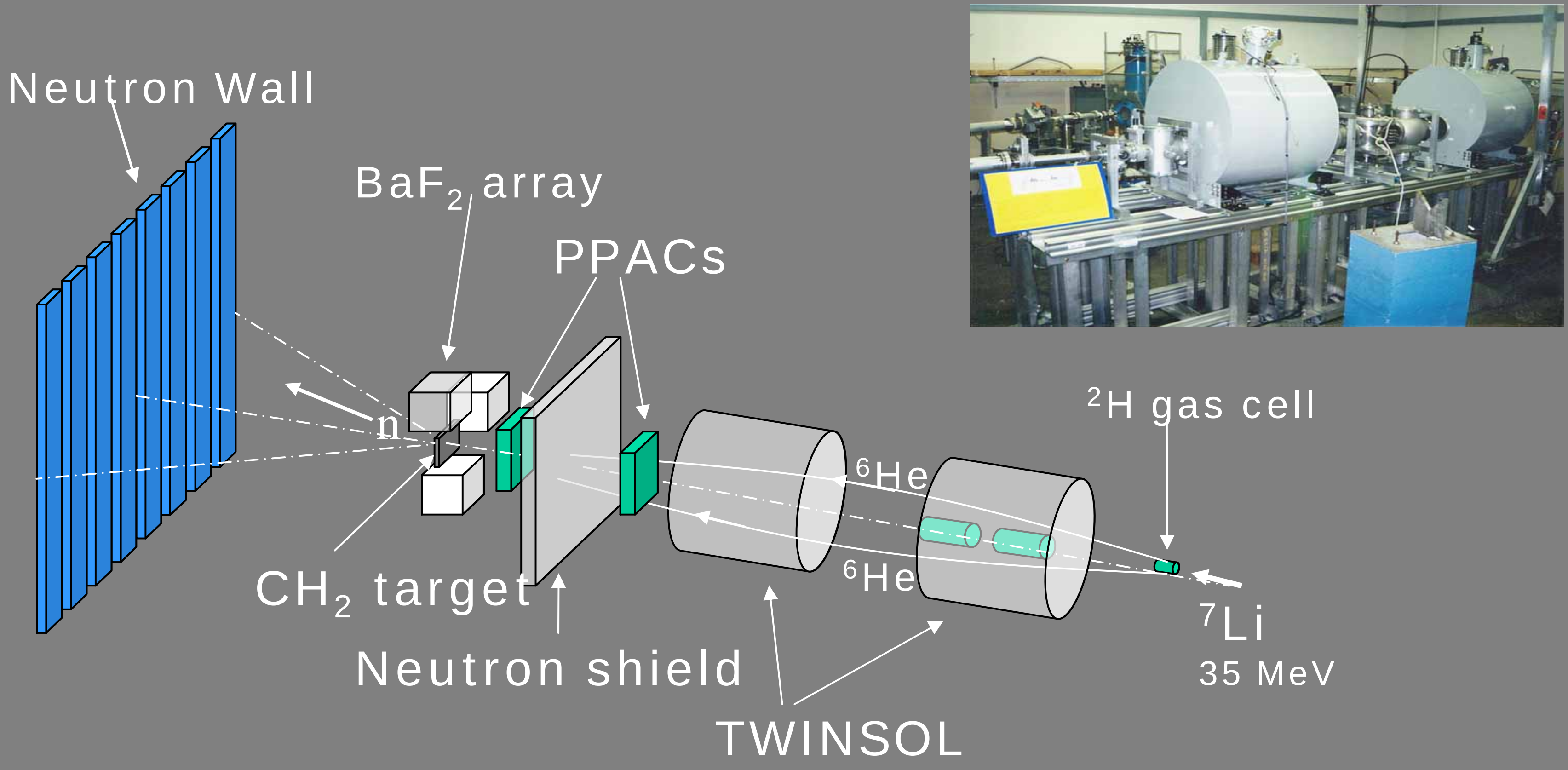

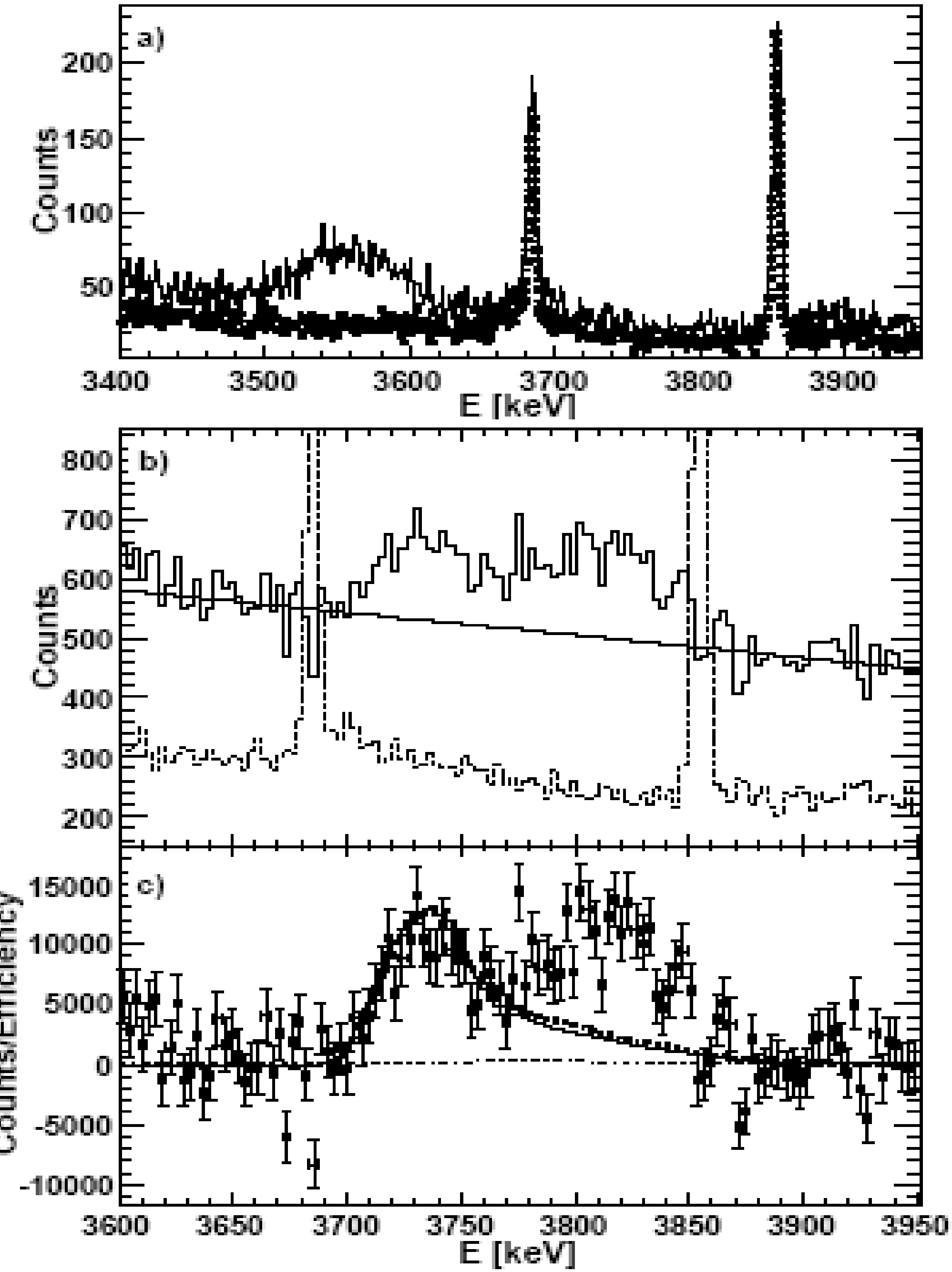

a) Part of the γ-ray spectrum from the 90^0 Ge detector. The solid curve was obtained with a CH_2 target, the dotted curve was taken with a carbon target

.

b) The spectrum in the 0^0 Clover detector obtained by subtraction of the carbon contribution, the dotted curve was taken with a carbon target. The Compton background is approximated by a straight line as shown.

c) The final spectrum of the Doppler shifted 3.56 MeV γ-rays. The solid line shows the contribution from the known T=3/2, $J^\pi = 3/2^-$ state in ^{7}Li. The dotted line includes the effect of T=1/2 resonances.

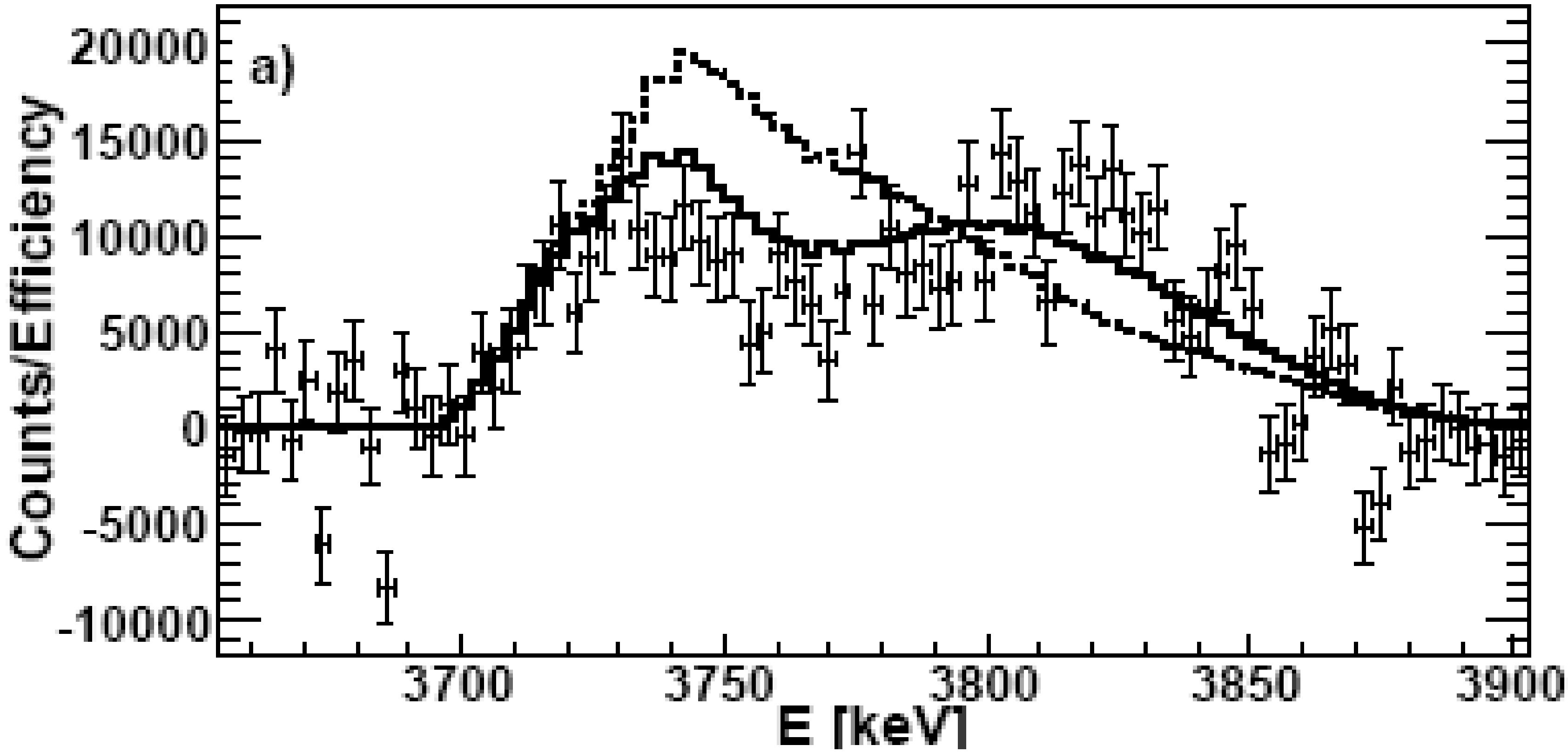

The solid curve shows a calculation of the γ-ray spectrum including the analog of the $^{7}He_{g.s.}$ and a $1/2^{-}$, Eex = 3.1 MeV, Γ = 6 MeV excited state. The dotted line is the effect from the *g.s.* resonance plus a state at E_{ex} 0.6 MeV having Γ=1 MeV.

M. Meister et al., Phys. Rev. Lett. 88, 102501 (2002).

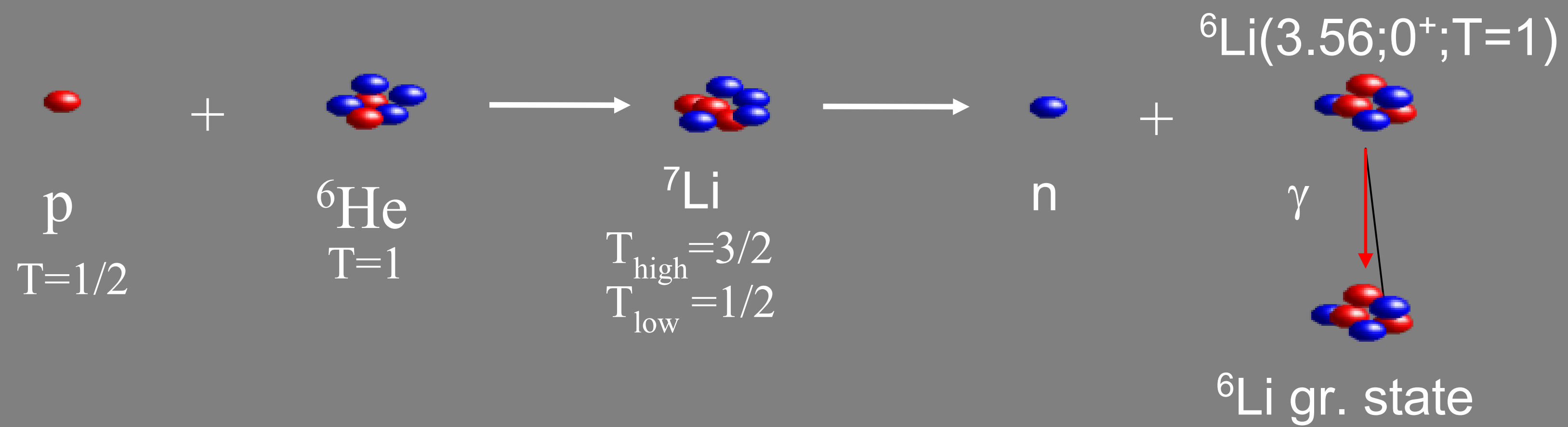

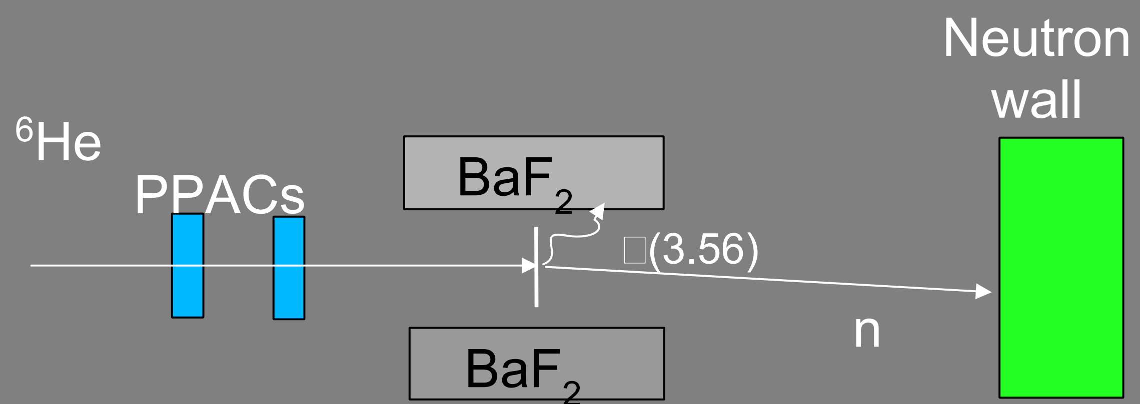

$^6Li(0^+)$ decays only by γ emission!

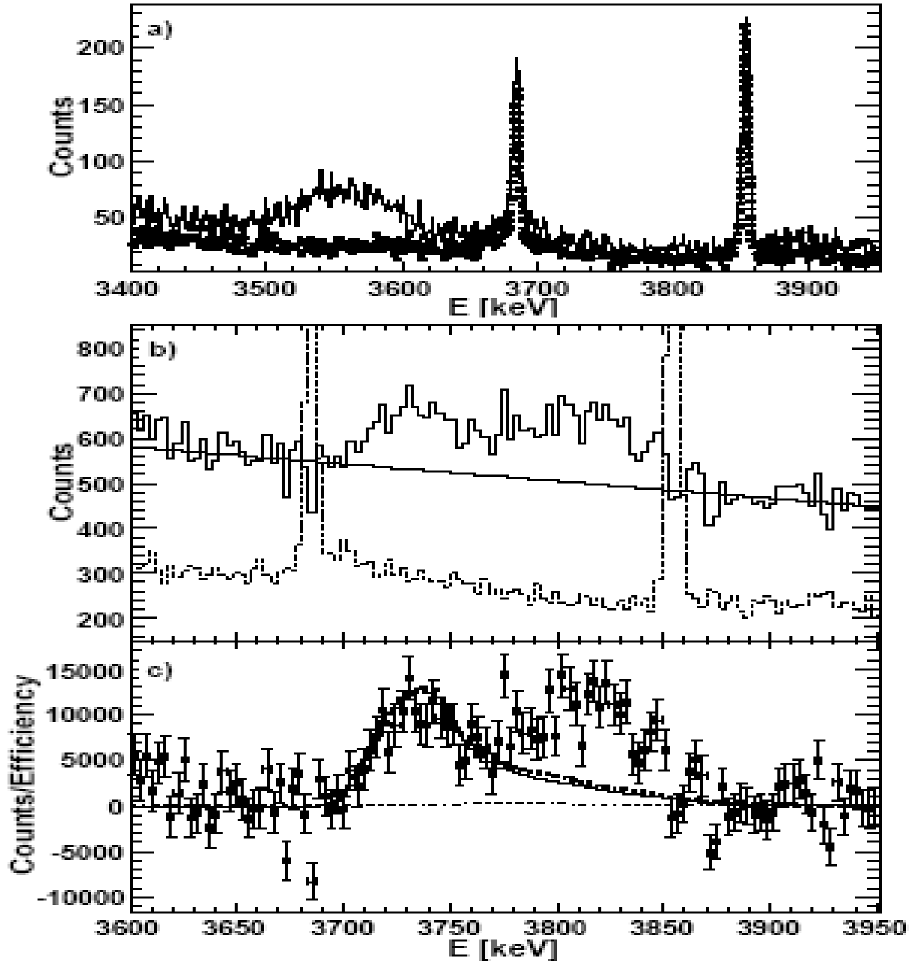

Figure 2: a) Part of the γ-ray spectrum from the 90^0 Ge detector. The solid curve was obtained with a CH_2 target, the dotted curve was taken with a carbon target. b) The spectrum in the 0± Clover detector obtained by subtraction of the carbon contribution, the dotted curve was taken with a carbon target. The Compton background is approximated by a straight line as shown. c) The final spectrum of the Doppler shifted 3.56 MeV γ-rays. The solid line shows the contribution from the known T=3/2, $J^\pi =3/2^-$ state in ^{7}Li. The dotted line includes the effect of T=1/2 resonances.

^{7}Be discrimination

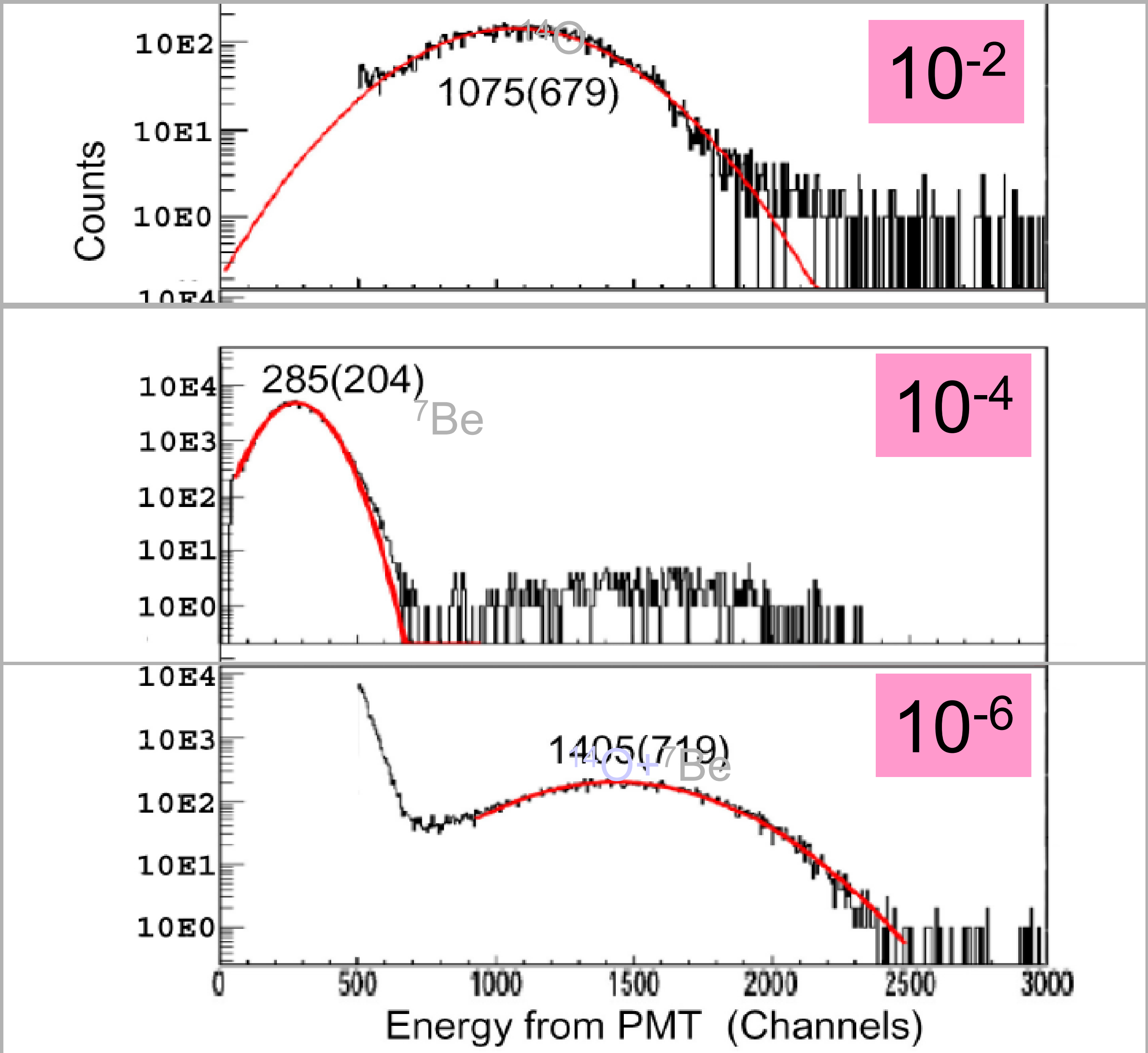

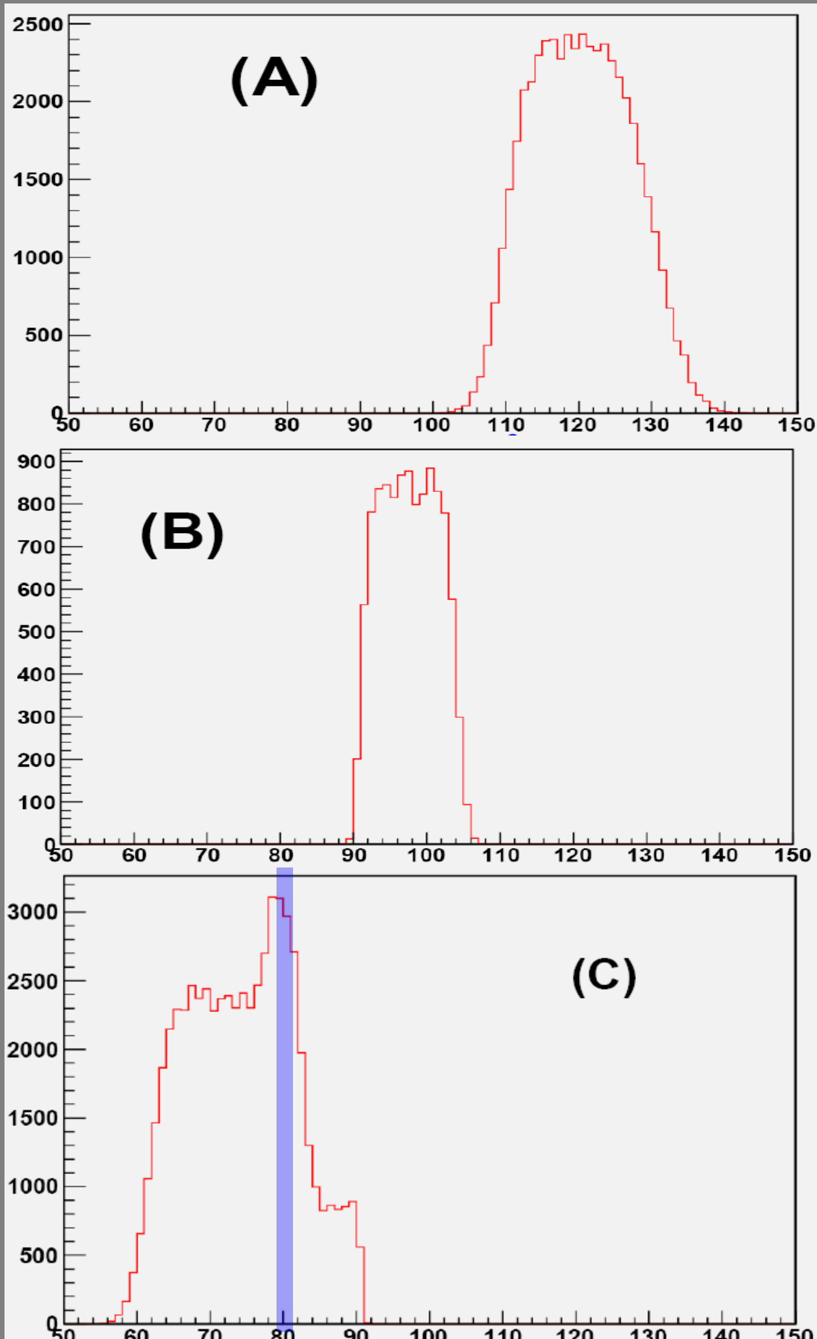

Energy spectra of ^{14}O

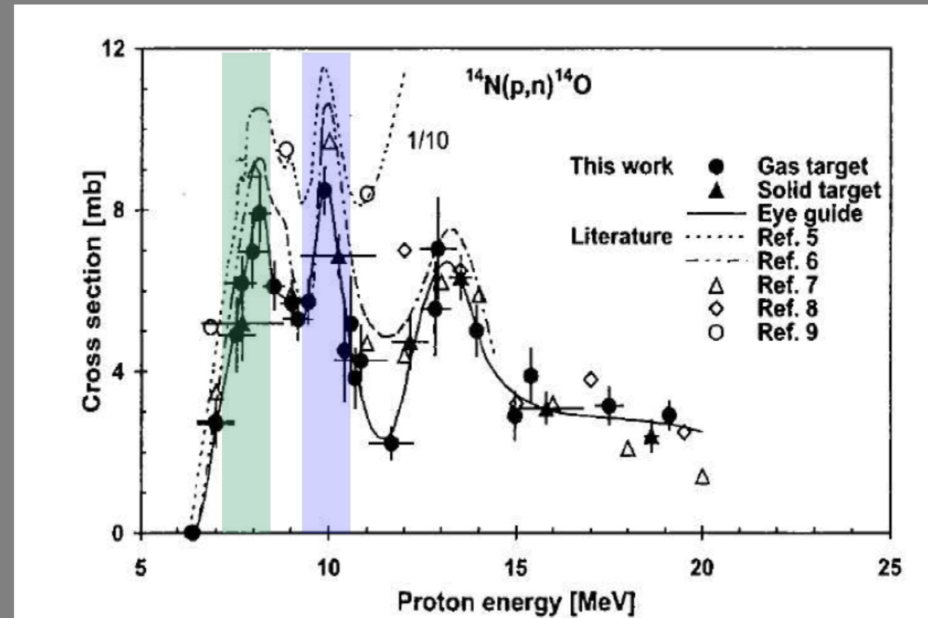

From Radiochim. Acta 91(2003)185

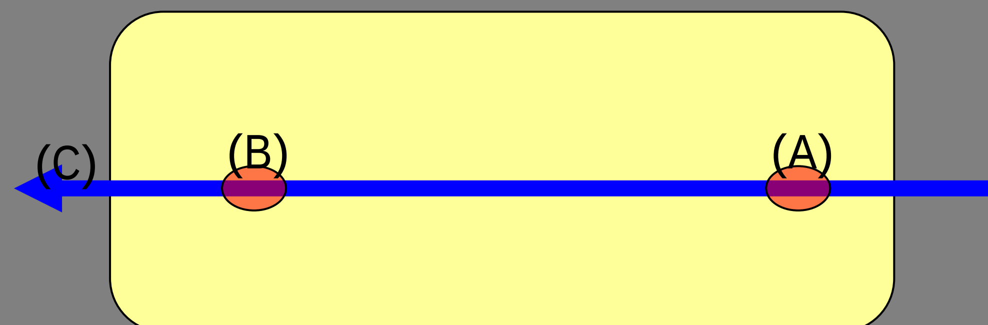

Two channels multi level expression was used to make the R-matrix fit. All notations are the same as in the article of A.M. Lane and R.G. Thomas (1958) [***U*-**collision matrix, *L*c –logarithmic derivative of the outgoing wave functions at the channel radius, E_λ-level position, and the $\gamma_{\lambda l}$ is the reduced width amplitude]

$$U_{cc}^{J\ell} = U_{cc}^{J\ell} pot + \frac{\exp[2i(\omega_\ell + \delta_{J\ell})]2iP_\ell[R_{11}^{J\ell} - L_2^\ell(R_{11}^{J\ell}R_{22}^{J\ell} - R_{12}^{J\ell\,2})]}{(1 - R_{11}^{J\ell}L_1^\ell)(1 - R_{22}^{J\ell}L_2^\ell) - L_1^\ell R_{12}^{J\ell\,2} L_2^\ell}$$

$$U_{cc}^{J\ell} pot = \exp[2i(\omega_\ell + \delta_{J\ell})],$$

$$R_{mk}^{J\ell} = \sum_\lambda \frac{\gamma_{m\lambda}^{J\ell}\gamma_{k\lambda}^{J\ell}}{E_\lambda - E},$$

$$\delta_{J\ell} = \lambda + i\mu$$